Fishery Manuscript No. 07-11

The Feasibility of Using a Split-beam Sonar to Estimate Salmon Passage on the Nushagak River as a Potential Replacement for an Echo-counting Bendix Sonar

by

Suzanne L. Maxwell,

Don Degan,

April V. Smith,

Lee McKinley,

and

Nancy E. Gove

December 2007

Alaska Department of Fish and Game **Divisions of Sport Fish and Commercial Fisheries**

Symbols and Abbreviations

The following symbols and abbreviations, and others approved for the Système International d'Unités (SI), are used without definition in the following reports by the Divisions of Sport Fish and of Commercial Fisheries: Fishery Manuscripts, Fishery Data Series Reports, Fishery Management Reports, and Special Publications. All others, including deviations from definitions listed below, are noted in the text at first mention, as well as in the titles or footnotes of tables, and in figure or figure captions.

Weights and measures (metric)

centimeter	cm
deciliter	dL
gram	g
hectare	ha
kilogram	kg
kilometer	km
liter	L
meter	m
milliliter	mL
millimeter	mm

Weights and measures (English)

cubic feet per second	ft^3/s
foot	ft
gallon	gal
inch	in
mile	mi
nautical mile	nmi
ounce	oz
pound	lb
quart	qt
yard	yd

Time and temperature

day	d
degrees Celsius	°C
degrees Fahrenheit	°F
degrees kelvin	K
hour	h
minute	min
second	s

Physics and chemistry

all atomic symbols	
alternating current	AC
ampere	A
calorie	cal
direct current	DC
hertz	Hz
horsepower	hp
hydrogen ion activity (negative log of)	pH
parts per million	ppm
parts per thousand	ppt, ‰
volts	V
watts	W

General

Alaska Administrative Code	AAC
all commonly accepted abbreviations	e.g., Mr., Mrs., AM, PM, etc.
all commonly accepted professional titles	e.g., Dr., Ph.D., R.N., etc.
at	@
compass directions:	
east	E
north	N
south	S
west	W
copyright	©
corporate suffixes:	
Company	Co.
Corporation	Corp.
Incorporated	Inc.
Limited	Ltd.
District of Columbia	D.C.
et alii (and others)	et al.
et cetera (and so forth)	etc.
exempli gratia (for example)	e.g.
Federal Information Code	FIC
id est (that is)	i.e.
latitude or longitude	lat. or long.
monetary symbols (U.S.)	\$, ¢
months (tables and figures): first three letters	Jan,...,Dec
no data	ND
registered trademark	®
trademark	™
United States (adjective)	U.S.
United States of America (noun)	USA
U.S.C.	United States Code
U.S. state	use two-letter abbreviations (e.g., AK, WA)

Measures (fisheries)

fork length	FL
mideye-to-fork	MEF
mideye-to-tail-fork	METF
standard length	SL
total length	TL

Mathematics, statistics

all standard mathematical signs, symbols and abbreviations	
alternate hypothesis	H_A
base of natural logarithm	*e*
catch per unit effort	CPUE
coefficient of variation	CV
common test statistics	(F, t, χ^2, etc.)
confidence interval	CI
correlation coefficient (multiple)	R
correlation coefficient (simple)	r
covariance	cov
degree (angular)	°
degrees of freedom	df
expected value	*E*
greater than	>
greater than or equal to	≥
harvest per unit effort	HPUE
less than	<
less than or equal to	≤
logarithm (natural)	ln
logarithm (base 10)	log
logarithm (specify base)	log_2, etc.
minute (angular)	'
not significant	NS
null hypothesis	H_O
percent	%
probability	P
probability of a type I error (rejection of the null hypothesis when true)	α
probability of a type II error (acceptance of the null hypothesis when false)	β
second (angular)	"
standard deviation	SD
standard error	SE
variance	
population	Var
sample	var

FISHERY MANUSCRIPT NO. 07-11

THE FEASIBILITY OF USING A SPLIT-BEAM SONAR TO ESTIMATE SALMON PASSAGE ON THE NUSHAGAK RIVER AS A POTENTIAL REPLACEMENT FOR AN ECHO-COUNTING BENDIX SONAR

by

Suzanne L. Maxwell
Alaska Department of Fish and Game, Division of Commercial Fisheries, Soldotna

Don Degan
Aquacoustics, Inc.

April V. Smith
Alaska Department of Fish and Game, Division of Commercial Fisheries, Soldotna

Lee McKinley, and Nancy E. Gove
Alaska Department of Fish and Game, Division of Commercial Fisheries, Anchorage

Alaska Department of Fish and Game
Division of Commercial Fisheries, Research and Technical Services
333 Raspberry Road, Anchorage, Alaska 99518

December 2007

This project was partially funded by Western Alaska Disaster Grant No. NA96FW0196. In 1998, the U.S. Congress funded an initiative for "… the State of Alaska to develop disaster research and prevention relative to the 1998 Bristol Bay, Kuskokwim and Yukon fishery resource disaster." The intent was to provide funds for research to mitigate unexpectedly low returns of salmon. A total of $336,800 was appropriated for the Alaska Department of Fish and Game to implement and test a modern acoustic system to estimate adult sockeye salmon passage on the Nushagak River.

The Division of Sport Fish Fishery Manuscript series was established in 1987 for the publication of technically-oriented results of several years' work undertaken on a project to address common objectives, provide an overview of work undertaken through multiple projects to address specific research or management goal(s), or new and/or highly technical methods. Since 2004, the Division of Commercial Fisheries has also used the Fishery Manuscripts series. Fishery Manuscripts are intended for fishery and other technical professionals. Fishery Manuscripts are available through the Alaska State Library and on the Internet: http://www.sf.adfg.state.ak.us/statewide/divreports/html/intersearch.cfm This publication has undergone editorial and peer review.

Suzanne L. Maxwell and April V. Smith
Alaska Department of Fish and Game, Division of Commercial Fisheries,
43961 Kalifornsky Beach Road, Suite B, Soldotna, AK 99669-8367, USA

Don Degan
Aquacoustics, Inc.
P.O. Box 1473
Sterling, AK 99672-1473

Lee McKinley, and Nancy E. Gove
Alaska Department of Fish and Game, Division of Commercial Fisheries,
333 Raspberry Rd., Anchorage, AK 99518-1599, USA

This document should be cited as:
Maxwell, S. L., D. Degan, A. V. Smith, L. McKinley, and N. E. Gove. 2007. The feasibility of using a split-beam sonar to estimate salmon passage on the Nushagak River as a potential replacement for an echo-counting Bendix sonar. Alaska Department of Fish and Game, Fishery Manuscript No. 07-11, Anchorage.

TABLE OF CONTENTS

Page

LIST OF TABLES

Table **Page**

LIST OF FIGURES

Figure **Page**

LIST OF FIGURES (Continued)

Figure **Page**

LIST OF FIGURES (Continued)

LIST OF APPENDICES

ABSTRACT

A split-beam sonar was tested on the Nushagak River as a potential replacement for an existing Bendix sonar used to enumerate migrating adult salmon *Oncorhynchus spp*. The Bendix counter is an echo-counting sonar deployed at a fixed location nearshore with the beam directed perpendicular to current flow. In 2000, limited datasets were collected alternately off the right and left banks with 2 split-beam transducers, 1 nearshore and 1 offshore. From 2001–2003, we collected paired data along the right bank between the split-beam and the Bendix sonar. Hardware and software difficulties created numerous setbacks in data collection and processing. Calibration and aiming protocols were developed to help standardize procedures and make it easier for technicians to set up the split-beam system. Diagnostic plots displaying the river bottom and vertical and range position of fish targets showed that the 2-transducer, split-beam system was inadequate for detecting fish. Due to changing water levels, a wider transducer beam might ensonify more of the water column, but the range would be compromised. A program developed to autotrack the split-beam sonar data failed because the riverine data was extremely noisy, and the signal processing removed many of the echoes needed to track the fish. We looked at the cross-river salmon distribution by using a wave drag model coupled with flow data to predict where the salmon should be, and then tested the model with range information from 2 sonars and drift gillnetting catch data. We compared 5, 10, 15, and 30 min/h sampling periods from a continuous split-beam sonar dataset and selected a 10 min/h sampling strategy. Paired data comparisons from the sonar's did not produce a relationship similar to 1. The difference between counts was most pronounced in 2001 and 2003, while 2002 was more similar. It was determined that the split-beam sonar was not the best replacement for the Bendix sonar. During the study period, we began testing a dual-frequency identification sonar (DIDSON). The DIDSON is proving to be a better choice for the Bendix sonar replacement because of its wider viewing angles, higher resolution of fish targets, and ease of operation.

Keywords: Split-beam, Bendix, sonar, salmon, hydroacoustic, sonar transition, Bendix replacement, sockeye salmon, Chinook salmon, *Oncorhynchus nerka*, *Oncorhynchus tshawytscha*.

INTRODUCTION

The sonar project along the Nushagak River, located in Southwestern Alaska (Figure 1), has been providing daily estimates of adult salmon *Oncorhynchus spp*. escapement for 20 years using an echo-counting, single-beam sonar, the Bendix[1] counter. Five species of Pacific salmon, sockeye *O. nerka*, Chinook *O. tshawytscha*, coho *O. kisutch*, chum *O. keta*, and pink salmon *O. gorbuscha*, migrate up the Nushagak River past the sonar site. Drift gillnetting was used to apportion the sonar counts to species (McKinley 2003). This study was developed to test a split-beam sonar as a potential replacement for the Bendix counter, determine the suitability of the existing sonar site and, if necessary, select an alternate site.

At the sonar site, the Nushagak River is approximately 300 m across. In strong river currents sockeye salmon typically migrate close to shore. The Bendix counter was originally designed to count shore-based migrating salmon but, over the years, fishery managers have become increasingly reliant on the sonar system to provide estimates of both Chinook and coho salmon, which migrate farther offshore. A split-beam sonar system has the potential to sample farther offshore, distinguish between upstream and downstream fish travel, and provide amplitude and angle information to help distinguish fish targets from non-fish targets. In addition, the replacement of the Bendix counters is needed because many electrical components are beginning to fail and some of the replacement parts are obsolete.

The Nushagak River flows approximately 390 km from its headwaters to Bristol Bay. The existing sonar site was selected because it is primarily a single channel (a small slough flows

---

[1] Product names used in this report are included for scientific completeness but do not constitute a product endorsement.

behind the site), its proximity to the commercial fishing district 40 km downstream, and because few fish have been observed milling in the area. The sonar site is located approximately 4 km downstream from the village of Portage Creek within tidal influence. The river current slows during high tide, but no flow reversal occurs. The river's turbidity precludes the possibility of enumerating migrating salmon from a counting tower. Alternative sites are limited because of the 2 primary channels upstream of Portage Creek and the multiple channels located downstream.

The feasibility of using a Bendix counter on the Nushagak River was first investigated in 1979 (McBride 1981). Since then, inseason salmon escapement estimates produced by the Bendix counter have become an important information source for commercial and sport fishery managers in the Bristol Bay area. Many management decisions are based on meeting escapement goals derived from the historical escapement estimates of sockeye salmon. The Bendix counters were used to estimate predominately sockeye or chum salmon passage on many rivers throughout Alaska (Barton 2000; Chapell 2001; Dunbar 2001; Westerman and Willette 2003). Because the use of Bendix counters is not widespread, a short description of their operations is included. More information on the system can be found in Gaudet (1990).

Bendix counters are deployed nearshore at a fixed location with the beam pointed offshore perpendicular to the river's current. At the Nushagak River, 2 counters were deployed; one nearshore and the second positioned a short distance offshore where the slope flattens. Bendix transducers were positioned close to the river bottom and aimed just high enough to avoid receiving echoes from bottom structure. Start and end ranges were set to maximize the counting range while avoiding false counts from bottom structure. Bendix transducers alternately transmit a 4^o beam from the transducer to the half range and a 2^o beam from the half range to the end range. Echoes that exceed the voltage threshold are counted and divided by range-dependent, hard-wired, echo/fish criteria. To adjust for changes in fish swimming speed and behavior, an operator periodically 'calibrates' the system by counting echo returns displayed on an oscilloscope for a set period of time and adjusting the ping rate until oscilloscope and machine counts match. The counters run continuously during the field season, except during brief periods of downtime, producing estimates available to fishery managers hourly.

Split-beam sonars have been used since 1995 to enumerate Chinook salmon on the Kenai River (Miller and Burwen 2002) and chum salmon on the Chandalar River (Osborne and Melegari 2002). Fish are manually tracked from electronic echograms but neither river has the fish densities observed at the sockeye salmon sites. Split-beam sonars use timing differences in the arrival of echoes at each of 4 transducer quadrants to determine the echo position in the X and Y axis. The echo position is used to plot the upstream or downstream movement of a fish and its vertical position, an advancement over the single-beam Bendix system. To count high densities of sockeye salmon, we pursued an automated tracking program. A cooperative effort between the Department of Fisheries and Oceans (British Columbia, Canada), Peter Withler (software developer), the Alaska Department of Fish and Game (ADF&G), and Hydroacoustic Technologies Inc. (HTI), led to the development of an autotracking software program using Blackman's algorithm (Blackman 1986). The state contracted Peter Withler to develop a software program capable of autotracking fish targets. With the lack of useful editing software, the state also contracted Withler to provide an integrated tracking and editing program and leave the algorithms open to the public domain. The Polaris software was developed, but problems with the program forced ADF&G to move to a new program, SonarData's Echoview (http://www.sonardata.com). Echoview integrated

Peter Withler's autotracking program into a program capable of tracking, editing, and exporting the echo data.

The aim of the split-beam or single-beam (Bendix) transducer is critical for detecting migrating fish. Salmon typically swim near the river bottom to take advantage of the reduced current flow and avoid surface drag. However, tidal influences and seasonal water level fluctuations can alter the current flow and fish may rise up off the bottom. Inside the Bendix counter, all processing is accomplished by the electronics; the only output is a count for each range sector. The split-beam sonar's output includes dimensional information on each echo (time, horizontal, vertical, and range), echo voltage, target strength, and various other parameters for each echo that crosses the sonar threshold and meets the single echo criteria. This information can be used to determine the effectiveness of the aim and monitor changes in fish behavior or the environment, which can necessitate changing either the aim or the deployment position.

The Bendix counter samples only 20%–30% of the Nushagak River's overall width (Miller 2000). The limited range of the sonar is due to a combination of a nonlinear profile of the river bottom and the low power output of the Bendix sonar (less than 1 Watt) coupled with a relatively high frequency (515 kHz). But is more range necessary? To answer this question, we needed to know where fish swim as they migrate upstream. Knowing the cross-river and vertical limits of the fish migratory corridors is important for selecting transducer deployment sites and understanding what proportion of migrating fish a sonar system is capable of detecting. The Bendix counter receives the majority of echoes from the nearshore transducer indicating that either migrating salmon are shore-oriented or fish detection drops off sharply with range. To learn more about how far offshore salmon migrate at the sonar site, the drift gillnetting project was expanded to include the entire river width during the 1998 and 1999 field seasons (Miller 2000). Although gillnets provide a relatively poor estimate of abundance due to variable catch rates among species and individuals and other environmental factors, the study showed that a potentially large proportion of salmon migrate offshore of the range ensonified by the Bendix sonar. A total of 83% of Chinook, 20% of sockeye, 55% of chum, and 56% of coho salmon were captured outside the range of the Bendix sonar.

Existing theories on the energy costs of migration (Brett 1995; Hinch and Rand 2000; Webb 1995), predict that salmon of all sizes will migrate close to the riverbank to minimize the water velocity against which they have to swim. In order to explain the cross-river distribution observed by Miller (2000), a new model that incorporates wave drag was developed to predict the cross-river distribution and speed of migrating salmon. Wave drag occurs when a fish swims near the water's surface. An increase in drag is experienced with the formation of waves. This wave drag can be considerable, up to 4 times the drag a fish would experience if swimming 3–4 body diameters below the surface. The wave drag model combines river depth and velocity with the energetics of swimming fish to predict the location of the migratory corridor that will minimize the cost-per-unit distance traveled upstream (Hughes 2004). Because it accounts for this previously neglected source of resistance, the wave drag model can explain why smaller fish restrict themselves to a narrow migration corridor, while larger fish are able to swim farther offshore in deeper water, even though this means swimming against faster current. If the model can accurately predict the location of these corridors, it would help us in positioning the sonar where the power of the beam and the river bottom profile provide the best coverage of migrating fish. We might also be able to select sites that maximize lateral segregation between species. This should improve species identification, which would be particularly helpful in situations where it important to assess the numbers of less abundant species, like Chinook salmon, migrating alongside a more abundant species like sockeye salmon. As part of this study, we also looked at range measures from the sonars and drift gillnetting catch information to test the wave drag predictions.

The specific objectives for this study were to:

1. Select deployment sites.
    a. Profile the river bottom at the Bendix deployment sites.
    b. Profile sites in the vicinity of the Bendix site and at single-channel locations upriver and downriver.
    c. Select a site along each side of the river to deploy the split-beam sonar.
2. Test the split-beam sonar and optimize the sampling and autotracking parameters.
    a. Determine the optimal beam size and select equipment.
    b. Field calibrate the split-beam system.
    c. Determine the best aim and optimal sonar parameters for sampling at the selected site.
    d. Analyze split-beam sonar echo data to diagnose problems with equipment and to determine autotracking parameters.
    e. Optimize the autotracking parameters.
    f. Test sampling plans for data collection and determine how much information is lost by subsampling.
3. Outline the cross-river salmon distribution at the selected deployment site.
    a. Develop a model based on the wave drag theory to predict the migratory corridors of Chinook and sockeye salmon at the Nushagak River sonar site.
    b. Measure bathymetry and flow characteristics of the river in the vicinity of the sonar site.
    c. Examine the cross-river salmon distributions obtained from the split-beam sonar and drift gillnetting data.
    d. Using the drift gillnetting data, determine the percentages of Chinook, sockeye, and chum salmon that travel in the nearshore and offshore regions along both sides of the river.
4. Determine whether the estimates from the split-beam sonar and Bendix counter are equivalent.
5. If the split-beam sonar proves to be a feasible alternative to the Bendix counter, assess the management plan and escapement goals for the Nushagak River based on the 2-sonar comparison.

METHODS

SELECTING A DEPLOYMENT SITE

River bottom profiles were created using a down-looking Lowrance X-15 chart recording Fathometer (192 kHz with a 20^{o} circular beam) and a laser range finder to measure the distance from shore. The Lowrance transducer was attached to the transom of a small skiff. Charts showing the depth versus time were produced as the boat moved cross-river from one side of the river to the other. The boat's range from shore was measured in meters with the laser ranger-finder in varying increments and marked on the charts. The distance between each measured range depended on how long it took the observer to note the range, mark the chart, and record the measured range in a field log. We profiled the river bottom at the Bendix site, in the vicinity of the Bendix site, and at selected upstream and downstream single-channel segments of the river.

A more detailed bathymetric map was produced in the region of the sonar site using a down-looking BioSonics' DT sonar system with a 201-kHz 6° circular beam and a Trimble DSM212H GPS, which received differential corrections from a Trimble DSM212 Reference Station setup along the shore. The BioSonics' transducer was positioned along the side of the boat. The boat was motored back and forth focusing the heaviest sampling in the regions of the Bendix sonar deployment site. Position and depth data were imported into ArcView software to produce a bathymetry map of the region, and cross-river depth profiles were generated for sites with the most uniform slope and minimal bottom obtrusions.

TESTING THE SPLIT-BEAM SONAR

Equipment and Deployment

We selected an HTI Model 241 echosounder with elliptical split-beam transducers to test on the Nushagak River. HTI Model 661H rotators with remote controllers and relative feedback were used to remotely aim each transducer. A BioSonics' attitude sensor was affixed to each transducer to provide absolute pitch and roll information. For each year of data collection, a nearshore and offshore transducer were deployed. We used an H-shaped mount made from aluminum poles held together with slightly larger diameter aluminum poles welded into T-shapes (Figure 2). The rotators were attached to a hanging bracket on the mount, and the transducers were affixed to a metal plate mounted to the rotators. The BioSonics' attitude sensor was held on the side of the transducer using large metal hose clamps. The apparatus was deployed nearshore at a fixed location with the sonar beam directed perpendicular to the current flow. For the nearshore deployments, the H-mount and equipment were walked into the water until the transducers were far enough underwater that the tidal changes would not leave them dry. The legs of the H-mount were sandbagged to prevent the transducer from moving. For the offshore deployment, an anchor attached to a long rope with a buoy on the end was dropped far enough upstream that the buoy landed at the desired deployment location. Next, a rope was attached to the 2 upright poles of the H-mount and pulled over the gunnels of the boat, hanging the H-mount from the side of the boat. The boat traveled directly to the floating buoy dragging the cables from shore. The buoy was disengaged from the rope and attached to the upstream leg of the H-mount. The H-mount was then slowly lowered to the river bottom. The upstream leg attachment to the anchor kept the mount from spinning on its way down.

The nearshore and offshore split-beam transducers were positioned close to the river bottom with enough space to make small adjustments to the transducer pod without damaging the transducer. The center of each transducer beam was approximately 18–20 cm from the river bottom. A weir was positioned downstream of the nearshore sonar to prevent fish from passing inshore or within the 1.7 m near field region of the transducer (Figure 3). We tried to keep the weir approximately 2 m beyond the transducer. The offshore transducer was positioned along the secondary, more flattened slope. Most of the work for this study was performed off the right bank (facing downstream) of the river. Only a short period in 2000 was devoted to testing the split-beam system on the left bank.

Off the right bank in 2000, a 4^o by 10^o split-beam transducer was deployed nearshore and autorotated between 3 vertical aims: the first, low along the river bottom, the second, a beam width higher, and the third, 2 beam widths high. The small size beam with multiple vertical aims was chosen because larger beams have been shown to have poorer detection abilities (Enzenhofer et al. 1998). A 2^o by 10^o split-beam transducer was attached to the offshore mount and deployed where the slope flattened. This transducer automatically rotated between 2 aims; the first, low along the river bottom and the second, 1 beam width higher. Later in the 2000 field season, only the low aim was used. Few fish were observed in the uppermost aim of either transducer. In 2001, we dropped the uppermost aim on the nearshore transducer and autorotated between the 2 lower aims. In 2002 and 2003, a 6^o by 10^o split-beam transducer, on loan from the U.S. Department of Fish and Wildlife, was substituted for the 4^o by 10^o and aimed low along the river bottom. Based on detection difficulties observed by Enzenhofer et al. (1998) using an 8^o vertical beam, we were hesitant to move to the larger beam. The primary reason for selecting the larger beam was the uncertain detection rate of fish along the beam edges. Fish tracks or portions of fish tracks near the beam edge had the potential of appearing in the lower or upper beam. We decided the larger beam with a single aim would be less biased, and easier to process data from, than the multiple beams. The same 2^o by 10^o offshore split-beam transducer was used each year. For each year, the sample time within each hour was divided between each transducer aim.

Off the left bank in 2000, we deployed the 4^o by 10^o split-beam transducer nearshore and autorotated between 2 aims, and the 2^o by 10^o transducer offshore autorotated between 3 aims. No further split-beam data was collected off this side of the river.

Personal laptop computers were used to operate the sonar and process the data. All raw and processed files were written on compact disks.

Calibrations and Aiming

The HTI transducers were calibrated at the HTI laboratory facility against a standard transducer using reciprocity techniques (Appendix A1). In addition, we field-calibrated the HTI system at the start of each field season using a 38.1 mm tungsten carbide sphere (calibration sphere) suspended outside the near field of each transducer in the middle of the beam. The calibration sphere was moved up, down, right, and left to obtain echoes throughout each of the 4 split-beam transducer quadrants. The theoretical target strength of the calibration sphere for a 200 kHz frequency rounds to –39.5 dB for water temperatures ranging from 9–15^{o}C (Faran 1951).

Prior to deploying the transducers, the attitude sensors were tested and leveled using a bubble level onshore. We aimed the nearshore transducers by suspending an approximate acoustic salmon-size target (10.16 cm plastic sphere filled with bb's) above the river bottom in front of the transducer. The target strength of the plastic sphere was measured using the split-beam sonar to determine its similarity acoustically to a salmon. We adjusted the transducer pitch to match the river bottom slope then fine tuned the aim by rotating the transducer until the target echoes in 2-dimensional position plots appeared just below the centerline of the beam. For the remaining vertical aims, the transducer was positioned a beam width above the lower aim. The offshore transducer was aimed by first matching the aim to the bottom slope then affixing the plastic sphere to a pole with monofilament line and lowering it from the side of the boat into the beam.

The target was lowered to the river bottom then pulled up approximately 4 inches to test the aim. This technique was repeated at 2 or 3 ranges.

Sonar Parameters

Although we desired as low a threshold as possible for the sonar system, the river is a noisy environment. Because the sound beam is squeezed between the river bottom and surface boundaries, sound reflecting off microscopic or macroscopic objects in the water and off the boundaries themselves can bounce back to the receiver, creating large numbers of unwanted echoes. In this report, unwanted echoes are referred to as noise regardless if their source is from ambient noise or sound reverberation. To enhance fish detection, we strove to obtain a minimum signal to noise ratio of 10 dB across the ensonified range. The sonar settings for the transmit, receiver gain, and voltage threshold all were adjusted to achieve as high a signal to noise ratio as possible while maintaining the lowest possible threshold. The pulse length was set small enough to provide maximum resolution of targets, but high enough that we were not unnecessarily limiting the amount of power being transmitted. The pulse repetition rate was set as high as the range limitation would permit and the acoustic transmitter was capable of to achieve as high a resolution as possible at close ranges. To obtain accurate range measures of echoes, the sound speed was calculated based on water temperature (MacLennan and Simmonds 1992) and input into the configuration file.

Split-beam Sonar Data Processing and Analyses

To process the split-beam sonar data, we tested a series of programs designed to display the data and allow the user to edit and autotrack the data. We began using a program borrowed from the Pacific Salmon Commission in British Columbia (PSCSplitBeamFishTrack). The program had poor viewing capabilities and was very slow to use. In 2001, we began using a beta version of the Polaris program developed by Peter Withler along with a separate tracking program (ABTracker), until we discovered the edited data was not being stored. We quickly switched to Echoscape, an HTI echo-processing program. The entire season’s data was manually tracked and edited. We later discovered the concatenating function, used to process and store data from multiple files in 1 grouping, was flawed. It collapsed fish tracks from the multiple files into single fish, rendering the processed data useless. In 2002, we went into the season with a new program, Echoview, developed by SonarData. Discovering no serious flaws, we went forward with the processing of the data. The same program was used in 2003 and later used to go back and reprocess the 2001 data.

The split-beam system outputs both amplitude and positional data for each echo. The most powerful viewing tool from this data is a fish-profile plot. To create this plot, we plotted the river bottom profile in a range versus depth graph then converted the positional information from the fish echoes to the same coordinate system. The average position of each fish was plotted as a separate point. Each point was then ‘pitched’ to match the recorded pitch angle of the transducer that produced it. The averaged, pitched echoes were then plotted on the charts. The position of the nominal beam was overlaid resulting in a plot that showed the fish position in relation to both the transducer beam and the river bottom. This information was used to judge the effectiveness of the multiple aims and the aiming pitch of the transducer. Ideally, we wanted to produce daily fish-profile plots in season. With this tool, we would be able to adjust the aim as needed. For example, if fish targets were concentrated in the upper edge of the beam, the transducer beam could be raised. Daily plots would show which portion of the beam the fish were most concentrated in and whether fish were moving inshore or offshore.

Other diagnostic tools included plots of the average position of individual fish in the horizontal (upriver/downriver) and the vertical (up/down) planes. In the horizontal plane, there should be an equal number of echoes on the upstream side and the downstream side. If the cluster of echoes is tipped, it might mean the transducer is rolled or directed too far upstream or downstream. In the vertical plane, the echoes should be predominately located in the lower quadrant if fish are swimming along the river bottom. Movement up can indicate a change in fish behavior that might necessitate a change in the transducer's pitch. We monitored the average target strength of fish, calculated by first averaging echoes from an individual fish then averaging overall. Changes in this value could indicate a problem with the transducer sensitivity or the receiver card. Target strength values for individual echoes were calculated by first logging the data, and then obtaining an average. Average fish velocity and the number of echoes per fish were needed for the automated fish-tracking program. For each measure, individual echoes were averaged within a fish track then an overall average was obtained by year. The velocity of a fish traveling through the beam was obtained by regressing the horizontal position of each echo within a fish track against time. The velocity of each fish track was then averaged to obtain an overall velocity by year and by transducer. These diagnostic tools allowed us to monitor the sonar system, alerted us to problems that might otherwise go unnoticed, and make needed adjustments in a timely fashion.

Testing the Autotracking Program

Autotracking parameters were optimized by using datasets, from each transducer aim, where fish passage was low enough that individual tracks could be seen on the echogram. Autotracked counts were compared with counts obtained from visually tallying fish traces from an echogram. SonarData's Echoview software was used for both autotracking and displaying fish tracks for visual counts. We originally intended to work with a few sample files to develop the needed parameters, and then track a broad range of files using these parameters. However, because of the large disparity in counts from the autotracking program compared to the visual counts, further tracking was halted and the reasons for the problems were examined.

Testing a sample design

During its many years of operation, the Bendix system has been operated continuously throughout the field season except during brief down periods when calibration, testing, or moving and re-aiming the system is required. With a new system, there are many reasons to subsample. If multiple aims are needed to adequately ensonify the water column where the fish are, or if time constraints prevent inseason data processing, subsampling is required. ADF&G investigated subsampling migrating sockeye salmon at several tower sites and determined that 10 min/h samples were adequate (Seibel 1967; Reynolds et. al 2007). Because sockeye salmon tend to migrate in schools and passage rates are not even throughout the day, we confined our subsampling to sampling for a portion of an hour every hour. The simulations we performed investigated the effects of subsampling on the estimated counts and the variance of these counts on a daily basis. The simulations were based on the 2001 Nushagak sonar data collected from the same BioSonics' DT system used to collect the bathymetry data in the earlier section. A single BioSonics' split-beam transducer was deployed alongside the HTI system off the right bank sampling 1 aim directed along the river bottom. For a simulations iteration, we counted salmon for 5, 10, 15, and 30 minutes out of each hour; expanded each count to an hourly estimate; and summed the hourly estimates for each day. For each subsampling interval length, the daily mean, standard deviation, CV, 0.05 quantile, 0.95 quantile, and the cumulative mean, standard deviation, and quantiles were calculated. For each interval length, 500 iterations were used.

OUTLINING THE CROSS-RIVER SALMON DISTRIBUTION

Methods for predicting the fish migration corridor are found in Hughes (2004). In order to make the predictions, the river velocity and channel topography were measured using an integrated GPS, hydroacoustic bottom profiling, and Acoustic Doppler Profiler sampling package deployed at the sonar site by staff from Utah State University. The objective of the sampling was to obtain an accurate 3-dimensional (3D) representation of the channel topography velocity that would allow for the direct overlay of fish data. The basic mapping data was to be reduced to provide an interpolated computational mesh for use in hydraulic simulations of the water surface elevations and velocity fields for a range of discharges and tidal readings employing either a 2-dimensional (2D) or 3D hydraulic model. Approximately 3–4 discharges were to be simulated representing the range of flows during which fish observation data would be correlated with hydrodynamic properties at the study reach. However, these objectives were not met. Bathymetry and flow data collection was limited and no modeling of the data was performed. Instead, we used cross-river slices of the flow data to obtain a sense of how the flow changed from one side of the river to the other.

We used range information from the HTI and Bendix sonar systems to determine the cross-river distribution for the combined fish species within the range of the sonars. The output from the HTI system includes the range (measured from the transducer) of each echo. All echoes from a tracked fish were averaged to obtain a single range value per fish. Range values from the nearshore and offshore transducers were binned into 1 m bins. To combine the range information from the 2 transducers, we added the distance between the 2 transducers to each offshore fish range value to produce a continuous range plot, starting from the nearshore transducer and ending at the end range of the offshore transducer. When the nearshore transducer was moved offshore, new distance values were recorded and the offshore range data was adjusted accordingly. The Bendix counter's sampling range is divided into 16 sectors. The output is the number of fish/sector. To convert to a range value in meters comparable to the HTI range values, we subtracted the start range from the end range and divided by 16. Data from the Bendix nearshore and offshore transducers were combined using the distance between the 2 transducers as the adjustment value. Settings and sampling methods for the Bendix counter are described in McKinley (2003). Because of the distance between the 2 HTI and Bendix system deployments and the differences between the river bottom profiles, we did not expect the 2 range plots to be identical.

Drift gillnetting catch information was used to apportion the Bendix sonar counts to species. A nearshore and offshore region were marked along each side of the river with floating buoys to correspond to the nearshore and offshore sampling regions of the Bendix transducers. However, as the water level declined and the nearshore transducer was pushed offshore, matching the sonar and drift-gillnet regions became less precise. A suite of gillnets 18.3 m (10 fathoms) in length with mesh sizes of 20.6 cm (8.125 in), 15.2 cm (6.0 in), 13.0 cm (5.125 in), and 11.4 cm (4.5 in) were each drifted for 2.5 min/drift. The 4 drifts spanned approximately 25% of the river width. Two drifts were conducted with each net at each station 3 times daily during the peak of the sockeye run and twice daily during the remainder of the season. More detailed methods describing this sampling technique are found in McKinley (2003). The species, station, fish length, drift time, and drift number were recorded for each captured fish.

COMPARING BENDIX AND SPLIT-BEAM SONAR ESTIMATES OF MIGRATING SALMON

We collected paired Bendix and HTI split-beam sonar data along the right bank of the Nushagak River. No paired data from the left bank was obtained. The nearshore and offshore split-beam transducers were located approximately 40 m upstream from the Bendix transducers. Weirs were positioned downstream of each sonar (Figure 3). The Bendix sonar was operated 24 h/d. The Bendix sonar setup and operation are described in McKinley (2002, 2003) and Brazil (2007). The sonar counts were paired by matching full-hour Bendix counts with the 10-min split-beam sonar counts multiplied by 6. For both systems, the nearshore and offshore counts were summed each hour to obtain a single hourly count.

Fish passage estimates from the 2 sonars were compared using both time series and least squares regression techniques. The time series plots were used visually to compare differences between the 2 sonars by day. We used the regression analysis to test the hypothesis that the slopes between the paired Bendix and split-beam sonar estimates were equal to 1. Because we can not assume that either method is without error, we calculated regression lines using each counting method as the independent variable to determine the extent of the variability from each sonar. Regression techniques were applied to both daily and hourly samples. For the daily samples, the data for the entire day was summed to provide a single data point. For the hourly samples, each hour count was treated as an individual sample.

To assess the diurnal pattern of the migrating fish, we summed the season's data for each hour of the day and divided the sum by the total fish within each year to obtain the percentage of fish passage by hour. The seasonal fish passage per hour data were visually examined by year to look for annual trends and differences between the 2 sonars.

This was not a true blind comparison. The topside components of both sonars were positioned across from each other in the same tent. Although different staff members monitored and obtained counts from each system, there was an exchange of information between them. To reduce potential observer effects, in 2003, the split-beam sonar data was processed 3 days behind the Bendix. In 2001 and 2002, no counts were obtained from the HTI sonar until postseason. However, visually observing the HTI echogram and being aware of the Bendix count could potentially create a bias. For example, if 1 sonar was obviously detecting more fish than the other, the system with lower counts would likely be checked for transducer aim and position, a check that might not have occurred without the additional information. In addition, a crewmember might unconsciously count more or less fish when calibrating the Bendix if he/she feels the count should be lower or higher. Crewmembers visually counting fish traces on the HTI system may count more or less fish if the Bendix count is known. The potential bias from this sharing of information is unknown, but is most likely to occur during the periods of highest fish passage when technicians are less sure of their counts.

RESULTS

The data collection phases for the Bendix replacement began in the summer of 1999 with the initial upriver and downriver profiling. In 2000, bathymetry and flow data were collected, and the new sonar was deployed and tested for the first time. Additional bathymetry data were collected in 2003. During the 2001–2003 field seasons, paired data from the Bendix and HTI split-beam sonar were collected. The 2003 field season was shortened to include only the Chinook and sockeye salmon runs due to budgetary constraints. The final data processing and analyses occurred in the fall of 2004.

SELECTING A DEPLOYMENT SITE

In 1999, we collected a series of river bottom profiles at the existing Nushagak River sonar site and at single channel locations both downriver and upriver (Figure 4). At the sonar site where the Bendix counters are deployed, the cross-river profiles are nonlinear. Off the right bank, there are 2 primary slopes nearshore followed by a flattening toward the river's center (Figure 5). The left bank Bendix transducers are deployed approximately 225 m upstream of the right bank deployment site. Here, a smooth linear slope extends to approximately 40 m then the river bottom flattens. In the center of the river, a wide hump is visible which is the downstream edge of a gravel bar. Sites profiled downriver were predominately U-shaped with a broad flat region in the central portion of the river (Figure 6). Upriver, where the 2 forks meet, the river channel was narrower (~200 m across). Here the profiles were mostly V-shaped, but irregular (Figure 7). What's not apparent from the upriver profiles is the long flat shallow region along the right bank where we were unable to motor the boat. Onshore, the flat terrain extends inland to form a wide flood plain. Because of the tidal influx and the shallowness, the amount of area underwater is highly variable and would require a long weir to keep fish offshore of the transducer during high water. With no promising alternative, we narrowed our search to within the vicinity of the sonar site and profiled it more intensively.

In 2000 and 2003, bathymetry maps were created in the vicinity of the sonar site from acoustic surveys. From these maps we were able to examine the cross-river depth profile at the existing Bendix site and, to extract the most promising cross-river depth profiles for deploying the new sonars. Figure 8 shows the locations of the Bendix, HTI, and BioSonics' systems. Along the right bank, the selected profile contained a smoother slope and fewer slope changes compared to the Bendix site (Figure 9, top). Along the left bank, the selected site drops fairly smoothly from out to about 30 m before the slope flattens (Figure 9, bottom). The Bendix site is shallower and more irregular from shore to 30 m.

TESTING THE SPLIT-BEAM SONAR

Equipment and Deployments

In 2000, we began testing the split-beam sonar. Tests ran from June 22–July 3 to sample sockeye and Chinook salmon and August 1–4 to sample pink and coho salmon. The HTI system was first installed close to the Bendix counter. On June 26, the system was moved 40 m upstream of the Bendix counter. From the drift gillnet catch we learned that initially the sockeye catch was high, but rapidly declined by July 1 when the HTI system was moved to the left bank 90 m downstream of the Bendix counter. The system was removed July 3 and then re-deployed in August on the right bank at the same 40 m upstream location. During each of the remaining 3 sampling years (2001–2003), the split-beam system was deployed for the bulk of the field season 40 m upstream of the right bank Bendix transducers with a downstream weir that extended 3 m beyond the nearshore split-beam transducer.

We struggled with equipment and software problems throughout the whole of this study. During the first 2 years of operation, the network connecting the HTI sonar to the controller computer crashed frequently (especially during the night) resulting in much lost data. Prior to the 2002 field season, HTI worked out the incompatibility problems making the system more stable. The HTI rotators were not robust enough to handle the constant rotation schedule in 2001 and needed repairing following the field season. During cold weather, the wet end rubberized plugs become very rigid and difficult to plug in. Several of the plugs either failed or were close to failing by the end of the study. In 2003, 2 laptop computers failed within minutes of each other. It was later determined the motherboard went out in both of them. The failure was most likely caused by moisture. The area had experienced heavy rainfalls, everything was damp inside the wall tents, and the stoves were not yet in operation. Either a ruggedized computer or a reliable heat source should prevent this problem in the future.

Calibrations and Aiming

Field calibration results from the tungsten carbide and plastic sphere are listed in Tables 1 and 2 for each of the transducers used in this study. In each case, the target strength values were higher than expected. There were no field calibrations performed in 2000 and only the 4 ^{o} by 10^{o} transducer was field calibrated in 2001. For each calibration, echoes were received across each of the transducers' quadrants (Figures 10–12). The echo patterns were not completely random; however, each quadrant contained numerous echoes indicating that all 4 quadrants of the sonar were receiving and processing echoes. In 2002 and 2003, we raised the receiver sensitivity 3 dB for both HTI transducers (6^{o} by 10^{o} transducer from -170.83 to -167.83 dB; 2^{o} by 10^{o} transducer from -171.41 to -168.41) to compensate for the difference between the measured and theoretical values of the calibration sphere. The data reported for this period reflects the 3 dB correction.

Table 1.–Field calibration results for the 38.1 mm tungsten carbide sphere using the 200 kHz split-beam sonar.

Transducer	Year	Target Strength (dB)	Theoretical Target Strength (dB)	# of Echoes
HTI 4^{o}x10^{o}	2001	-37.7 ± 1.3	-39.5	1,464
HTI 6^{o}x10^{o}	2002	-36.8 ± 1.2 [a]	-39.5	6,184
HTI 6^{o}x10^{o}	2003	-36.0 ± 1.5 [a]	-39.5	5,716
HTI 2^{o}x10^{o}	2001	ND	-39.5	ND
HTI 2^{o}x10^{o}	2002	-37.4 ± 2.4 [a]	-39.5	3,445
HTI 2^{o}x10^{o}	2003	-37.8 ± 2.5 [a]	-39.5	2,655

Note: The theoretical target strength for this sphere is -39.5 dB based on the environmental and sonar parameters at the time of the calibrations.

[a] The receive sensitivity was raised 3 dB to correct for the high target strength values.

Table 2.–Target strength calculations for the 10.16 cm plastic sphere using the 200 kHz split-beam sonar.

Transducer	Date	Target Strength (dB)	Range (m)	# of Echoes
HTI 6^o	6-13-02	-29.8 ± 1.0	1.8	1,385
HTI 6^o	6-14-02	-30.0 ± 2.8	7.6	1,523
HTI 6^o	6-15-02	-36.0 ± 5.5	2.2	1,332
HTI 2^o	6-17-02	37.4 ± 4.6	10.1	4,789
HTI 2^o	6-12-03	-33.5 ± 4.1	12.7	1,782

In 2001, the low aim on the nearshore 4^o by 10^o HTI transducer was -8.1^o below level, the high aim -2.4^o (the effective beam size was widened to 6^o during this period). On July 16, the transducer stuck between the 2 aims at a pitch of -6.0^o. On July 25, the transducer was moved farther offshore and the low aim was readjusted to -8.3^o and the high aim to -4.0^o. As the season progressed, the low aim was lowered to -10.1^o and the high to -6.0^o. The offshore transducer was pitched -0.6^o to align the beam with the river bottom for the duration of the field season. The plastic sphere was visible in the center of the beam 20–38 cm above the river bottom at 10.2 m and on the bottom at 18.2 and 25 m from the transducer. In 2002, the 6^o by 10^o nearshore transducer was initially pitched -6.2^o to maximize the detection of the plastic sphere hung within 10 cm of the river bottom. The pitch was lowered to -8.3^o on June 30 after moving the transducer farther offshore then raised July 31 to -7.4^o. The offshore transducer was initially pitched 0.3^o then lowered to -1.0^o and -1.5^o to better view the plastic sphere. In 2003, the nearshore pitch remained close to -6.4^o and the offshore to -1.8^o throughout the field season.

Sonar Parameters

The north bank and right bank split-beam sonar parameters for 2001–2003 are listed in Table 3.

Table 3.–Split-beam sonar parameters for the right bank operations on the Nushagak River, 2001–2003.

	Right Bank Nearshore			Right Bank Offshore		
Parameters	2001	2002	2003	2001	2002	2003
Sound speed	1485 m/s [a]	1447 m/s	1457 m/s	1485 m/s [a]	1447 m/s	1457 m/s
Water temp.	ND	10 ^{o}C	13 ^{o}C	ND	10 ^{o}C	13 ^{o}C
Receiver gain	-12 dB	-6 dB	-6 dB	-12 dB	-6 dB	-6 dB
Pulse repetition rate	5 pings/s	5 pings/s	5 ping/s	5 pings/s	5 pings/s	5 pings/s
Pulse width	0.2 ms	0.2 ms	0.2 ms	0.2 ms	0.2 ms	0.2 ms
Threshold	-45 dB	-53 dB	-45 dB	-45 dB	-53 dB	-45 dB
Transmit	8 dB	8 dB	8 dB	8 dB	8 dB	8 dB
Effective beam width	6^ox10^o	8^ox10^o	8^ox10^o	4^ox10^o	4^ox10^o	2^ox10^o [b] 4^ox10^o
Max off-axis criteria	15 dB	12 dB	12 dB	15 dB	12 dB	6 dB 12 dB
Absorption coefficient	0 dB/km	0 dB/km	0 dB/km	0 dB/km	0 dB/km	0 dB/km

[a] The sound speed was not adjusted; the sonar was set at 1485 m/s, which is slightly higher than the actual sound speed would have been.

[b] Both 10 and 20 min/h samples were collected on the offshore transducer in 2003. The effective beam width & max off-axis criteria used different parameters, respectively.

The transducer sampling range was highly dependent on water level. As the field season progressed the water level dropped, and the nearshore transducer was moved offshore toward the slope change, reducing the ensonifiable range. The range of the offshore aim was also dependent on water level, but for different reasons. In 2001 our sampling range was shortened due to lowered water levels and the resulting interference between the transducer beam and the river's bottom and surface. For the low aim of the nearshore transducer, the maximum sampling range in 2001 was 8 m until August 8 when the end range was reduced to 3.3 m. For the high aim of the nearshore transducer, the end range started out at 12 m and was reduced to 7.5 m on August 8. For the offshore transducer, the end range extended out to 80 m in 2000, but this long range was not achieved again during the study years. The end range was reduced to 27 m for the whole of 2001. In 2002, the end range for the single nearshore aim began at 12 m then was reduced to 5.5 m on June 30 and 3.0 m on August 7. The offshore end range started out at 26 m then decreased to 20 m on June 30. In the shortened field season of 2003, the nearshore transducer end range remained at 8 m and the offshore at 20 m.

Split-beam Sonar Data Processing and Analyses

All the final data processing was performed with SonarData's Echoview software program. All the prior data processed with earlier programs was flawed and unusable. Although the Echoview software quickened the data processing substantially, it was still too time-consuming to process 24 hours of data within a single day. In 2002, we attempted to track and process all the data daily during the field season. This created a large backlog of data by the end of the field season. To trim the data collection to what could be processed daily, we began processing only the first 10 min/h of data from each transducer and aim. Even this level of processing was too time-consuming to be performed daily. To further reduce the processing time, we began manually counting the 10 min/h files visually using a tally counter and recording the counts on a Microsoft Excel spreadsheet. Downstream targets were not subtracted from the count because the information is not available from a visual count. This method was used to count or re-count the data from all 3 years (2001–2003). To obtain the needed diagnostic tools, we processed data by manually tracking the fish tracks electronically and saving the amplitude and positional echo data for each fish in Microsoft Excel files. Two 20-min files per day for each of the 3 aims were processed for the 2001 data; 122 twenty-min samples per aim were tracked. In 2002, 10 min/h files were processed for each transducer; 1,385 ten-min samples for each transducer were tracked. In 2003, 2 full hours daily were recorded; a total of 18 h of data were processed from each transducer for the field season. Identifiable downstream targets were removed. Because of the software difficulties, daily processing of the information was only accomplished in the final data collection year, 2003. For all prior years, needed information was processed at the start of the season but the majority of processing occurred postseason. To produce the diagnostic plots presented here, we combined all or part of the field season's data.

The 2000 field season was primarily a feasibility year and the data collected was limited to relatively short time periods. A fish-profile plot created from the 2000 split-beam sonar data showed that the majority of fish were located within the 2 lower beams of the nearshore transducer with few fish in the top nearshore aim (Figure 13, top). The offshore beam shows the fish dispersed throughout the single aim (Figure 13, bottom).

In 2001, the nearshore transducer was rotated between 2 vertical aims, a low aim and a second aim 1 beam width higher, while the offshore transducer sampled a single aim. A total of 1,447 fish were tracked from echoes received in the high aim of the nearshore transducer, 9,182 fish from the low aim of the nearshore transducer, and 889 fish from the offshore beam. The water level changed dramatically during this season forcing us to continually push the nearshore transducer offshore toward the slope change shortening the ensonified range. Because of the changes in the transducers' aims and positions, it was necessary to create 5 fish-profile plots, 1 for each new aim and position of the transducer (Figures 14 and 15). We produced the plots early in the season to assist us in adjusting the transducer aim and to determine whether the sonar beam adequately covered the portion of the water column used by migrating fish. The fish targets filled the beam from edge to edge in the central portion of the nearshore beam, but at farther ranges, the fish swam closer to the river bottom. From the end of the nearshore transducer to the start of the far field of the offshore transducer, there is a fairly large gap where an unknown number of fish may pass. With the 2 different bottom slopes, there is no way to get around this situation with either a single- or split-beam sonar. In Figure 14 (bottom), the top and bottom beams are overlaid on the profile plot. This occurred when the autorotator got stuck in 1 position halfway between the 2 aims. Unfortunately, because we were not able to plot the diagnostic plots daily, this problem was not detected for about a week, and we were not able to get someone out there to correct the problem and re-aim the transducer for several days. An unknown number of fish may have traveled beneath or over the transducer beam during this time. As the water level dropped, the fish began to move farther offshore and became concentrated across the region where the change in slope occurred (Figure 15).

In 2002, sampling was accomplished with the 6^o by 10^o transducer using a single aim. The fish-profile plots were divided by month for this year, which provided a reasonable break between transducer movements and adjustments in the pitch angle. A total of 84,479 fish were tracked from echoes received by the nearshore transducer and 2,750 fish from the offshore transducer. The fish-profile plots from this year were crowded with fish in the nearshore with targets filling the transducer beam from top to bottom (Figure 16). Again, there is a large gap between the end range of the nearshore transducer and the start range of the offshore transducer. The offshore transducer received more fish echoes in July and August compared to June.

In the shortened 2003 field season, the change in water level was less dramatic, the nearshore and offshore transducers were able to remain in the same position throughout the field season. All the fish echoes from the field season were plotted on a single plot (Figure 17). A total of 4,209 fish were tracked from echoes received in the nearshore transducer and 1,439 fish from the offshore transducer. In the nearshore, the fish were congregated in the central range and again filled the beam from edge to edge. At farther ranges, the number of fish in the upper portion of the beam dropped off. In the offshore transducer, fish targets stretched from edge to edge at close range then were found predominately in the lower half of the beam. Fish targets dropped off abruptly after about 26 m. Also on this plot, we overlaid the potential coverage from a new type of sonar, a dual frequency identification sonar (DIDSON) described in the Discussion section of this report.

Little sampling was done on the left bank. We deployed the HTI system on the left bank and collected data on July 2, 2000. From this dataset, we tracked 835 fish combined from 2 nearshore and 3 offshore aims. For the nearshore transducer, the majority of fish were found in the low aim, except close to the transducer where the beam is very small (Figure 18). For the offshore transducer, fish targets were spread from the river bottom to the uppermost edge of the top beam.

The average horizontal and vertical positions of each fish track were calculated from the split-beam sonar angular data and plotted. If the fish passes directly through the beam, echoes averaged in the horizontal (upstream-downstream) plane should all be located along the beam's centerline. Instead, the echoes were widely spread (Figures 19–21). In the vertical plane, as in the fish-profile plots, the echoes were usually spread from the lower to the upper edge of the nominal beam.

We calculated the average target strength (TS) of fish for the study years 2001–2003 for both the nearshore and offshore transducers (Table 4) then binned the averaged TS values into 1 m range bins and separated them by year and transducer (Figure 22). For both transducers, averaged TS values varied by year from –29.6 to –34.8 dB. In 2001 and 2003, TS values obtained from the nearshore transducer increased as range from the transducer increased. In 2002, TS values first increased with range, decreased, and then increased to a maximum at the end of the range. This same end range area contained contamination from river bottom reverberation. For the offshore transducer, 2001 and 2003 TS values were similar to each other and similar throughout the range sampled. In 2002, the TS was approximately 4 dB lower throughout the range and dropped off sharply at the end of the range.

For the study years 2001–2003, the average fish velocity by year ranged from 0.25 to 0.40 m/s (Table 4). Velocity was also averaged within 1 m range bins by year and transducer. The velocity was fairly consistent for both nearshore and offshore traveling fish except in 2003 where the velocity shot up to 1 m/s in the outer range of the offshore transducer (Figure 23).

The average number of echoes per fish was determined for the study years 2001–2003 for each transducer (Table 4) and averaged into 1 m range bins by year and transducer (Figure 24). The average number of echoes for fish from each transducer was highly variable. Some of the variation stems from the change in end range between the study years. As expected, the number of echoes for fish at close range to the transducer was low and the number increased with range. During 2002 and 2003, the number of echoes per fish from nearshore fish remained fairly consistent across the range sampled. In 2001, the number of echoes per fish remained consistent from 1–6 m then increased after 7 m. For the offshore, the 3 years were similar in the close range then diverged widely as the fish ranged farther from the transducer. We received the most echoes per fish in 2001 from both transducers.

Table 4.–Average target strength, velocity, and numbers of echoes per fish from tracked fish obtained from the HTI sonar along the right bank of the Nushagak River.

Year	Strata	Target Strength (dB)	Velocity (m/s)	Echoes/Fish (#)	Daily Sampling Strategy for Tracked Fish
2001	Nearshore	–31.2 ± 2.2	0.30 ± 0.15	31.0 ± 8.9	2 - 20 min samples per aim
2002	Nearshore	–34.1 ± 3.9	0.25 ± 0.24	14.8 ± 8.7	10 min/h samples
2003	Nearshore	–29.6 ± 3.2	0.29 ± 0.19	15.6 ± 5.9	1 h sample
2001	Offshore	–30.2 ± 3.0	0.33 ± 0.40	47.4 ± 37.4	2 – 20 min samples
2002	Offshore	–34.8 ± 3.3	0.29 ± 0.44	20.7 ± 15.9	10 min/h samples
2003	Offshore	–31.9 ± 2.1	0.40 ± 0.25	28.7 ± 17.1	2 – 30 min samples

Testing the Autotracking Program

Autotracking the HTI split-beam sonar data yielded poor results. After numerous tries with sample datasets, we stopped autotracking the data. Examining the echograms we found 3 primary reasons why the autotracker failed: 1) interference between fish echoes and non-fish echoes reflected off the river bottom or surface; 2) poor positional data due to multi-path echoes and from fish near the beam edges; and 3) too few fish echoes resulting from the restrictive split-beam signal processing. For the low aim of the nearshore transducer, when the water level was high, the majority of fish traveled midrange between the transducer and the change in slope, where the transducer beam first strikes the river bottom (Figure 25). At the range where river bottom echoes dominate, fish targets were difficult to discern. As water level dropped both the transducer and preferred fish travel zones were pushed closer to the slope change and fish echoes became interspersed with echoes from bottom reflections (Figure 26). The high nearshore aim was less problematic with no interference from the river bottom (Figure 27).

The poor positional information from non-fish echoes and from multi-path echoes caused the autotracker to create numerous false fish tracks. Here, we defined multi-path echoes as sound energy that passed through the fish, reflected off surface or bottom structure, and returned to the transducer. The degree of multi-pathing depended on the depth of the water and the composition of the river bottom. The multi-path echoes either formed traces similar to fish or resulted in a fountain of echoes ranging from beyond the fish to the end of the sampling range (Figure 28). Fewer multi-pathed echoes were visible on the offshore echograms, but the echograms often contained traces from what we believed to be plants floating downriver (Figure 29). A type of aquatic plant containing numerous small air sacs was frequently pulled from our anchors. Positional information from the plants (which float higher in the water column than fish) was far less noisy than from the tracked fish (Figure 30).

The problem of too few echoes became apparent from examining BioSonics' echograms created from raw amplitude data. (all HTI echograms were created from echoes that passed user-defined split-beam criteria.) Fish traces were broken up and many lost entirely after processing, even when the split-beam criteria was fairly unrestrictive. Figure 31 compares BioSonics' echograms created from the raw data (center panel), with the same file processed using single-beam criteria (left) and split-beam criteria (right). In the center panel, the pulse shapes make it relatively easy to visually distinguish fish from noise. Once the data was processed into echoes, the visual display became more difficult to interpret. Using single-beam processing criteria with few or no restrictions on the dataset creates an echogram dominated by noise echoes, but targets are distinguishable. With the more restrictive split-beam processing, we lost a large number of echoes. In the example shown, processing the file using single-beam criteria resulted in 40,489 echoes, while the restricted split-beam processing resulted in 18,045. The lost echoes were from both fish and noise targets. Figure 32 shows the same file with fish tracked in the single-beam and split-beam panels. A total of 2,580 fish targets were visually counted from the unprocessed dataset, 2,464 from the single-beam data, and 1,217 from the split-beam data.

Testing a Sample Design

We sampled a single aim continuously from June 15 to July 2 using the BioSonics' split-beam system. Our simulations showed that little information would be lost if the split-beam sonar data is subsampled. The 5-, 10-, 15-, and 30-min sample intervals provided unbiased estimates of daily counts (Figure 33, top). The standard deviation, CV, and quantile data (Figures 33–34) suggest that the longer intervals have less uncertainty than the shorter intervals; however, the difference between the different length intervals is not dramatic. All of the sampling intervals also produced reasonable estimates of the cumulative abundance (Table 5). Again, the larger the sampling interval, the smaller the variance, but even the difference between the 5 and 30 minute intervals is relatively small. Also, one gets the largest decrease in standard deviation per increase in sampling time from the change from 5-min to 10-min sampling intervals (Figure 35).

Table 5.–Cumulative counts as estimated from the simulations for hourly sampling intervals of different lengths.

Sampling	Mean	Standard Deviation	0.05 Quantile	0.95 Quantile
True Abundance	231,160			
5 min Interval	230,970	6,164	220,632	241,577
10 min Interval	231,982	5,413	222,947	240,589
15 min Interval	231,330	4,921	223,344	238,996
30 min Interval	231,017	3,795	224,798	237,446

Note: The mean, standard deviation, and quantiles were calculated from 500 simulation iterations.

One thing that was noticeable from the simulations is that the salmon do not pass at a continuous rate, but come in clusters (i.e. schools). The clustering is what causes much of the variation in the subsampling and affects even the 30-min intervals. Estimates of hourly counts will be affected by the schools observed and missed. However, the estimates of daily counts from the subsampling intervals track the counts based on sampling the entire hour.

OUTLINING THE CROSS-RIVER SALMON DISTRIBUTION

The ability of the wave drag model to predict the migratory routes used by sockeye and Chinook salmon in the Nushagak River (Hughes 2004) is illustrated in Figures 36 and 37. The model correctly predicted that sockeye salmon would prefer the most nearshore sections along both banks and Chinook salmon would prefer the second section from the bank on the left and the third section from the bank on the right. Hughes (2004) shows that the probability of getting predictions as accurate as this by chance is 0.05 for each species considered separately and 0.0025 for both species together.

River velocity and channel topography were measured June 13–15, 2000. A cross-river slice of the river during 1 instant in time shows the flow to be heavier (darker regions) in the offshore regions roughly 40–70 m and 150–200 m from the left bank of the river (Figure 38). The tidal flux is not strong enough to create a back surge; water continues to flow downriver during all tidal stages. Measured flow rates varied from 0–1.9 m/s, with a mean of 0.6 m/s. Fish distributions obtained from data collected in 2000 show that the majority of fish are concentrated along the bottom and in the shallower regions where the flow velocity is reduced (Figures 39).

We used range data from the HTI and Bendix sonars to plot the cross-river salmon distributions within the range of the sonars (note: these distributions were NOT species specific). The cross-river salmon distributions from both sonars along the right bank were similar to each other and across study years (Figures 40–42). The peak regions were slightly wider in each Bendix distribution. The percentage of fish detected by the nearshore transducer from the HTI and Bendix sonars was very similar. In 2001, using the HTI visual count data (10 min/h counts expanded to a full hour estimate) and the full hour Bendix counts, the nearshore estimate included 93% and 94%

of the total fish counted from the HTI and Bendix sonars, respectively. In 2002, the nearshore estimates were 97% (HTI) and 95% (Bendix) of the total. In 2003, the nearshore estimates were 95% (HTI) and 93% (Bendix) of the total. From the more limited tracked fish dataset, the percentage of fish counted from the nearshore transducer was 92% in 2001, 97% in 2002, and 75% in 2003. By lumping the nearshore and offshore fish together from the tracked fish dataset, 95% of fish traveled within 23 m of the transducer and 99% within 36 m in 2001, within 10 m and 29 m in 2002, and 16 m and 22 m in 2003. The preferred range for fish travel was 4–5 m from the nearshore transducer during all 3 years (Figures 40–42). On the left bank, the data was sparser due to the limited sampling time. In 2000, the preferred fish migration range was 2–4 m from the HTI nearshore transducer and 95% of fish traveled within 58 m (Figure 43).

Because the drift gillnetting catch was divided into nearshore and offshore drifts, we were able to obtain a crude measure of the cross-river distribution from this dataset. Datasets from 2002 and 2003 were examined. The catch numbers were comparable to a catch per unit effort (CPUE) because all the drift times were the same (2.5 min). Fewer total fish were captured in the left bank offshore strata in 2002, while in 2003 the number of fish captured in each strata was roughly equivalent. Breaking down the catch by species shows sockeye salmon were captured predominately in the nearshore (aka inshore) strata while Chinook salmon were more dominate in the offshore catch (Figure 44). Chum salmon, which are similar in size to sockeye salmon, were captured more frequently in the nearshore strata on the left bank, but on the right bank the catch from the 2 strata was very similar for both years. In 2002, pink salmon were predominate in the nearshore strata, but they also had a strong presence in the right bank offshore region, while coho salmon were captured in larger numbers in the offshore strata off both sides of the river (Figure 45). A total of 4,279 salmon were captured in 2002. Of this total, 27% were Chinook, 22% sockeye, 40% chum, 7% pinks, and 4% coho salmon. A total of 2,681 fish were captured in 2003, which was divided into 40% Chinook, 33% sockeye, and 27% chum salmon. Because of the shortened field season in 2003, no pink or coho salmon were captured. During the peak passage week, the combined catch was highest from the left bank nearshore stratum in 2002 and nearly equal between right and left bank nearshore strata in 2003 (Figure 46). The left bank offshore had the lowest catch during the peak week in 2002, but was substantially higher in 2003. Chinook and sockeye salmon catch compared daily (Figure 47) show that the catch is highly concentrated within a narrow time period. In 2002, the peak lasted longer compared to 2003. An early peak of Chinook salmon occurred in 2002; the majority of Chinook salmon were observed in the nearshore strata. Aside from this small peak, the bulk of the Chinook salmon run appears to coincide with the sockeye salmon run. This early Chinook salmon peak was not observed in 2003.

COMPARING BENDIX AND SPLIT-BEAM SONAR ESTIMATES OF MIGRATING SALMON

We collected paired Bendix and HTI split-beam sonar data along the right bank of the Nushagak River across 3 field seasons (2001–2003). No paired data from the left bank was obtained. In 2001, paired data from the HTI and Bendix sonars were collected from June 20 to August 16. Numerous network crashes causing the connection between the HTI sonar and the controlling computer to be lost, resulted in 116 hours of lost data in blocks ranging from 1 to 16 hours. Following the field season, it was learned that the Lantastic network used by the HTI system was not fully compatible with the computer's Windows 2000 operating system, even though the combined system was tested pre season by the vendor. The vendor resolved the problem prior to the next field season. In 2002, paired data was collected from June 18 to August 17. We planned an earlier start date but problems with the automatic sequencing of the HTI system caused delays in setting up the second transducer. We tested fast multiplexing between the 2 transducers, but this required reducing the ping rate of the nearshore transducer below acceptable levels. Instead, we returned to a slow multiplex sequencing. In 2003, paired data was collected from June 25 to July 2 and July 7 to 19. Two laptops failed causing a late start date and additional lost data from July 3 to 6. The early stop date resulted from budgetary decisions designed to reduce the project cost by not assessing the late run of coho salmon. Both the Bendix and split-beam sonars were pulled at this time.

Daily Bendix and HTI Estimates Compared

Daily estimates of migrating fish from the HTI and Bendix sonars were compared from 2001–2003. Because we were interested in comparative data and not daily passage, we removed rather than interpolated, the blocks of missing data that extended beyond 2 hours. Consequently, daily totals reported here do not always represent a complete day's estimate of salmon passage and will not match the numbers reported in the annual Nushagak River sonar reports (McKinley 2002, 2003) and (Brazil 2007). In each case, the data was missing from the HTI system, not the Bendix. Single or double hours of missed data from the HTI system were interpolated by averaging the prior and subsequent hours and dividing by 2. The data were summed across all sampled hours and from nearshore and offshore transducers to obtain a single daily estimate from each sonar. A total of 58 daily samples from each sonar were compared in 2001, 60 daily samples in 2002, and 21 daily samples in 2003.

Fish passage estimates for the days sampled were most similar between the HTI expanded estimates and Bendix estimates in 2002 (Figure 48). From this year, the expanded HTI estimate of 526,781 and a Bendix total count of 527,944 differed by only 1,163 fish (0.2%). In 2001 and 2003, the overall difference between the 2 estimates was considerably greater. In both cases, the HTI system estimated the run strength at roughly half the strength estimated by the Bendix counter. In 2001, the expanded HTI estimates totaled 417,751 while the Bendix estimate reached 795,762, a difference of 378,011 fish (47.5%). In 2003, the expanded HTI estimates totaled 165,020 while the Bendix estimate reached 320,405, a difference of 153,385 fish (47.9%). The HTI estimates were considerably lower during the 3 major peak periods in 2001 and 2003 and more similar during the low fish passage days (Figure 48).

The offshore counts were lowest during the start of the season when the water level was highest. During this period, the slope change was located farthest offshore. As the water level dropped and the nearshore transducers were pushed farther offshore, more fish were detected with the offshore transducers. In 2001, the HTI offshore counts began to rise on July 13 and reached a maximum of 60% of the total count (Figure 48). For the Bendix system, the offshore counts stayed fairly low until July 23 then rose to a maximum of 43%. In 2002, the HTI offshore counts first increased around July 18 then declined. A second increase began on July 26 and rose to a maximum of 75%. This increase in offshore targets occurred when the nearshore transducer was moved farther offshore as water level dropped. The range was shortened to 3 m on the nearshore transducer. During the entire 2002 field season, the Bendix offshore counts remained fairly low, peaking at about 19% of the total. Because of the longer reach of the nearshore slope where the Bendix transducer was located, the range was not shortened to the same degree the HTI was. In 2003, both sonars were pulled before a large change in water level occurred. During this year the HTI offshore counts peaked at 16% and the Bendix at 12%.

Regression results from the comparison of daily estimates between the 2 sonars showed a strong relationship each sample year as evidenced by the high r^2 (Table 6). The 95% confidence intervals around the slope values do not include 1 during any of the comparison years. In 2002, the variation in the data was lowest with the HTI as the independent variable but highest when the Bendix was the independent variable. This is the same year the final estimates were the most similar, and the slope was closest to 1. We plotted scatter plots with the data from the HTI sonar on the x-axis and the Bendix on the y-axis adding a regression line using the HTI data as the independent variable. A second regression line was added to the same plot using the Bendix data as the independent variable by solving the regression equation for the x-variable. The plotted regression lines show that the difference between the 2 slopes is minimal compared to the difference between each regression slope and a slope of 1 (Figure 49).

Table 6.–Regression results for the HTI and Bendix sonar comparison of daily counts.

Year	Regression Equation	S.E. (slope)	r^2	95% Confidence (slope)
HTI as Independent Variable				
2001	y = 1.82x + 577	0.08	0.91	1.67-1.98
2002	y = 0.72x + 2512	0.04	0.87	0.64-0.79
2003	y = 2.27x – 2559	0.18	0.90	1.90-2.64
Bendix as Independent Variable				
2001	y = 0.50x + 372	0.02	0.91	0.46-0.54
2002	y = 1.21x – 1874	0.06	0.87	1.09-1.34
2003	y = 0.40x+1828	0.03	0.90	0.33-0.46

Hourly Bendix and HTI Estimates Compared

We collected 1,274 h of paired HTI and Bendix data in 2001, 1,385 h in 2002, and 454 h in 2003. In this section, we treated the hourly data as individual samples and recalculated the regressions. The r^2 values from the hourly samples were all lower compared to the daily samples (Table 7). Like the daily samples, the 95% confidence intervals from the hourly samples do not include a slope of 1. The slope values obtained when the HTI was used as the independent variable were lower each year for the hourly samples compared to the daily samples. Using the Bendix estimates as the independent variable, the slope values from the daily and hourly samples were the same for 2 of the years. Compared to the daily estimate, there was considerably more spread in the data points from the hourly estimates and regression lines from the 2 predictors were more disparate from each other during each of the sample years (Figure 50).

Table 7.–Regression results for the HTI and Bendix sonar comparison of hourly counts.

Year	Regression Equation	S.E. (slope)	r^2	95% Confidence (slope)
HTI as Independent Variable				
2001	y = 1.52x + 127	0.02	0.75	1.47-1.57
2002	y = 0.68x + 121	0.01	0.73	0.66-0.71
2003	y = 1.80x + 53	0.05	0.71	1.69-1.90
Bendix as Independent Variable				
2001	y = 0.50x +19	0.01	0.75	0.48-0.51
2002	y = 1.06x –25	0.02	0.73	1.03-1.10
2003	y = 0.40x+83	0.01	0.71	0.37-0.42

Because the daily inseason estimate has the most value to fishery managers, we calculated a slope value from the 2 sonars using the hourly data for each day sampled to obtain a daily slope value. Daily slope values ranged between –0.8 and +4.7 with the 2 highest values occurring during low passage periods (Figure 51). In general, the slope values fluctuated between approximately 0.5 and 1.5.

The percentage of fish tracked for each hour was surprisingly similar between the 2 sonars (Figure 52). There was no obvious diurnal pattern when all 3 years were examined. The lowest fish passage occurred at 0400 hours in 2001 and 2002, shifting to 1000 hours during 2003. The highest points were more variable between years. The highest fish passage occurred from approximately 1700–0200 hours in 2001 with a series of high peaks. In 2002 and 2003, the high peaks were sharper at approximately 0800 and 1700 hours, respectively.

DISCUSSION

SELECTING A DEPLOYMENT SITE

Profiling the river bottom downriver and upriver from the existing site did not yield a better site for sonar assessment. Further downriver, we found only 1 site, where the river remained in a single channel. The profile was U-shaped, which would make it difficult to detect bottom-oriented fish. We investigated a V-shaped river channel upriver from the sonar site, but the irregularities in the profiles, the proximity to the channel fork near Portage Creek, and the long shallow region along the right bank provided obstacles for sonar assessment. The most promising sites were near the existing sonar site. Along the right bank, most profiles contained multiple slope changes, which would require several transducers to adequately ensonify our desired range. We selected a site with a relatively smooth profile containing only a single slope change within our desired range. Along the left bank, we selected a site with an ensonification range similar to the Bendix counter (30 m), but with a smoother slope. Ensonifying the middle of the river would be difficult because of the nonlinear bottom and the necessity of deploying multiple transducers in the fast current.

TESTING THE SPLIT-BEAM SONAR AND OPTIMIZING PARAMETERS

Averaged target strength values from field calibrations of the HTI transducers using the calibration sphere were higher than theoretical values for each study year. Laboratory calibrations were only performed following the purchase of each new transducer. It would be useful to recalibrate the systems in the lab to determine whether the amplified target strength values would occur under more controlled conditions. Although the echo patterns from the calibration sphere were not completely random, each quadrant contained numerous echoes. Therefore, there was no reason to suspect a problem with the transducers.

Aiming the transducers using the aiming protocol we devised (Appendix B1) gave us confidence in the positioning of the transducer beam. The protocol, which utilized both profile and sensor information, provided a means for technicians to re-aim the transducer successfully after a change in water level or disturbance to the transducer. Without this information, it would be difficult if not impossible to determine how well the beam is directed along the river's bottom. Using the echogram helps, but there are many situations where the echogram alone does not provide enough information to achieve an accurate aim.

The fish-profile plots (Figures 13–18) were the most useful tools for determining how well the split-beam system was working. However, daily plots are needed if we are to make adjustments in season as conditions change. Without this information, it is easy to miss problems that arise. The fish-profile plots clearly show that the 2-transducer, split-beam system is inadequate for counting fish on the right bank of the Nushagak River. Because of the poor positional data from the sonar on fish targets, it was impossible to determine how much overlap might occur when sampling multiple vertical aims at different time intervals. Fish-profile plots from the 6^{o} by 10^{o} HTI transducer data show fish targets from one edge of the beam to the other, indicating the beam width was not adequate. Another problem is the gap between the end range of the nearshore transducer and the effective start range of the offshore transducer. The end range from the nearshore transducer ends abruptly where the beam encounters the river bottom. To squeeze the offshore beam into the narrow water column of the secondary slope, a very small 2^{o} beam was used with a long, 7 m, near field. At ranges close to the offshore transducer, fish filled the beam from edge to edge, again indicating fish are traveling over the beam. The wider nearshore transducer is the most effective for sampling fish. But as the water level drops and this transducer is pushed farther offshore, it approaches the slope change making the nearshore aim ineffective. A wider beam is not the answer since the depth of the river is constantly changing. A better solution needs to be found for sampling this shore.

The autotracking program was not usable with the noisy split-beam data from the Nushagak River site. If the split-beam is used for sampling, the data will have to be visually counted using a sonar system that constructs the echogram from the raw data and not the processed echo data. Subsampling the data will be a necessity.

The simulations used to test potential subsampling intervals showed that estimating salmon passage from a portion of each hour should provide a reasonable approximation of hourly and daily passage. From these tests, we could have selected a 5 min/h sampling regime. We chose the 10 min/h interval because a 5-min interval is so short one is less likely to notice odd readings due to equipment problems. This 10 min/h sample also agrees with the sampling done at tower sites in Bristol Bay (Seibel 1967; West and Fair 2006). The variance, standard deviation, CV, and quantiles only quantify the uncertainty due to sampling portions of the hour. The uncertainty due to varying fish passage rates, sonar aiming, fish behavior, etc. will increase the actual variance of counts and should be considered when designing sampling plans.

OUTLINING THE CROSS-RIVER SALMON DISTRIBUTION

The partial cross-river fish distributions from the sonar and drift gillnetting were not in agreement. According to sonar estimates, the majority of fish passed through the nearshore region, while the drift gillnetting capture rates showed the nearshore and offshore regions to be roughly similar. Most disturbing was the overall number of captured Chinook salmon exceeded sockeye salmon, and in 2002, was as high as 50% of the sockeye catch within the nearshore strata. Apportioning the minimal offshore sonar counts to the offshore Chinook-dominated catch, made the Chinook salmon estimate appear reasonable. Miller (2000) observed from other indices that sockeye salmon greatly outnumbered Chinook salmon in the Nushagak River, and concluded that Chinook salmon were more vulnerable to gillnetting. The placement of gillnets may also amplify the estimate of 1 species over another. Drifting a gillnet further offshore during a nearshore drift, would increase the Chinook salmon catch. Chum salmon were captured in numbers similar to sockeye salmon in the nearshore strata, but were also captured in significant numbers in the offshore strata, particularly along the shallower right bank. This resulted in similar sockeye and chum estimates, which may not represent the true species mixture. In Miller's study (2000), 50% of chum salmon were captured beyond the sonar range, which would make total chum salmon count much higher than sockeye salmon. Changes in the cross-river fish distribution pattern may occur on a yearly basis. Conditions that could lead to changes include changing water levels and current flow, fish density, and gillnet placement. More information is needed to assess the accuracy of the species apportionment program.

Although the wave drag model (Hughes 2004) explains why Chinook salmon swim farther offshore than sockeye salmon, it does not explain why chum salmon, which are closer in size to sockeye salmon, are found equally in the nearshore and offshore strata along the right bank. The mean length for Chinook salmon in 2001 was 738 mm, sockeye salmon 582 mm, chum salmon 593, and coho salmon 575 mm (McKinley 2002). For 2002, the mean lengths for Chinook salmon were 693 mm, sockeye salmon 543 mm, chum salmon 589 mm, and coho salmon 565 mm (McKinley 2003). If size, depth, and flow were the only factors in outlining the corridor for each species, we would expect chum salmon to occupy a narrow corridor, similar to the sockeye salmon. Coho salmon are captured in large numbers in the offshore strata along both banks, yet they were smaller in length than sockeye in 2001 and only slightly larger in 2002. There were no reported lengths for the pink salmon in the annual Nushagak River reports, but traditionally they are smaller than the sockeye, yet a high percentage of them migrate in the offshore strata. The species-specific cross-river distribution may be more a factor of fish behavior than fish length. The small peak of Chinook salmon observed in 2002 also contradicts this theory. At this time, the Chinook salmon were almost wholly captured during the nearshore drift. The second and larger Chinook salmon peak occurred at the same time as the sockeye salmon run. Another possible explanation for the lateral segregation of Chinook salmon at the Nushagak River might be that the large numbers of sockeye salmon crowd the nearshore region and push the Chinook salmon further offshore. But this hypothesis does not explain why coho salmon, whose timing follows the sockeye run, migrate in the offshore region. The early Chinook salmon peak was not observed in 2003. Timing of the ice break up, river temperatures and level may all contribute to run timing of salmon. There may be a small early run of Chinook salmon that is only captured on years when environmental conditions retard their run timing.

Flow was measured in the vicinity of the sonar site, but we were unable to obtain a flow model. To be beneficial, the flow data needs to be collected at a variety of discharge and tidal stages. We still have a very poor understanding of how fish behavior changes as environmental conditions change. The fish-profile plots created with the season's data are informative, but a daily picture coupled with environmental data would provide a much better view of how the salmon are responding to the environmental changes. This subject needs further exploring. The Nushagak River is difficult to ensonify because of its width and uneven bottom profiles. If we better understood fish behavior under a wider range of circumstances, the sampling effort could be focused where it is most needed.

COMPARING BENDIX AND SPLIT-BEAM SONAR ESTIMATES OF MIGRATING SALMON

Because the HTI system appears to be inadequate for detecting fish, and the Bendix counter does not provide enough information to make such an assessment, neither can be viewed as the true number of migrating fish. Although the HTI system is a more modern system, the 2 sonars are still subject to many of the same problems, i.e., narrow beams that fish can swim over or under if the bottom substrate is uneven, multi-pathing of echoes from fish, large gaps in detection between the nearshore and offshore transducers, and interference of fish echoes with surface and bottom echoes. Features of the Bendix counter that can reduce fish detection include a narrower nearshore beam and less power (~1 Watt compared to 25 Watts). Because of the Bendix counter's inability to provide data that allows a user to distinguish fish and non-fish echoes of similar amplitude, the counter also has the potential to over count fish. The combination of an undercount bias from poorer detection and over count bias from counting noise echoes adds uncertainty to the Bendix count.

Management goals are based primarily on the Bendix counts. In each of the study years, the Bendix system counted more fish than the HTI with the peak passage days showing the greatest differences. In 2001 and 2003, the HTI system would have counted almost 50% fewer fish both years. In 2002, the 2 estimates were very close. Whether the Bendix over counted during 2001 and 2003 or whether the HTI experienced greater detection problems is unknown. It is unusual that in 2002, when the 2 estimates were most similar, the standard deviation was highest when the Bendix counts were used as the independent variable. The daily slope values displayed in Figure 51 are highly variable which brings into question how estimates from the HTI system might affect daily decisions made by commercial fishery managers.

SUMMARY

Understanding the interplay between fish behavior and current flow may have provided answers as to why the 2 sonars were so different in 2 years but similar in the 1. Unfortunately, water level was not recorded during the study period. With the tidal changes, recording a daily meaningful water level is difficult. A large decline in water level during the latter part of the field seasons can shrink the nearshore sampling range down to 3–4 m. A reduction in the range of the offshore transducer is less significant because of fewer fish observed at the outer ranges, but the greater number of fish traveling past the near field of the offshore transducer in the narrowest portion of the beam is a concern. The narrow beam (2^o) of the HTI and Bendix offshore transducers are necessary to fit the water column. The nearshore effects coupled with the extremely small beam (less than 0.2 m at 5 m) greatly reduce detection. In addition, the transducer has to be located on the secondary slope so there is a lag between the end of the nearshore sampling range and the position of the offshore transducer. It is unknown how many fish are missed between the 2 transducers. Range plots show that fish passage drops dramatically with range, but this may be due to poor detection.

The difficult environment of the Nushagak River is not easily ensonified with traditional sonars, whether the system is a modern split-beam system or an older single-beam system. They share many of the same problems. Because of these difficulties, ADF&G began researching a different type of sonar at this site, a dual-frequency identification sonar (DIDSON) (Belcher et al. 2001; Belcher et al. 2002). This multiple beam sonar gets around many of the problems of the more traditional sonars. The DIDSON produces a video-like image from the echoes. The moving fish targets are easy to discern from static noise so fish are detectable even if the beam interferes with the river bottom. Therefore, a larger transducer beam can be used. The yellow beam overlaid on the fish-profile plot in Figure 17 shows the potential coverage of this larger 14^{o} vertical beam. Because of the wide horizontal beam, direction of travel is easy to distinguish, making it possible to separate downstream-moving objects from upstream-migrating fish, even fish close to the transducer. We expected to experience numerous hardware and software problems with a new system, but were surprised to find we were able to operate the DIDSON with few problems and with an ease of operation unsurpassed by even the Bendix sonar. We are moving forward with research on this new system.

The apportionment program has been largely ignored due to the large amount of time invested in the sonar replacement. In the future, this program will have to be carefully examined. For the nearshore strata, comparisons between drift gillnetting and beach seining may be illuminating. The offshore strata are more difficult to assess. Alternative methods will have to be explored. A potential method for studying the interplay between fish behavior and netting is to deploy a DIDSON close to the shore and observe fish behavior as a gillnet is drifted by. A DIDSON could also be placed at the lower and upper range of a beach seine and used to observe fish behavior as the seining process occurs.

ACKNOWLEDGEMENTS

Konrad Mittlestad, ADF&G Fishery Biologist, spent long hours tracking and editing the sonar data and providing logistical support. Nick Hughes, University of Alaska Fairbanks, applied the wave drag model to the drift gillnetting results from the Nushagak River. Tim Mulligan, retired Department of Fisheries and Oceans Scientist, assisted in the design of the study and in setting up the split-beam system. The Nushagak River sonar crew provided logistical support for the project. Dave Daum, U.S. Fish and Wildlife Service Fishery Biologist, loaned us the 6^{o} by 10^{o} HTI split-beam transducer. Peter Dahl of the Applied Physics Lab calculated the theoretical target strength of the 38.1 mm tungsten carbide sphere. Tom Harding, University of Utah, supplied the flow data for this report. Anna-Maria Mueller assisted in the data analysis. Chuck Brazil, ADF&G Bristol Bay Biologist, provided the drift gillnetting plots. Lowell Fair, ADF&G Regional Research Biologist, reviewed the manuscript.

REFERENCES CITED

Barton, L. H. 2000. Sonar estimation of fall chum salmon abundance in the Sheenjek River. Alaska Department of Fish and Game, Division of Commercial Fisheries, Regional Information Report 2A00-27, Anchorage.

Belcher, E. O., B. Matsuyama, and G. R. Trimble. 2001. Object identification with acoustic lenses. Proceedings of MTS/IEEE Oceans 2001, Honolulu, Hawaii. 1:6-11.

Belcher, E. O., W. Hanot, and J. Burch. 2002. Dual-Frequency identification sonar. Pages 187-192 in Proceedings of the 2002 International Symposium on underwater technology, Tokyo, Japan, April 16-19.

Blackman, S. S. 1986. Multiple-target tracking with radar applications. Artech House, Inc., Dedham, Massachusetts.

Brazil, C. E. 2007. Sonar enumeration of Pacific salmon escapement into the Nushagak River, 2003. Alaska Department of Fish and Game, Fishery Data Series No. 07-37, Anchorage. http://www.sf.adfg.state.ak.us/FedAidPDFs/fds07-37.pdf

Brett, J. R. 1995. Energetics. Pages 3-68 in C. Groot, L. Margolis, and W.C. Clarke, editors. Physiological Ecology of Pacific salmon. University of British Columbia Press, Vancouver, B.C.

Chapell, R. S. 2001. Anvik River Chum Salmon Escapement Studies, 1997-1999. Alaska Department of Fish and Game, Division of Commercial Fisheries, Regional Information Report 3A01-12, Anchorage.

Dunbar, R. 2001. Copper River hydroacoustic salmon enumeration studies, 2000 and 2001. Alaska Department of Fish and Game, Division of Commercial Fisheries, Regional Information Report 2A01-3, Anchorage.

Enzenhofer, H. J., N. Olsen, and T. J. Mulligan. 1998. Fixed-location hydroacoustics as a method of enumerating migrating adult Pacific salmon: comparison of split-beam acoustics vs. visual counting. Aquatic Living Resource. 11(2):61-74.

Faran, Jr. J. J. 1951. Sound Scattering by Solid Cylinders and Spheres. J. Acoust. Soc. Am., 23, pp. 405-418.

Gaudet, D. M. 1990. Enumeration of migrating salmon populations using fixed-location sonar counters. Rapp. P. -v. Reun. Cons. Int. Explor. Mer. 189:197-209.

Hinch, S. G., and P. S. Rand. 2000. Optimal swimming speeds and forward-assisted propulsion: energy-conserving behaviors of upriver-migrating adult salmon. Canadian Journal of Fisheries and Aquatic Sciences. 57:2470-2478.

Hughes, N. F. 2004. The wave-drag hypothesis: an explanation for size-based lateral segregation during the upstream migration of salmonids. Canadian Journal of Fisheries and Aquatic Sciences. 61:103-109.

MacLennan, D. N., and E. J. Simmonds. 1992. Fisheries acoustics. Chapman & Hall, London, UK.

McBride, D. N. 1981. Nushagak River sonar enumeration studies, 1979. *Appendix A* in Nushagak sonar enumeration project, 1980. Alaska Department of Fish and Game, Division of Commercial Fisheries, Bristol Bay Data Report No. 83, Anchorage.

McKinley, W. L. 2002. Sonar enumeration of Pacific salmon into the Nushagak River, 2001. Alaska Department of Fish and Game, Division of Commercial Fisheries, Regional Information Report 2A02-25, Anchorage.

McKinley, W. L. 2003. Sonar enumeration of Pacific salmon into the Nushagak River, 2002. Alaska Department of Fish and Game, Division of Commercial Fisheries, Regional Information Report 2A03-05, Anchorage.

Miller, J. D. 2000. Sonar enumeration of Pacific salmon escapement into Nushagak River, 1999. Alaska Department of Fish and Game, Division of Commercial Fisheries, Regional Information Report 2A00-19, Anchorage.

Miller, J. D., and D. Burwen. 2002. Estimates of Chinook salmon abundance in the Kenai River using split-beam sonar, 2000. Alaska Department of Fish and Game, Fishery Data Series No. 02-09, Anchorage. http://www.sf.adfg.state.ak.us/FedAidPDFs/fds02-09.pdf

REFERENCES CITED (Continued)

Osborne, B. M. and J. M. Melegari. 2002. Use of split-beam sonar to enumerate Chandalar River fall chum salmon, 2000. U.S. Fish and Wildlife Service, Fairbanks Fishery Resource Office, Alaska Fisheries Technical Report 61, Fairbanks, Alaska.

Reynolds, J. H., C. A. Woody, N. E. Gove, and L. F. Fair. 2007. Efficiently estimating salmon escapement uncertainty using systematically sampled data. Pages 121–129 in C. A. Woody, editor. Sockeye salmon ecology, evolution, and management. American Fisheries Society Symposium No. 54, Bethesda, MD.

Seibel, M. C. 1967. The use of expanded ten-minute counts as estimates of hourly salmon migration past counting towers on Alaskan rivers. Alaska Department of Fish and Game, Division of Commercial Fisheries, Informational Leaflet No. 101, Juneau.

Webb, P. W. 1995. Locomotion. Pages 71-99 in C. Groot, L. Margolis, and W.C. Clarke, editors. Physiological Ecology of Pacific salmon. University of British Columbia Press, Vancouver, B.C.

West, F. W., and L. F. Fair. 2006. Abundance, age, sex, and size statistics for Pacific Salmon in Bristol Bay, 2003. Alaska Department of Fish and Game, Fishery Data Series No. 06-47, Anchorage. http://www.sf.adfg.state.ak.us/FedAidPDFs/fds06-47.pdf

Westerman, D., and T. M. Willette. 2003. Upper Cook Inlet salmon escapement studies, 2002. Alaska Department of Fish and Game, Division of Commercial Fisheries, Regional Information Report 2A03-24, Anchorage.

FIGURES

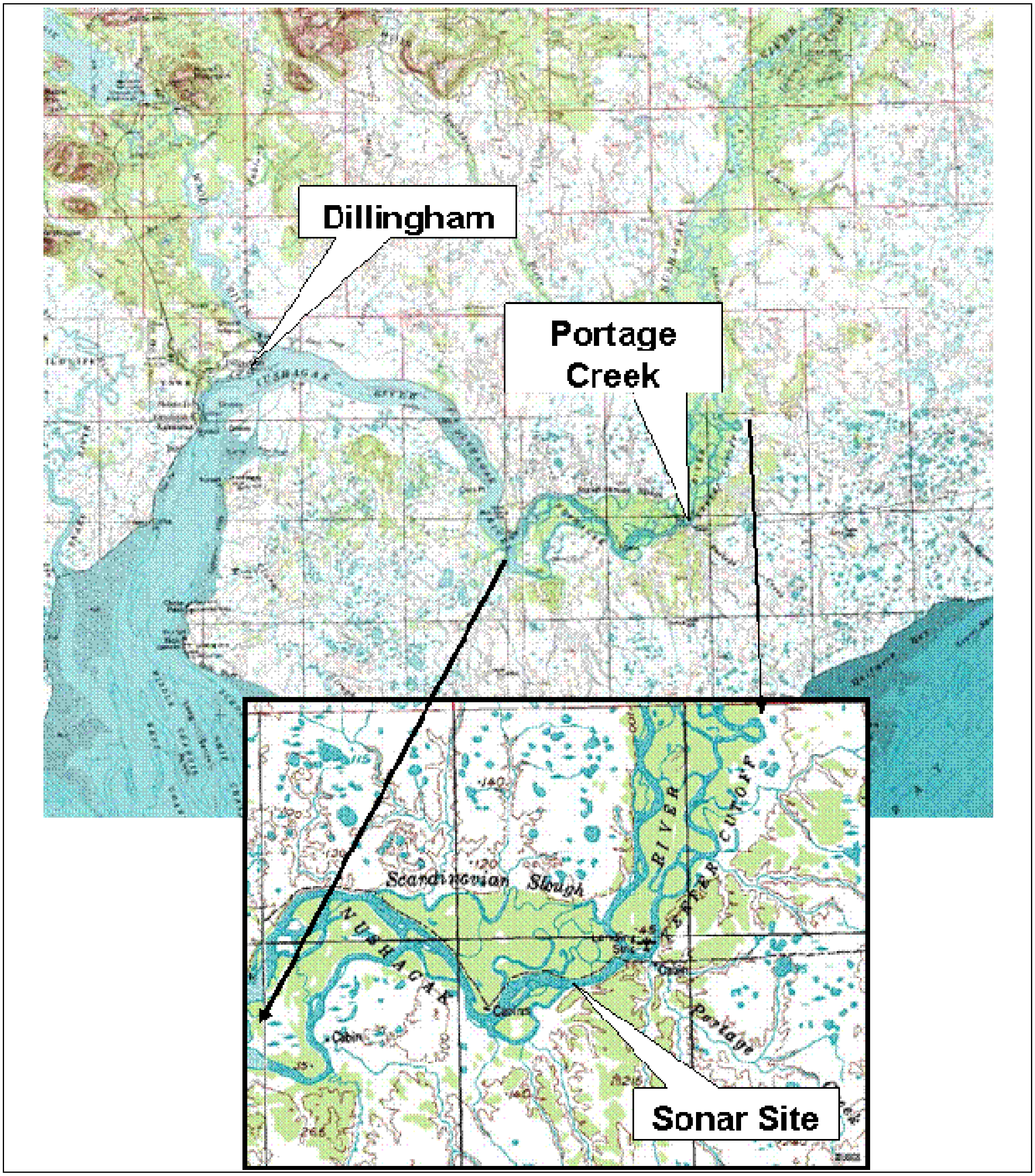

Note: The sonar site is located 41 km east of Dillingham and 4 km downstream of Portage Creek.

Figure 1.–Nushagak River, Alaska, and zoomed insert of the Nushagak River sonar site.

Figure 2.–H-mount made from aluminum poles with 2 single-axis rotators, a 4° by 10° HTI transducer, and a BioSonics' attitude sensor.

Figure 3.–Two weirs along the right bank of the Nushagak River for the Bendix nearshore transducer (foreground) and the HTI system (upstream), Nushagak River sonar, 2002.

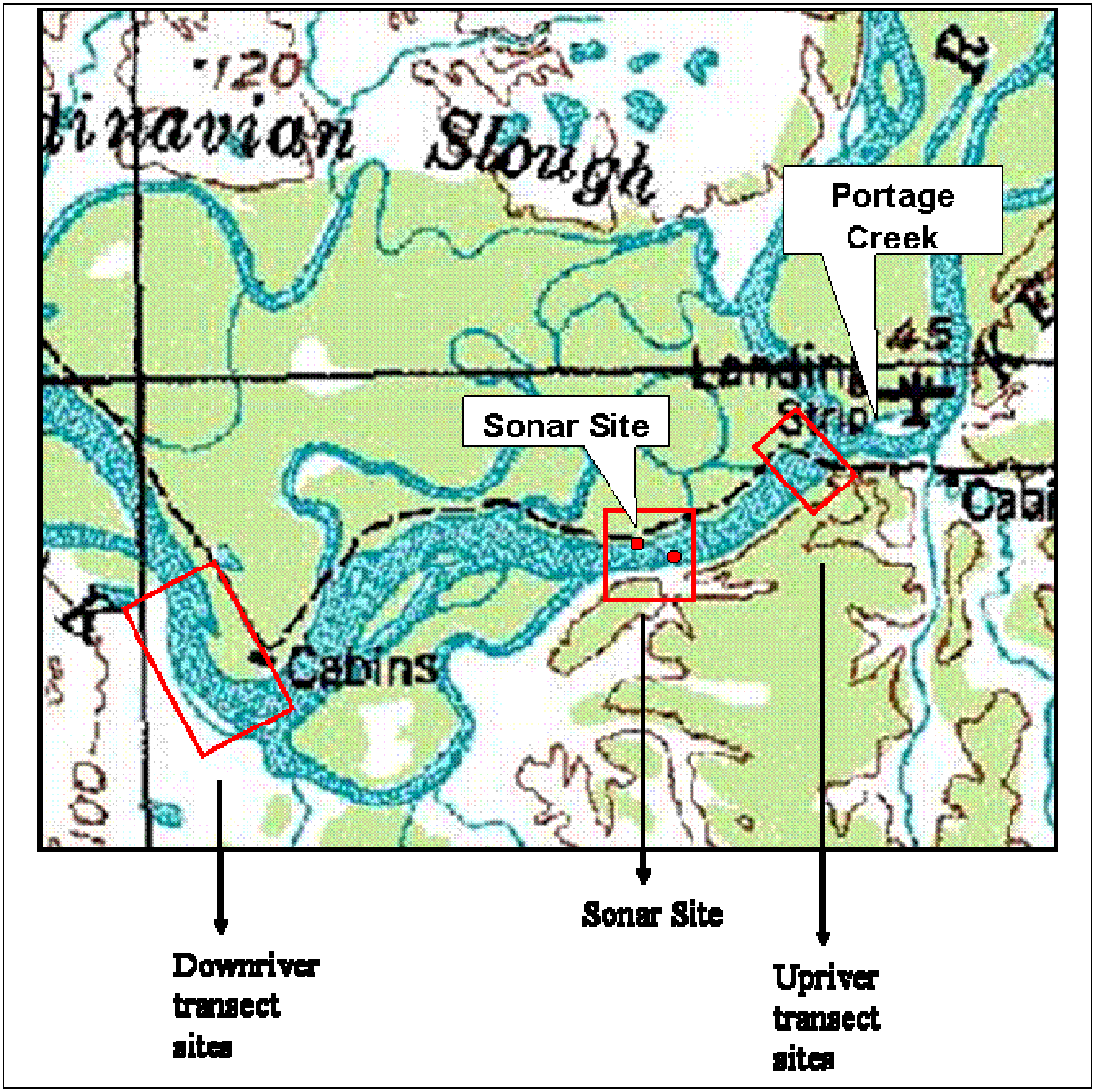

Figure 4.–The Nushagak River from Portage Creek downriver showing the approximate locations of the upriver sites profiled in 1999, the existing sonar site, and the downriver profiled sites.

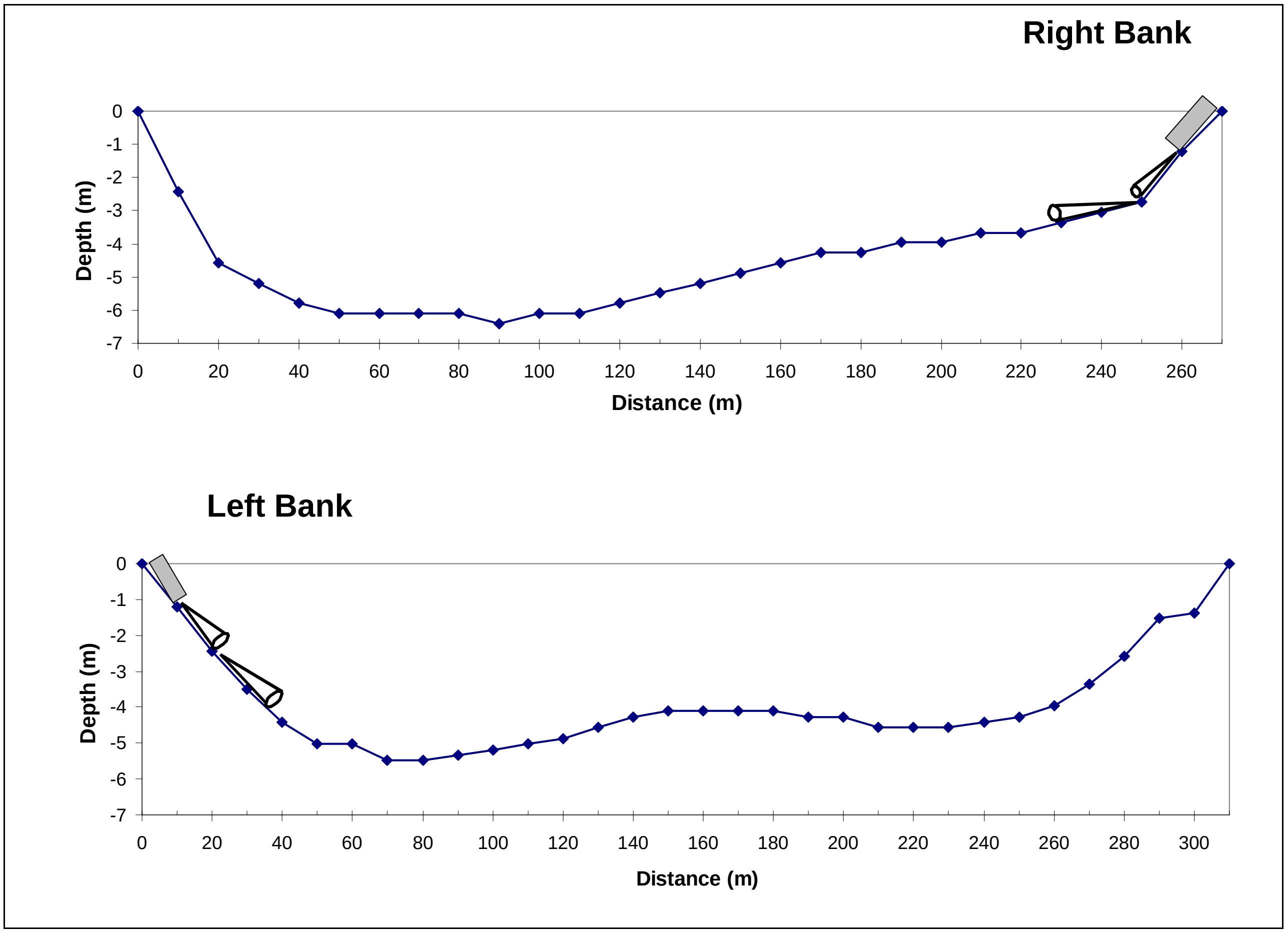

Figure 5.–Cross-river profiles at the right bank Bendix transducer site (top) and the left bank site (bottom) showing the approximate placement of the nearshore and offshore Bendix transducers, Nushagak River sonar site, June 10, 1999.

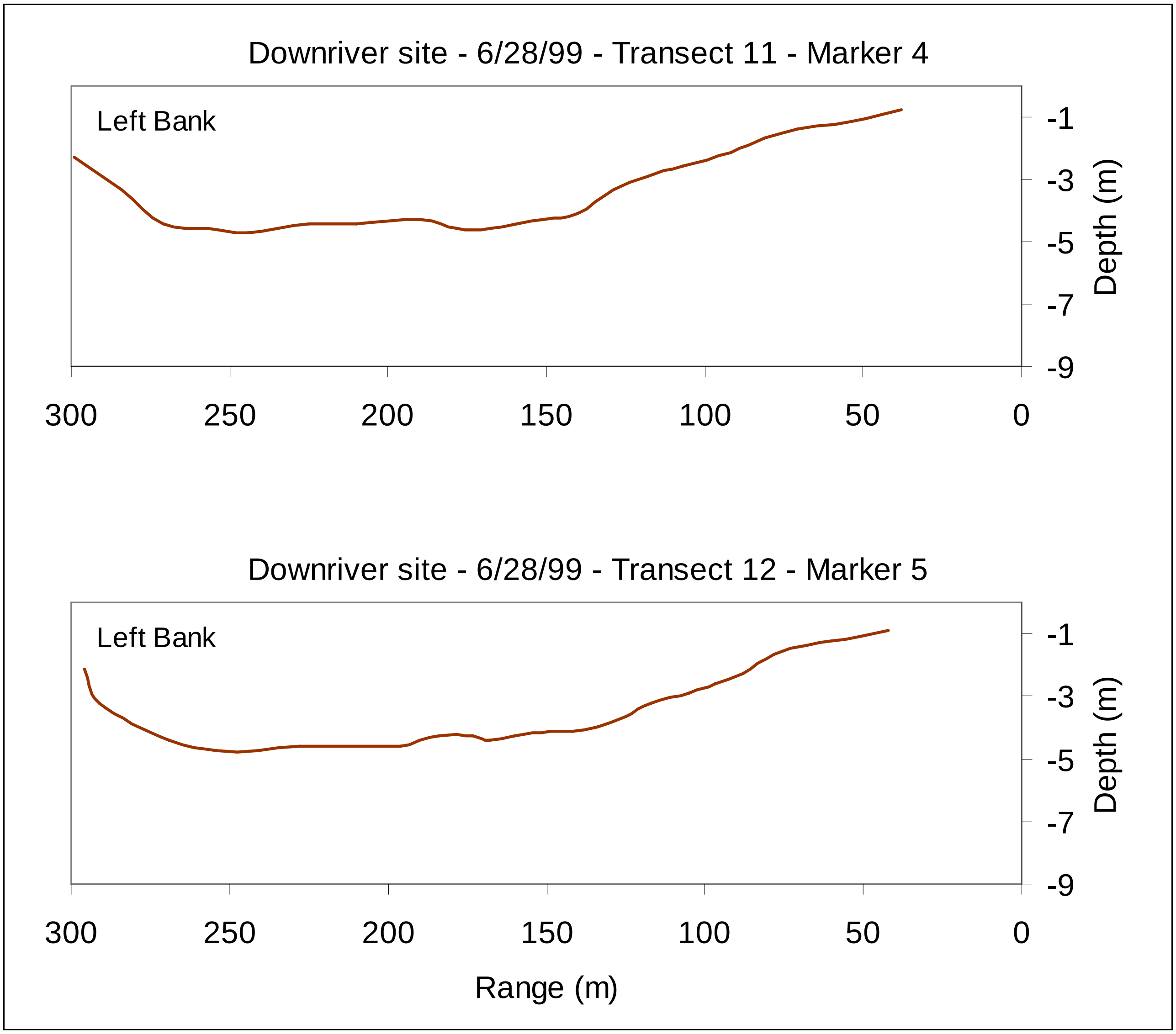

Figure 6.–A sample of the sites profiled downriver from the Nushagak River sonar site, 1999.

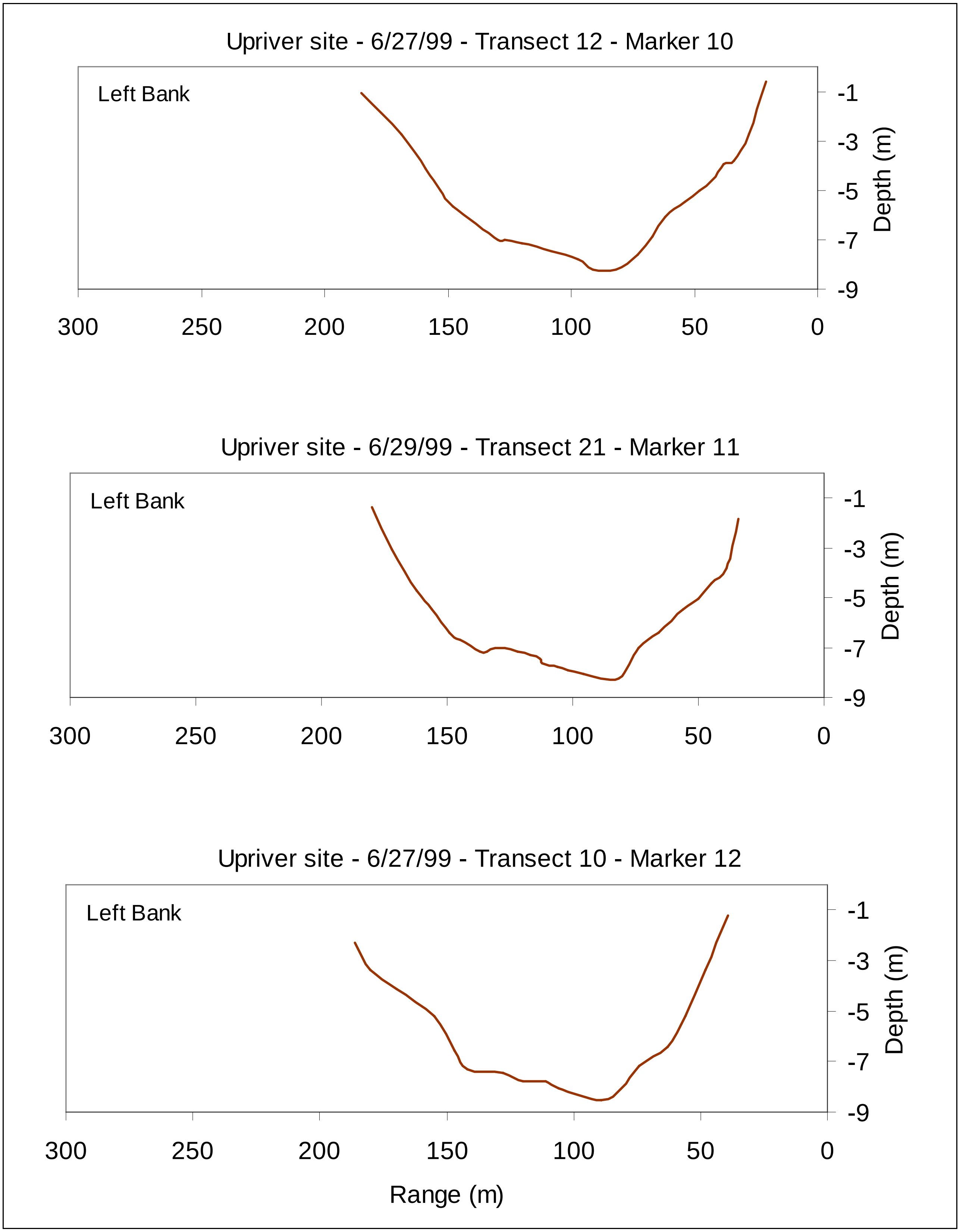

Figure 7.–A sample of the sites profiled upriver from the Nushagak River sonar site, 1999.

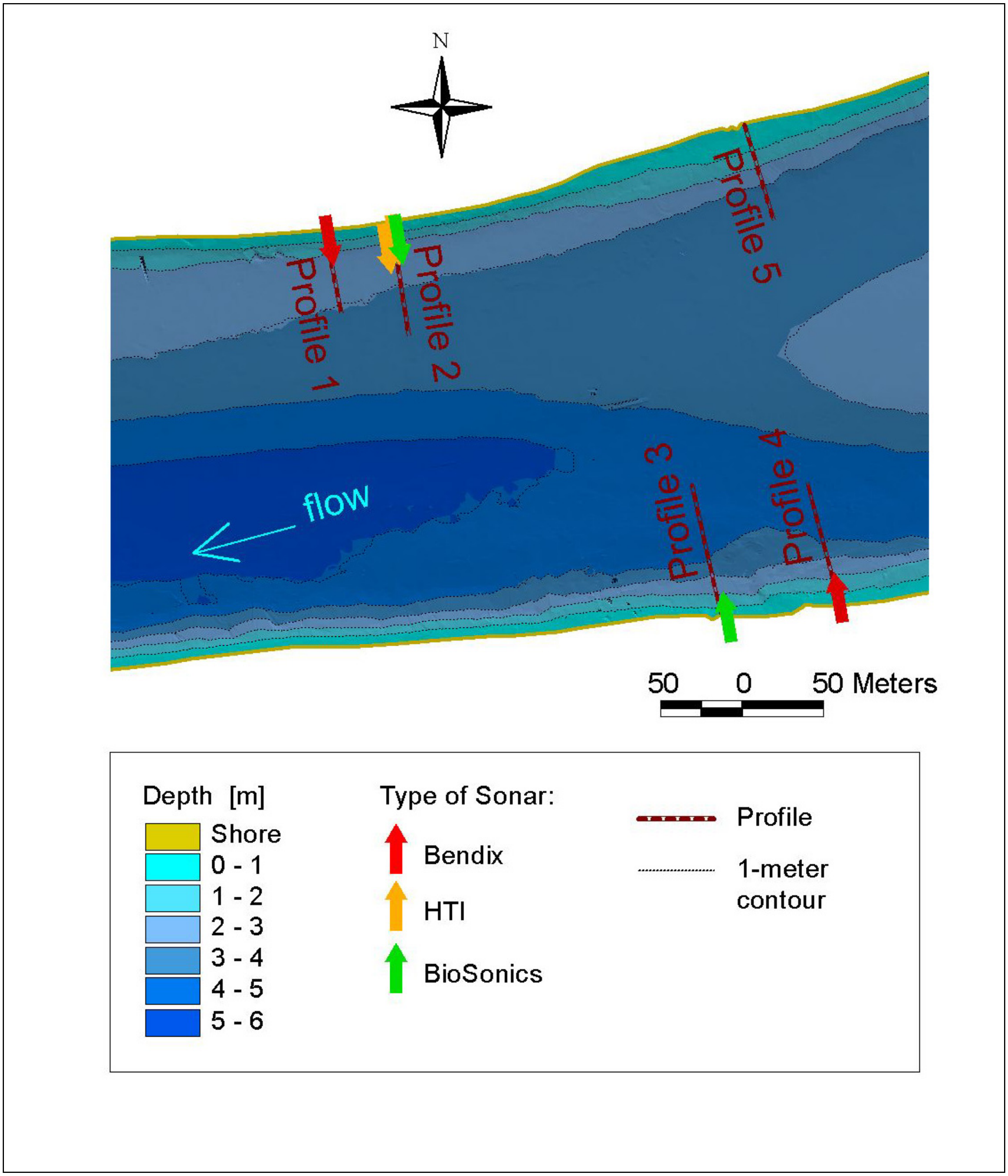

Note: Bathymetry is based on surveys from 2000 and 2003.

Figure 8.–Bathymetry map of the Nushagak River sonar site with the Bendix, HTI, and BioSonics' deployment sites marked.

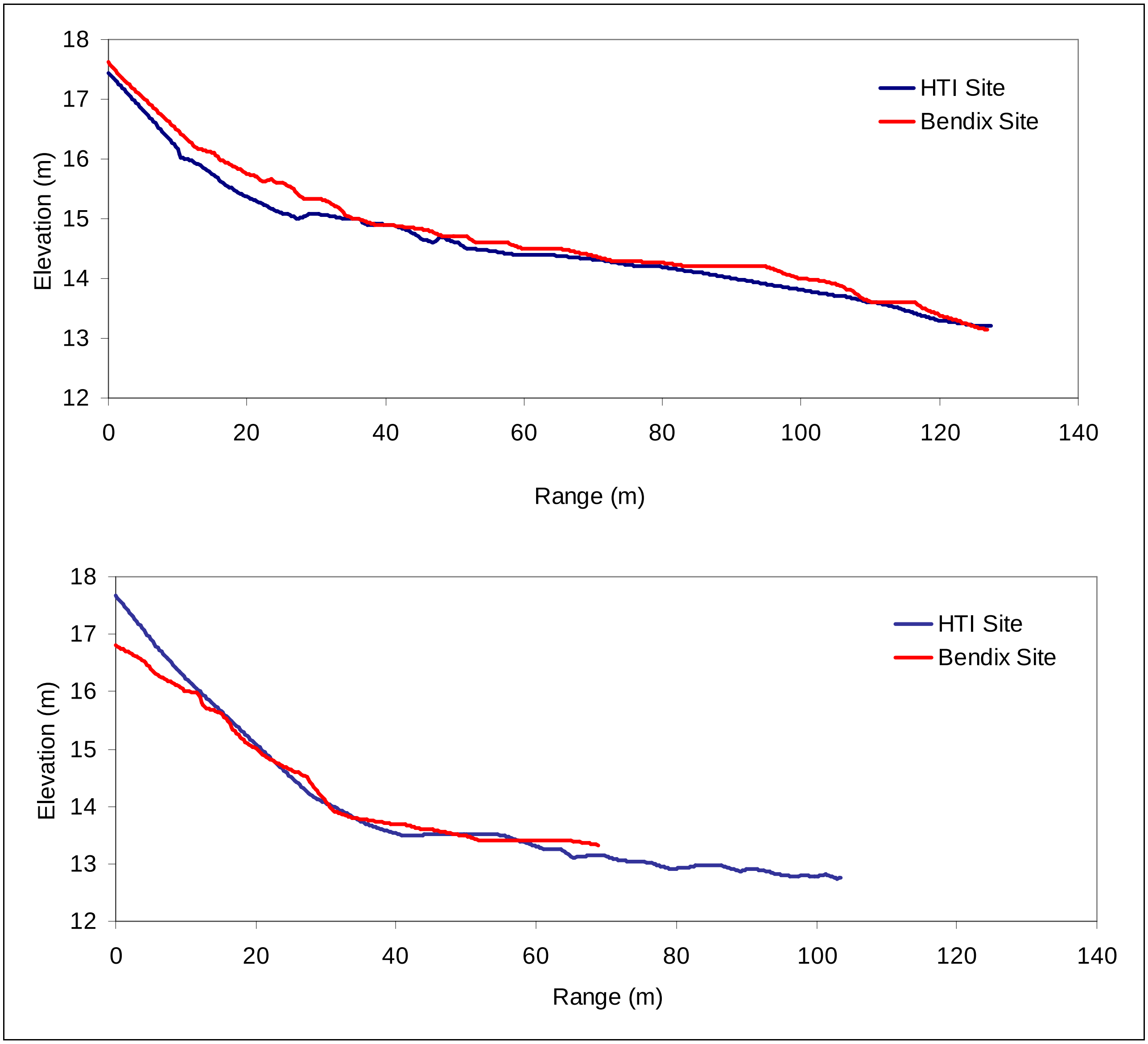

Figure 9.–River bottom profiles along the right bank (top) and left bank (bottom) of the Nushagak River at the deployment sites of the Bendix and HTI split beam sonars.

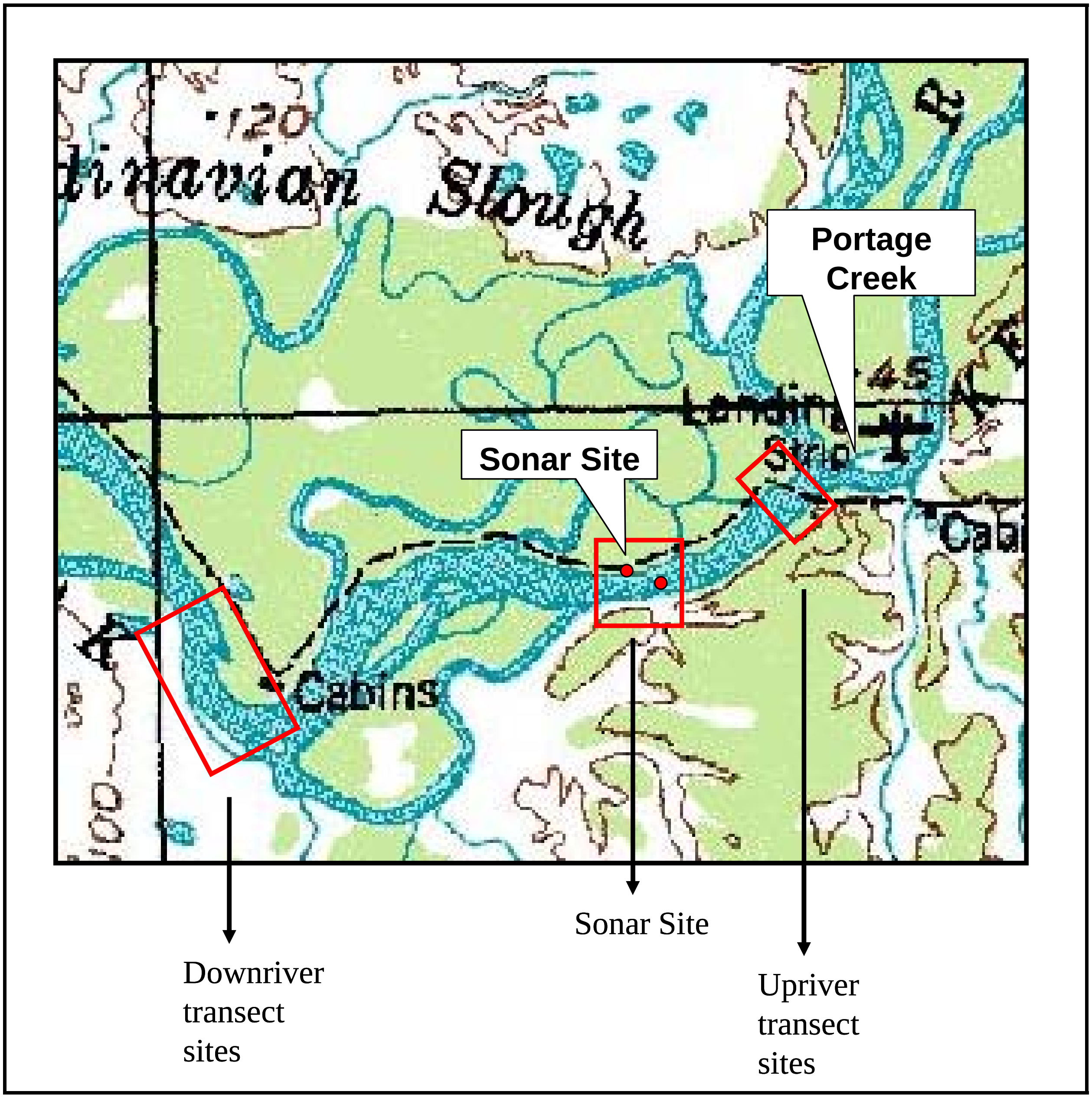

Figure 10.–The horizontal and vertical position of echoes reflected from the 38.1 mm tungsten carbide sphere with the nominal beam overlaid during calibration of the 4° by 10° transducer, Nushagak River sonar, 2001.

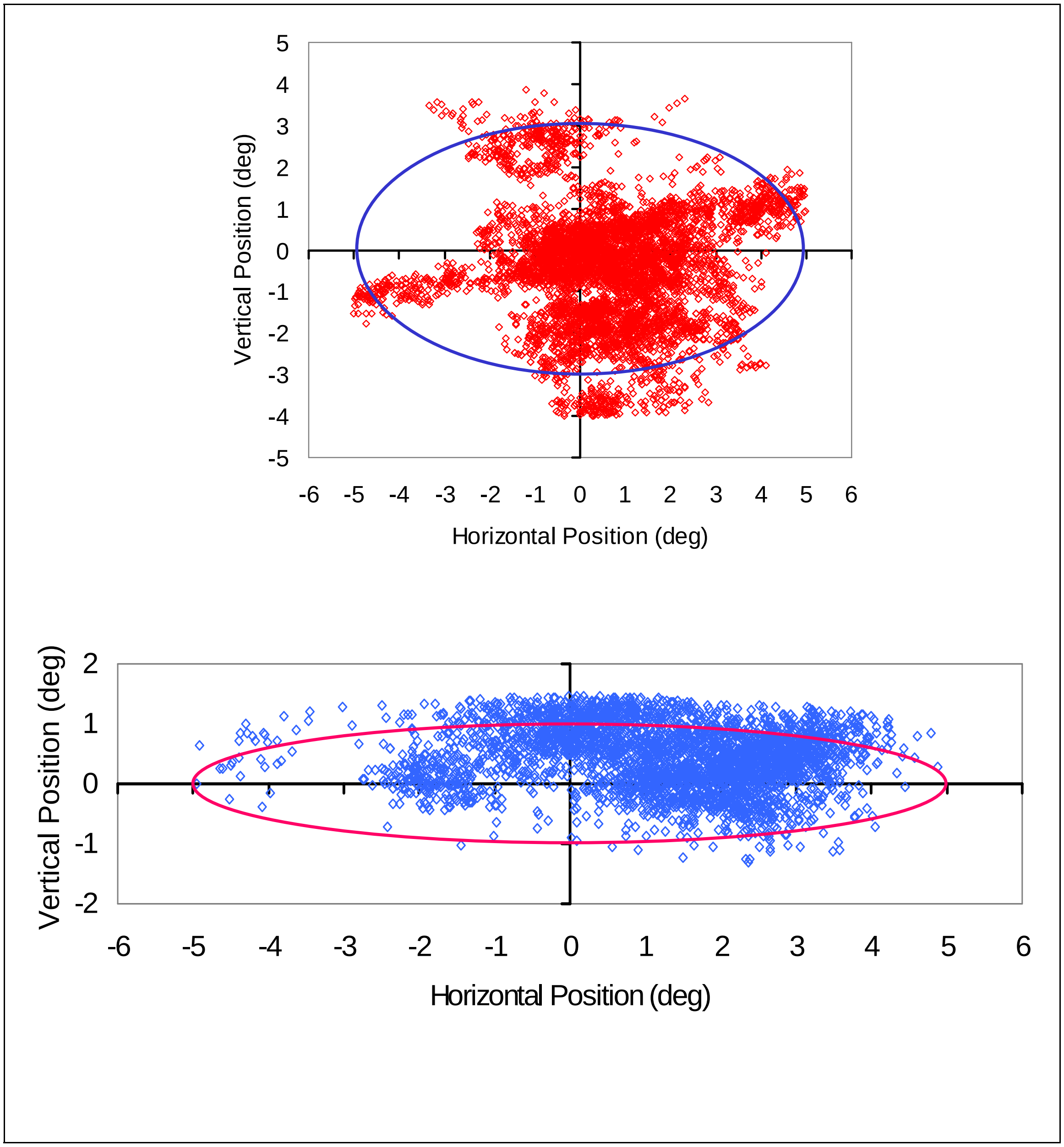

Figure 11.–The horizontal and vertical position of echoes reflected from the 38.1 mm tungsten carbide sphere with the nominal beams overlaid during calibration of the 6° by 10° (top) and 2° by 10° (bottom) transducers, Nushagak River sonar, 2002.

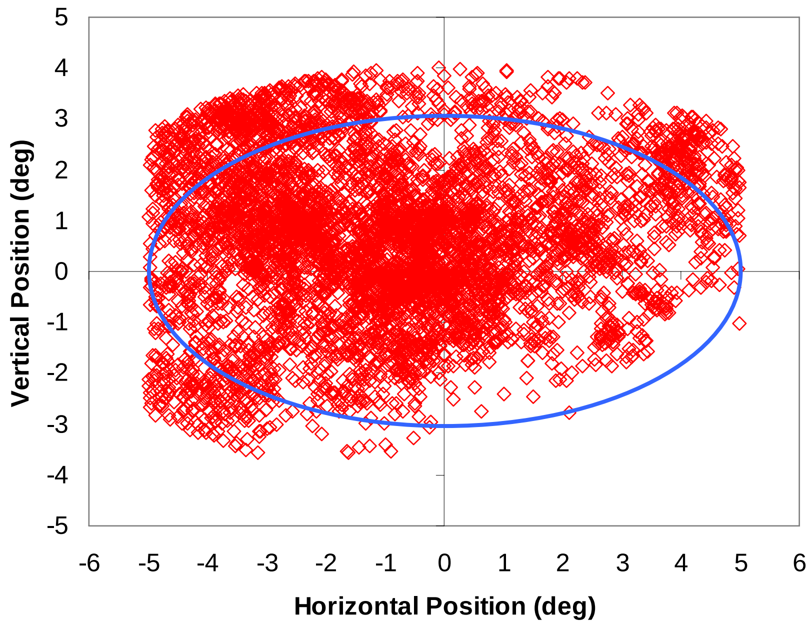

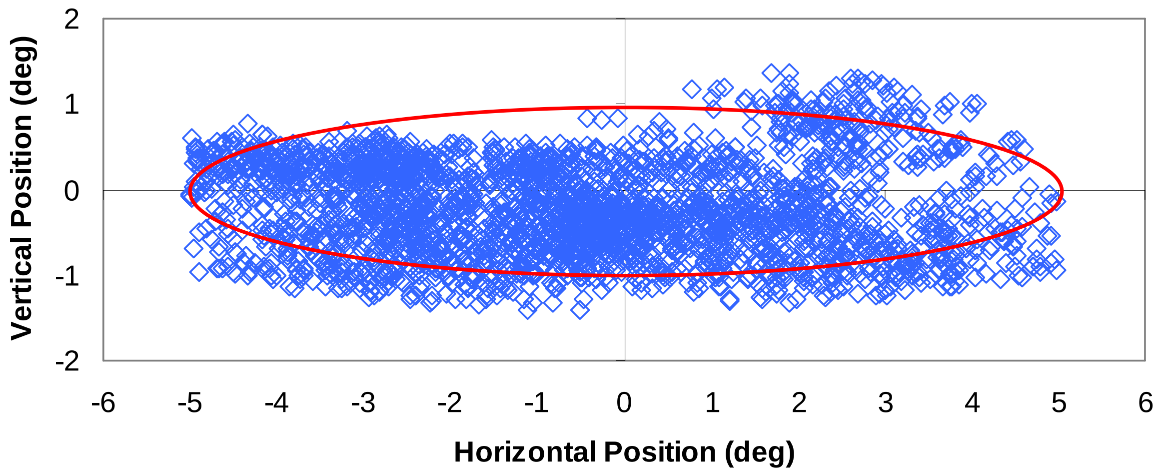

Figure 12.–The horizontal and vertical position of echoes reflected from the 38.1 mm tungsten carbide sphere with the nominal beams overlaid during calibration of the 6° by 10° (top) and 2° by 10° (bottom) transducers, Nushagak River sonar, 2003.

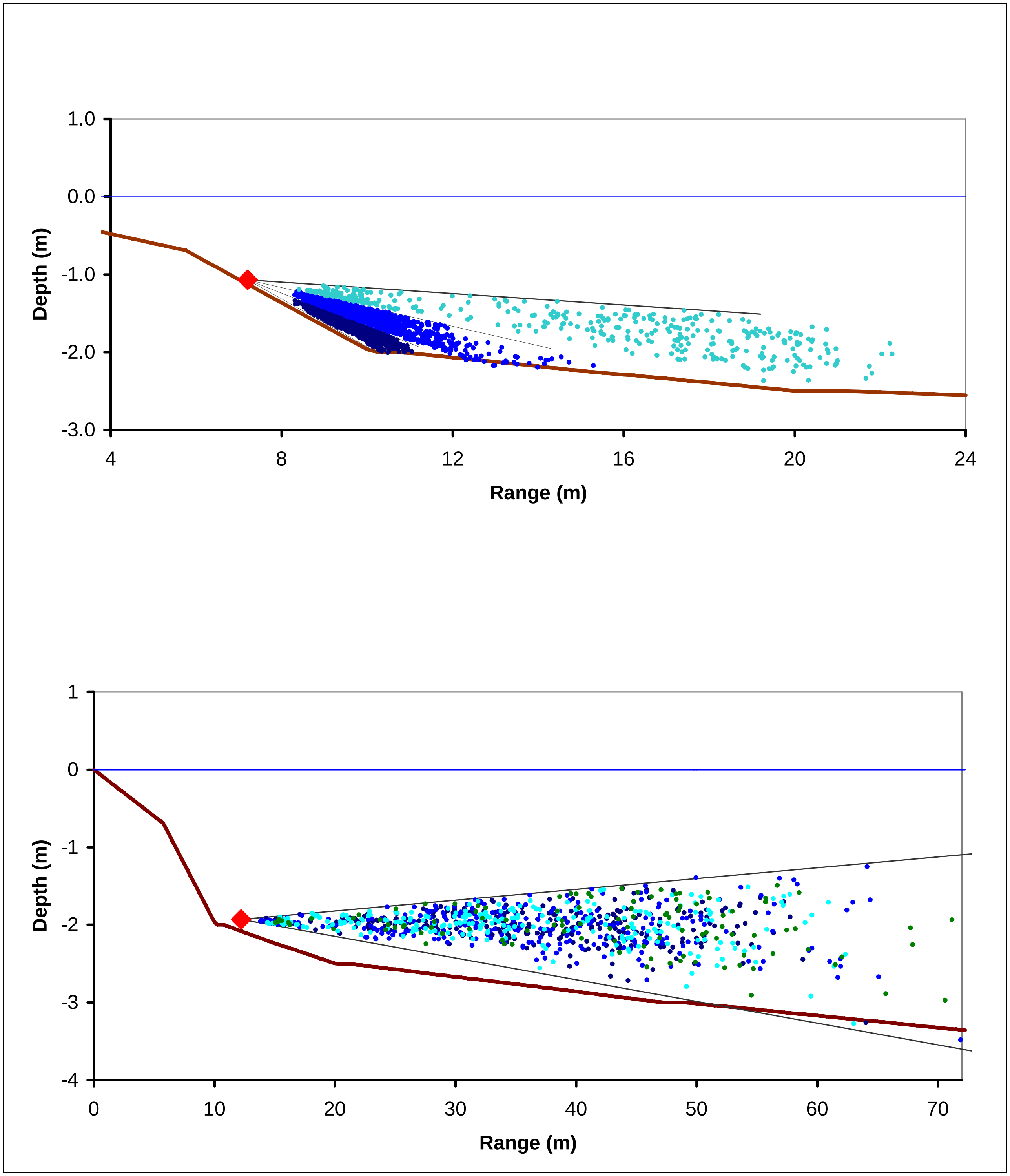

Figure 13.–The average range and vertical position of each tracked fish in relation to the beams and river profile for the 3 nearshore beam positions (top) and a single offshore beam position (bottom) along the right bank of the Nushagak River, 2000.

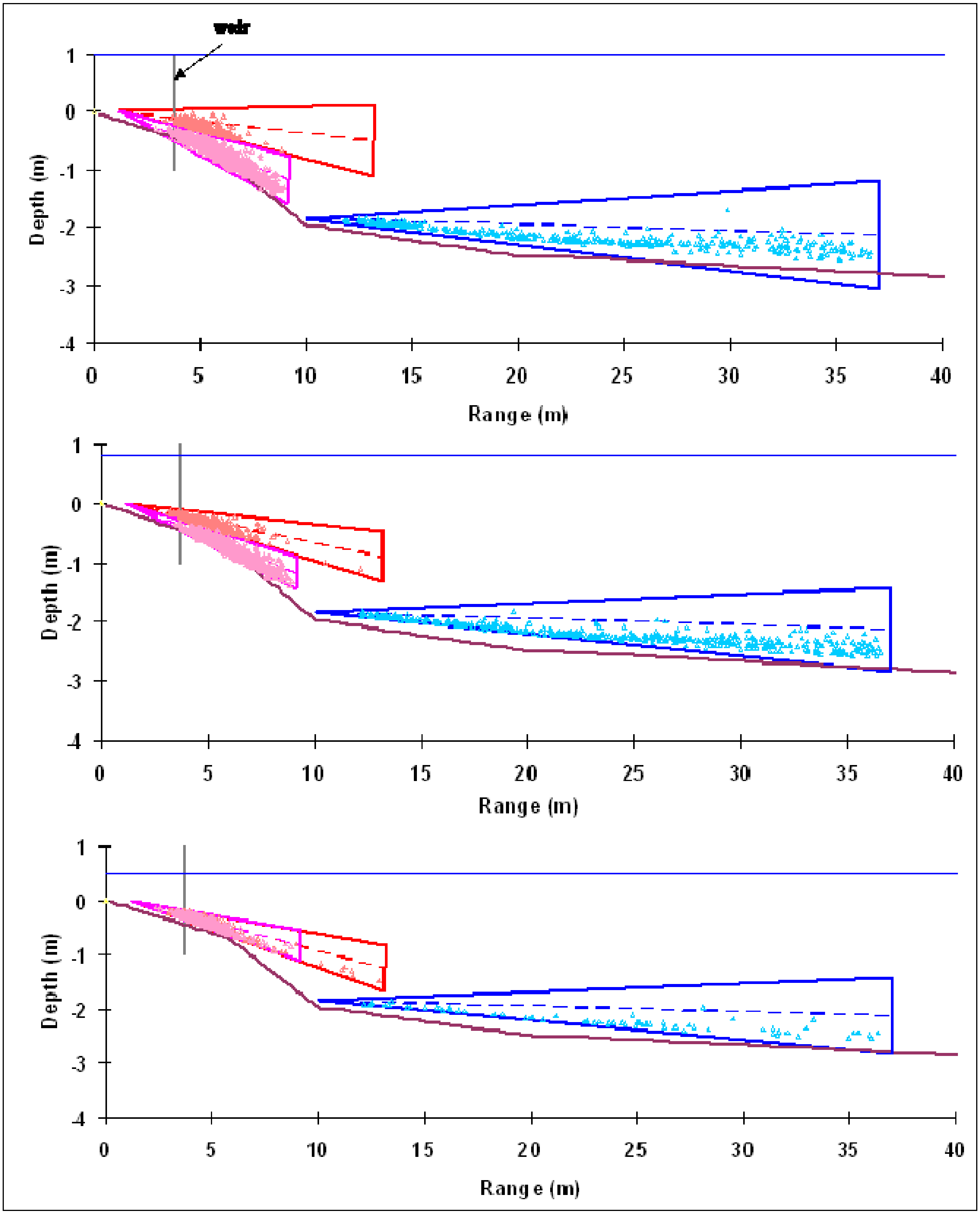

Figure 14.–The average range and vertical position of each tracked fish in relation to the beams and river profile, June 16–26 (top), June 26–July 15 (middle), and July 16–25 (bottom) along the right bank of the Nushagak River, 2001.

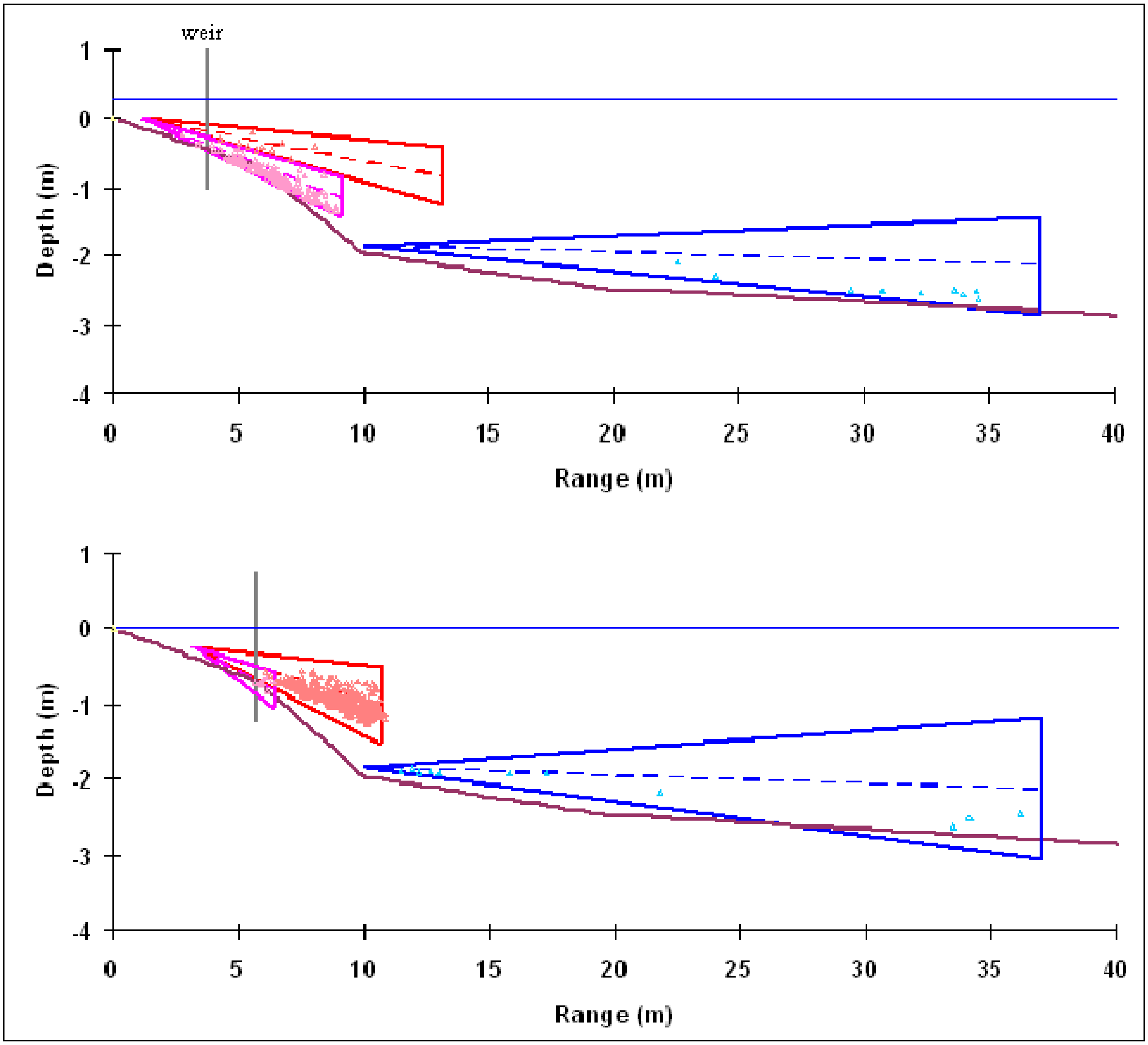

Figure 15.–The average range and vertical position on each tracked fish in relation to the beams and river profile, July 25–August 8 (top), August 8–16 (bottom) along the right bank of the Nushagak River, 2001.

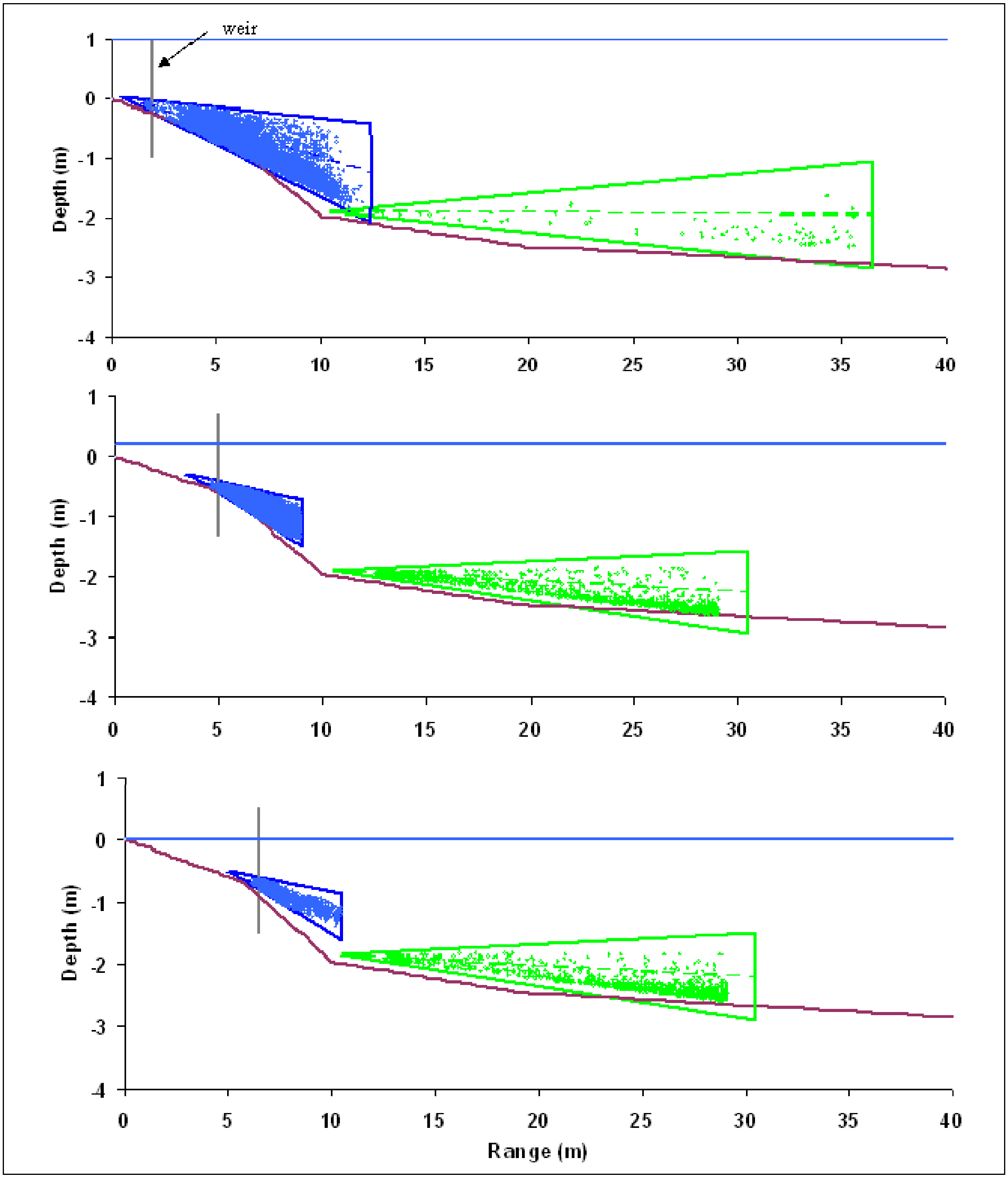

Figure 16.–The average range and vertical position of each tracked fish in relation to the beams and river profile separated by month, June (top), July (middle), and August (bottom) along the right bank of the Nushagak River, 2002.

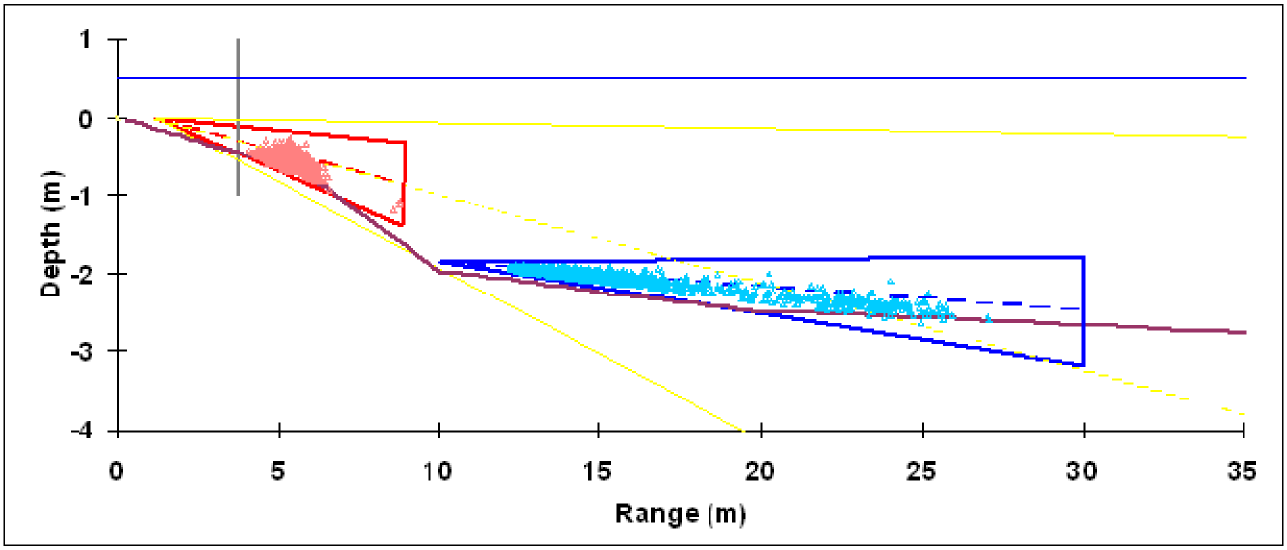

Note: The overlaid gray beam shows the potential coverage of a DIDSON 14° beam.

Figure 17.–The average range and vertical position of each tracked fish in relation to the transducer beams and river profile, June 26–July 18 along the right bank of the Nushagak River, 2003 (top).

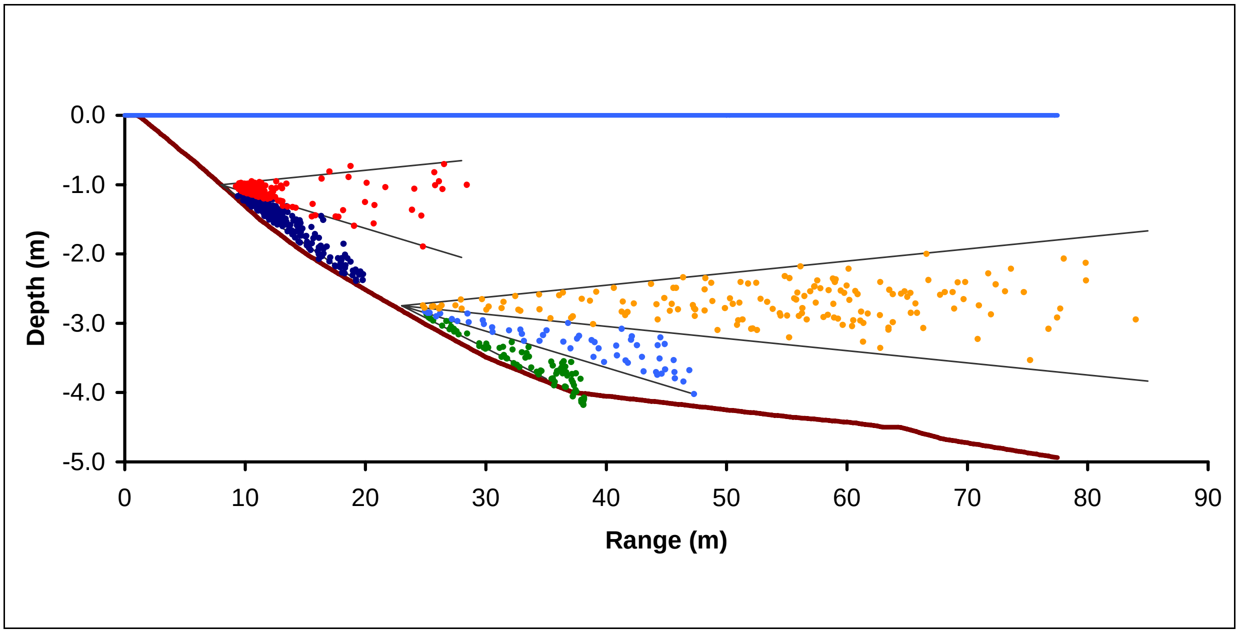

Figure 18.–The average range and vertical position of each tracked fish in relation to the beams and river profile along the left bank of the Nushagak River, July 2, 2000.

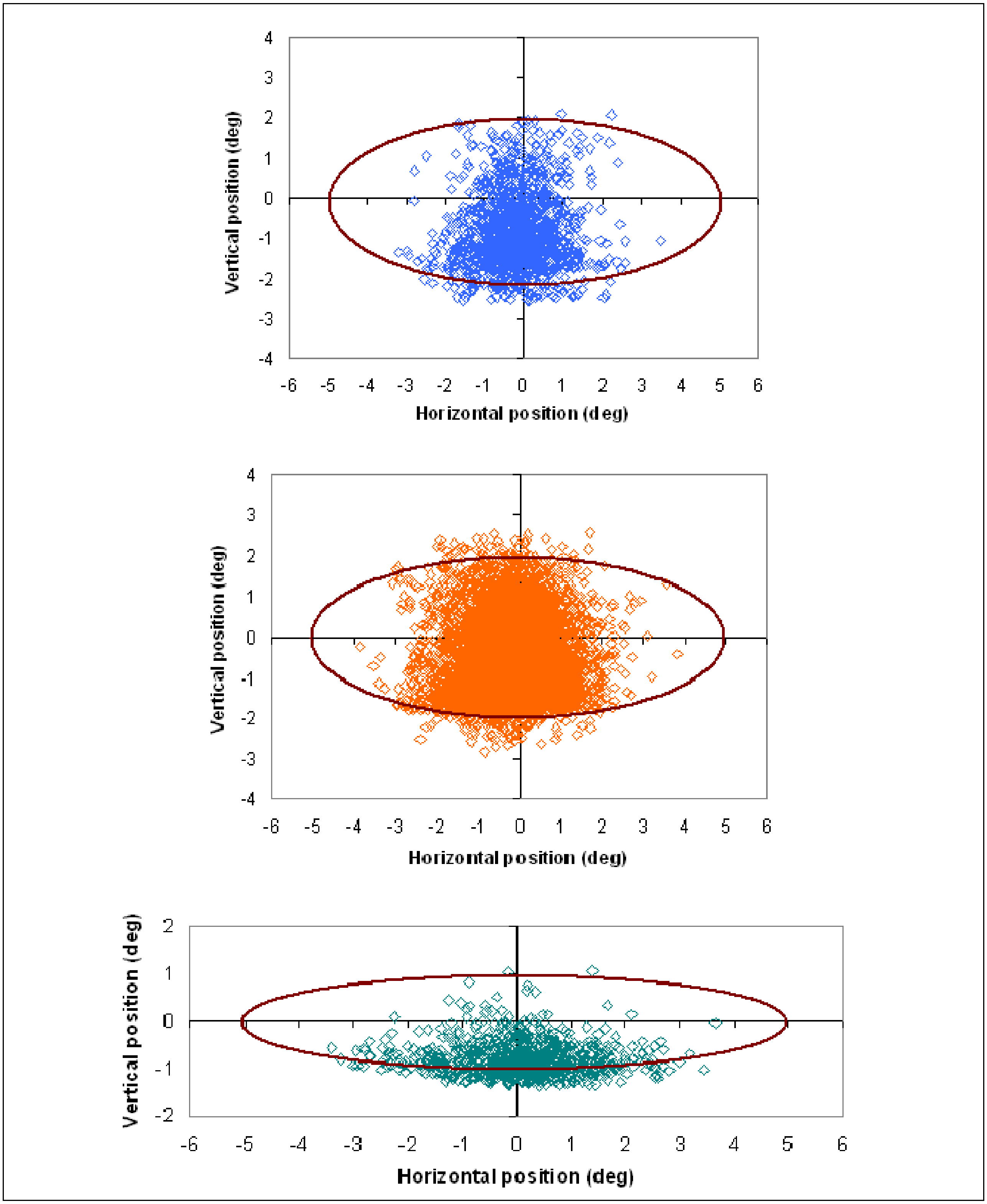

Figure 19.–The average position of echoes from individual fish tracks obtained from the nearshore transducer's high aim (top), low aim (middle), and offshore transducer's low aim (bottom) with the nominal beams overlaid, Nushagak River right bank, 2001.

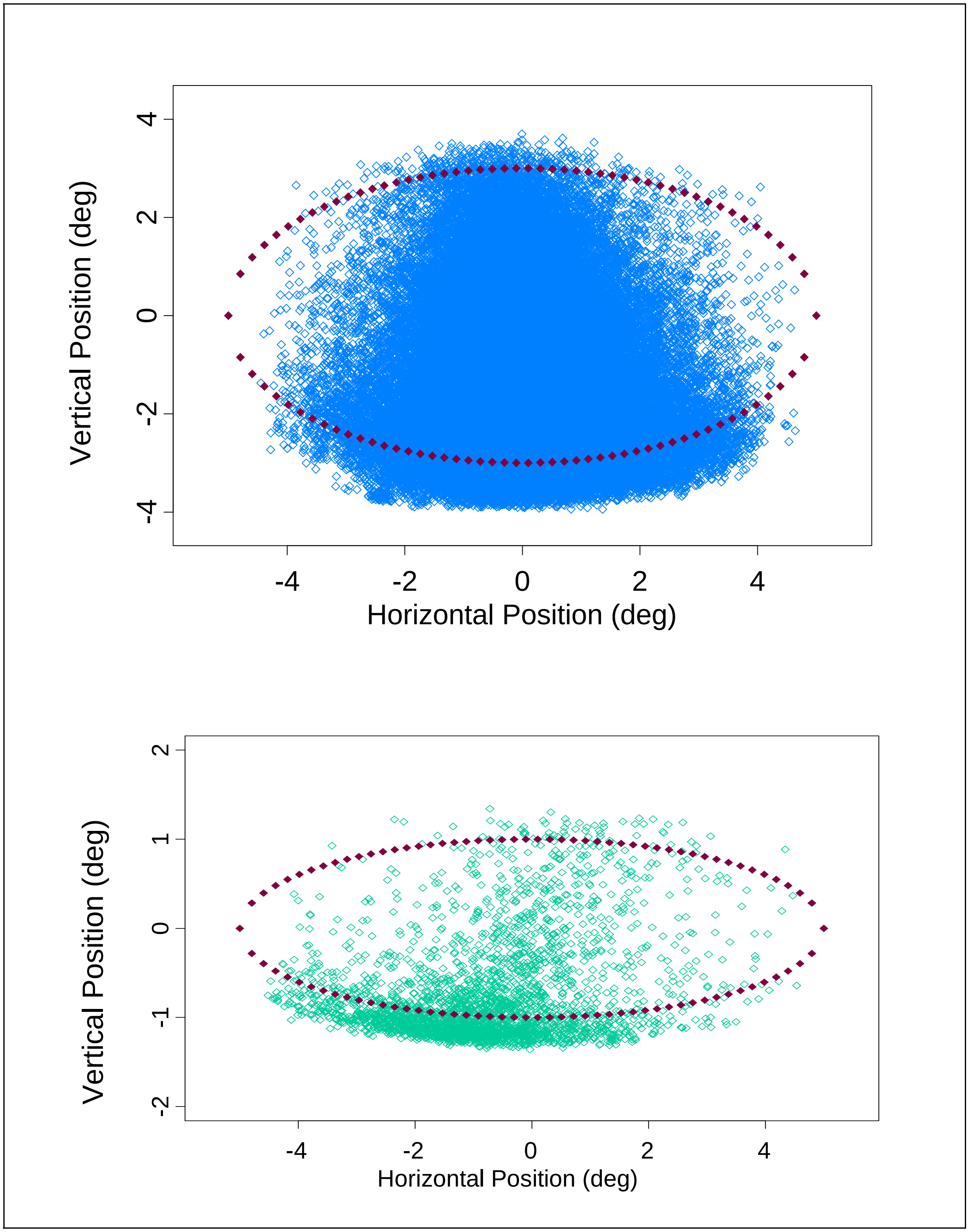

Figure 20.–The average position of echoes from individual fish tracks obtained from the nearshore transducer (top) and offshore transducer (bottom) with the nominal beams overlaid, Nushagak River right bank, 2002.

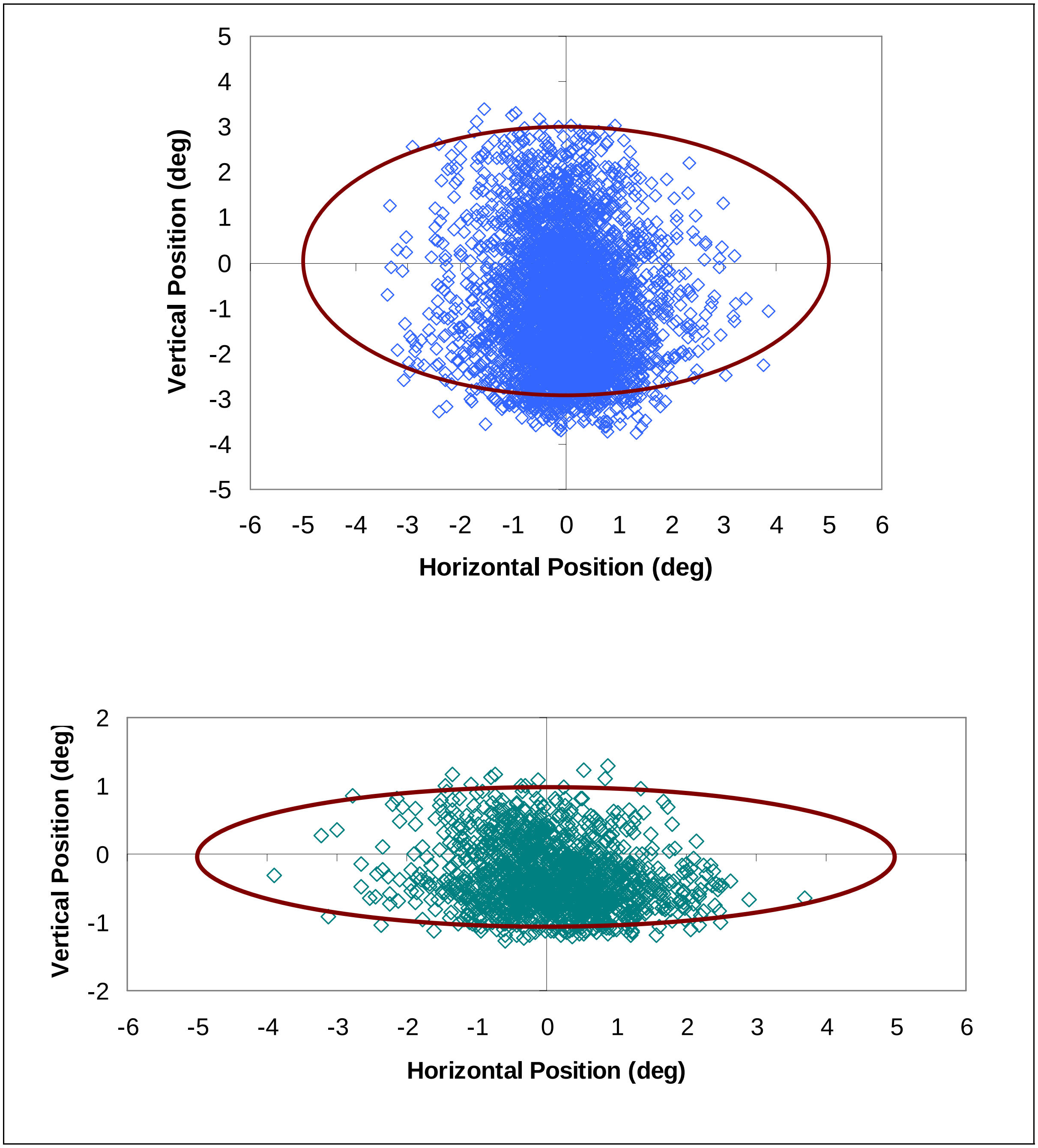

Figure 21.–The average position of echoes from individual fish tracks obtained from the nearshore transducer (top) and offshore transducer (bottom) with the nominal beams overlaid, Nushagak River right bank, 2003.

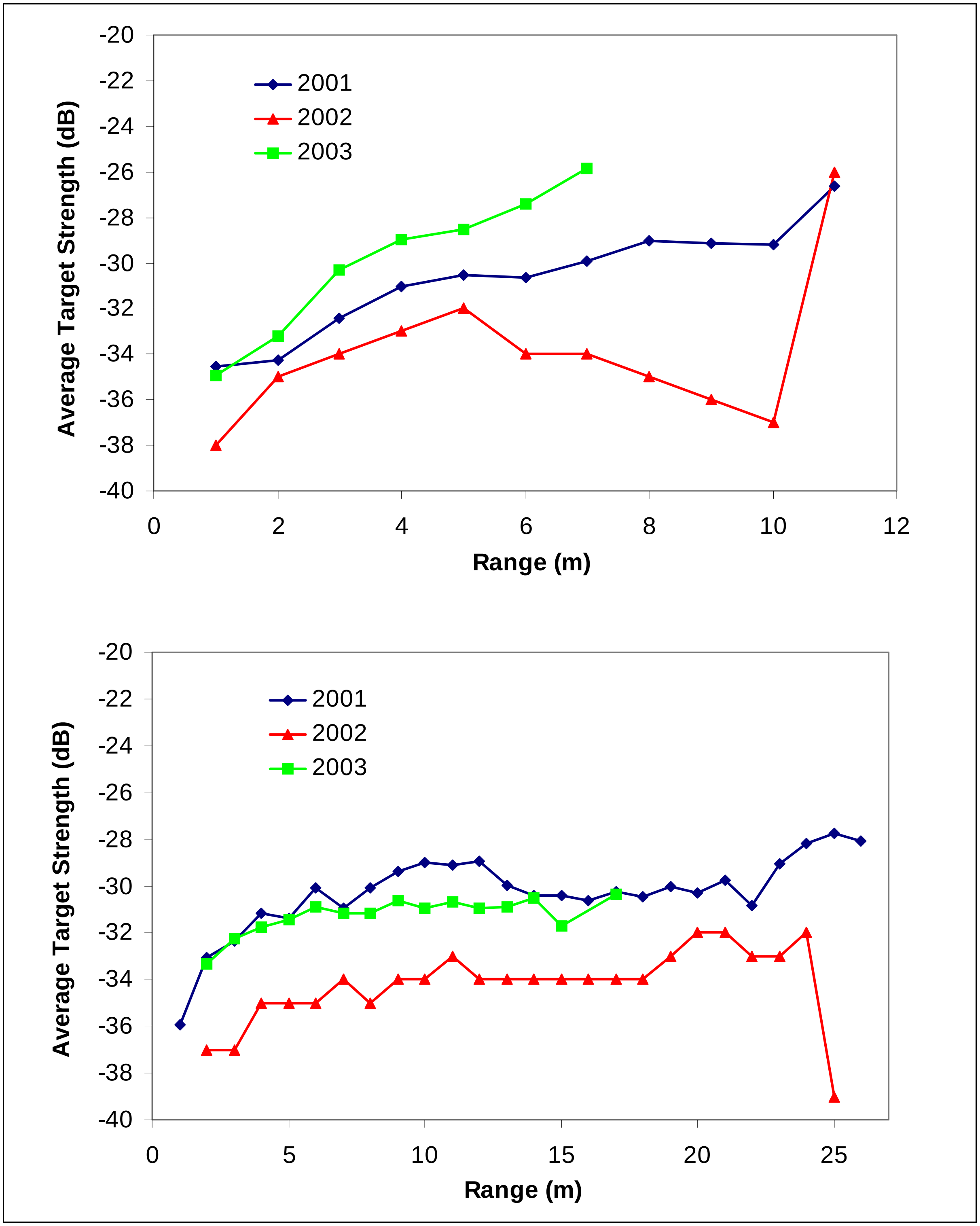

Figure 22.–Average target strength of tracked fish by range from the transducer nearshore (top) and offshore (bottom) along the right bank of the Nushagak River, 2001–2003.

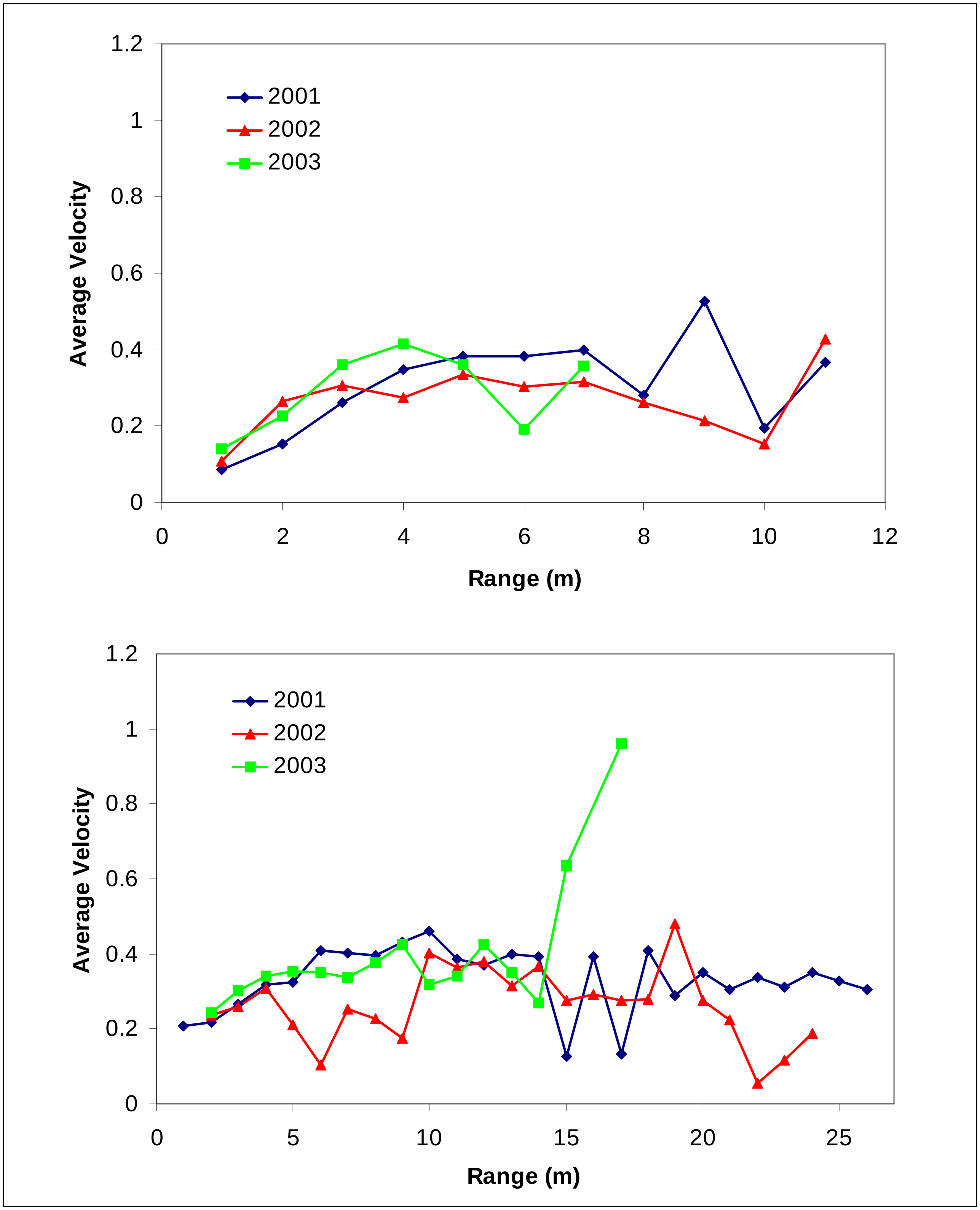

Figure 23.–Average velocity by range from the transducer for tracked fish nearshore (top) and offshore (bottom) along the right bank of the Nushagak River, 2001–2003.

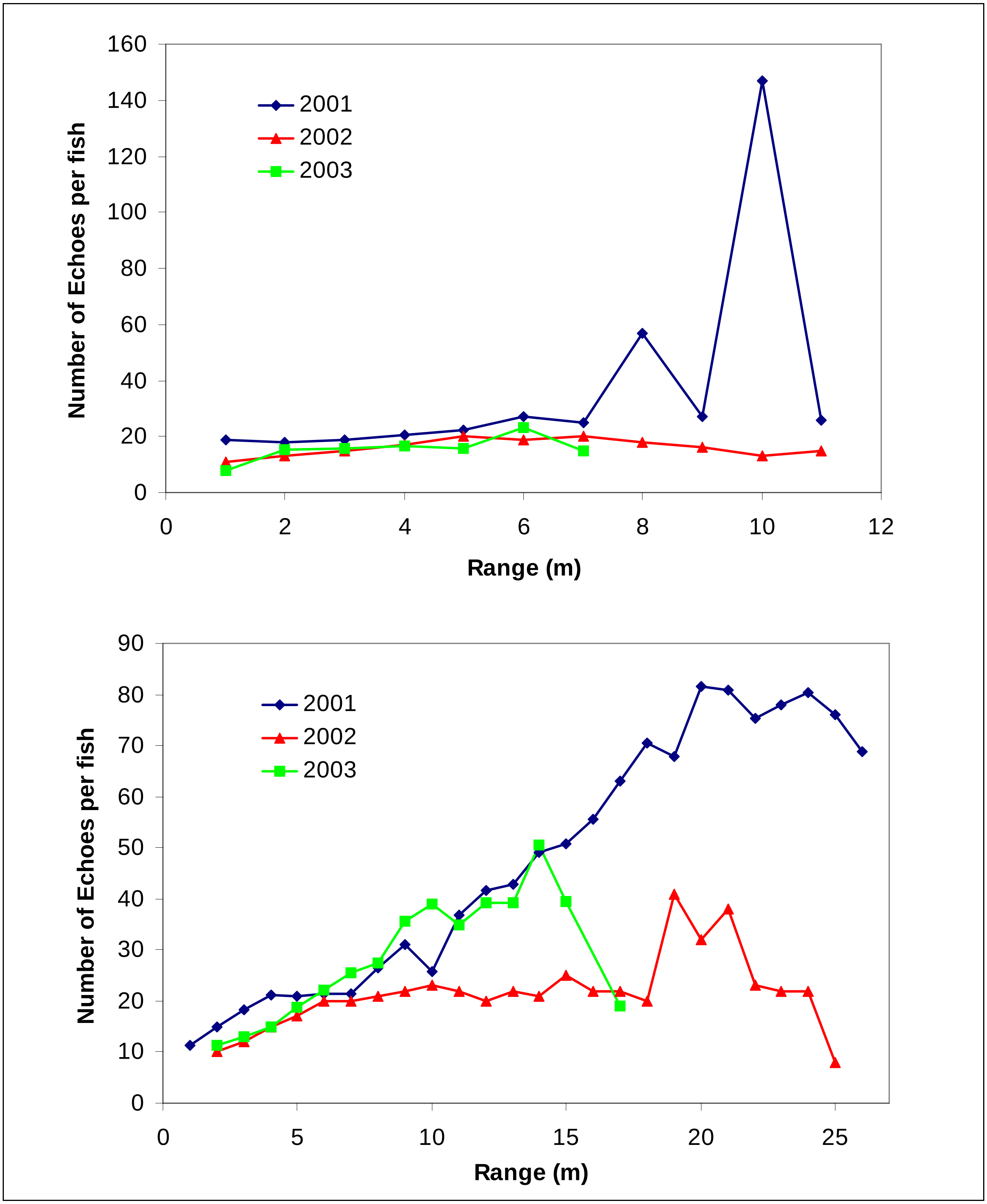

Figure 24.–The number of echoes per fish by range bin from the transducer for tracked fish nearshore (top) and offshore (bottom), Nushagak River, 2001–2003.

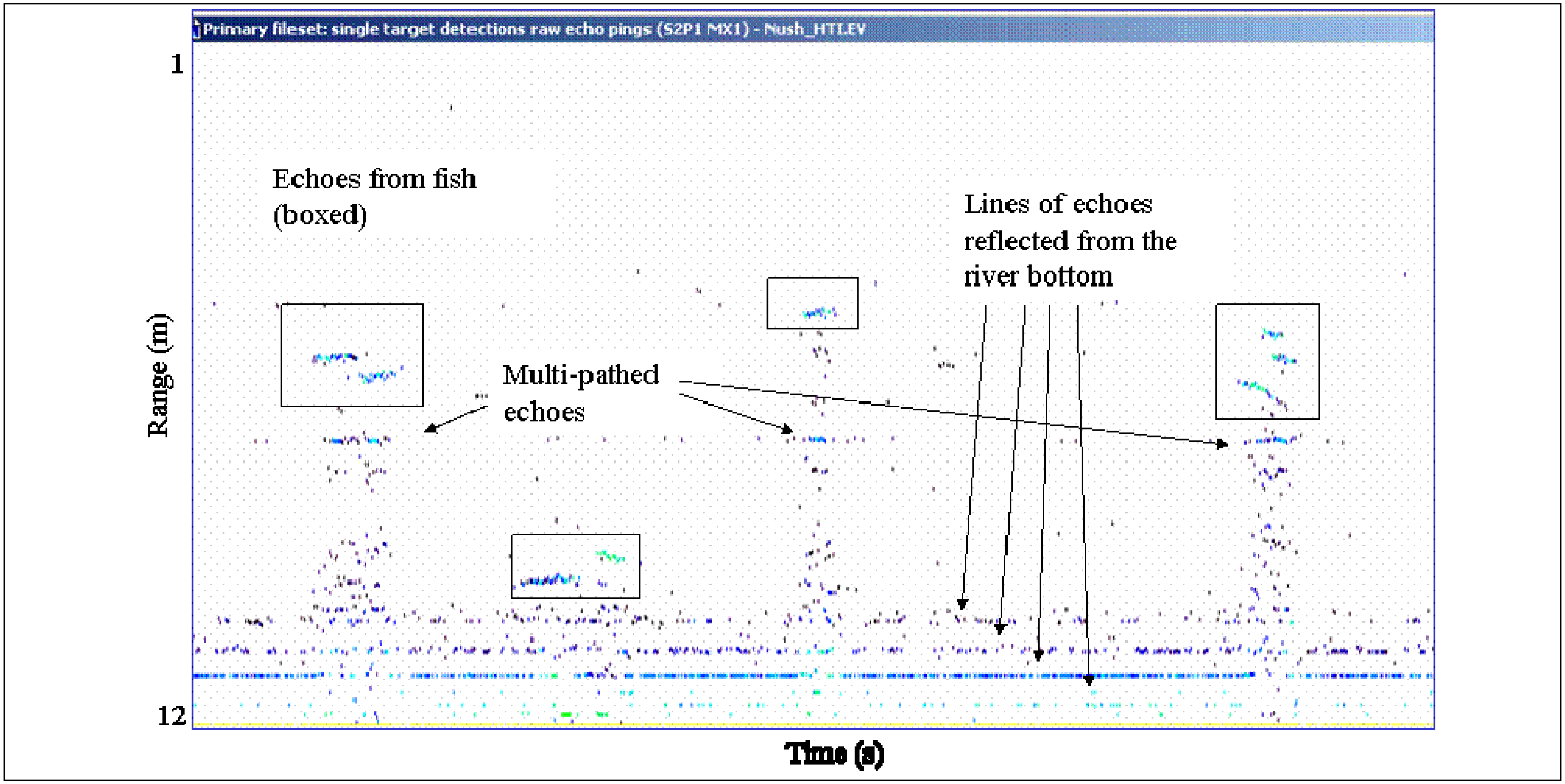

Note: The end range for this echogram is 12 m.

Figure 25.–An echogram from the nearshore transducer (low aim) showing fish echoes, reflections off the river bottom, and multi-path echoes, Nushagak River, June 22, 2002.

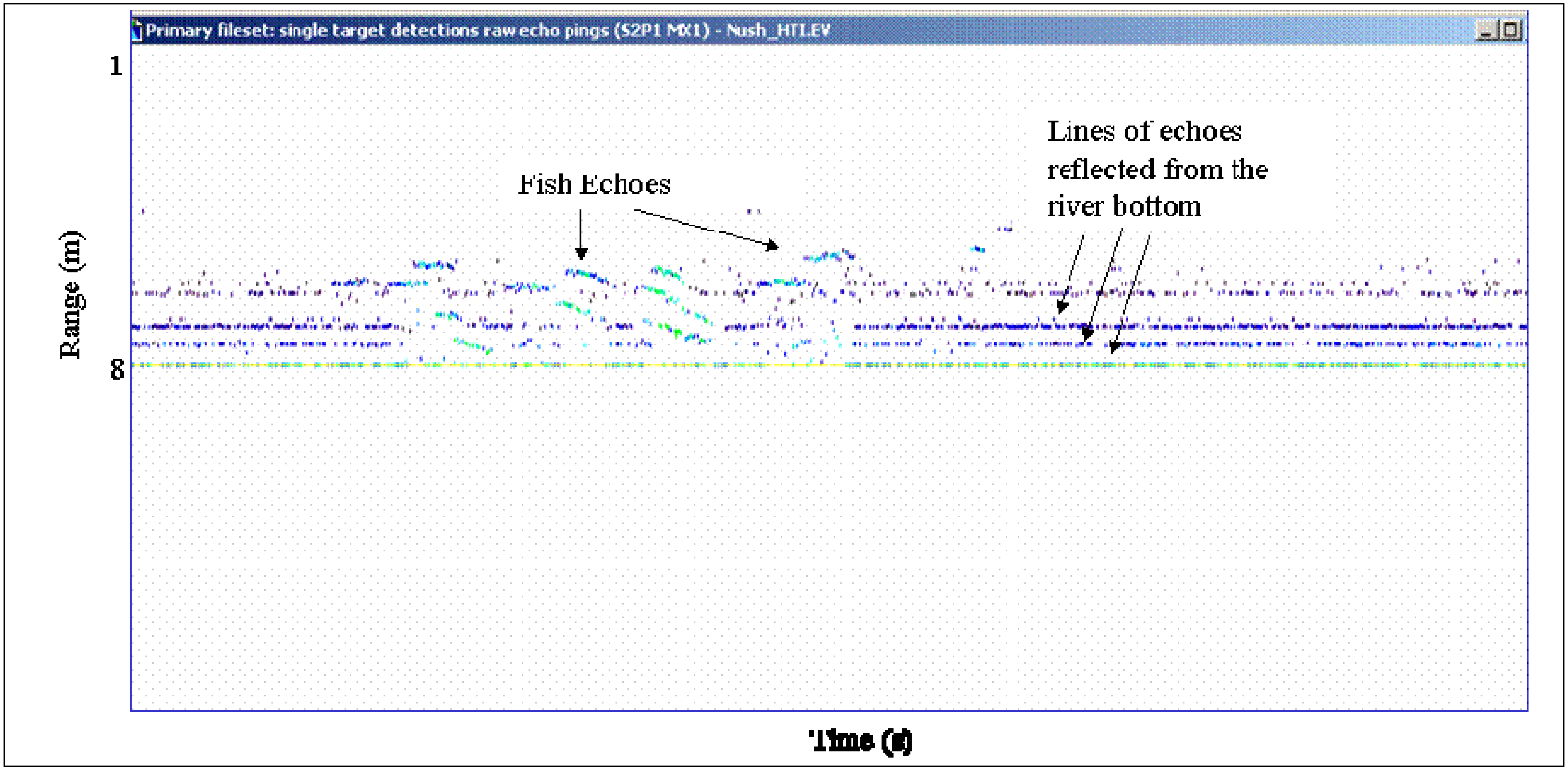

Note: The echogram also shows fish tracks and reflections off the river bottom.

Figure 26.–An echogram from the nearshore transducer's low aim after the transducer was pushed farther offshore and the end range reduced to 8 m, July 1, 2001.

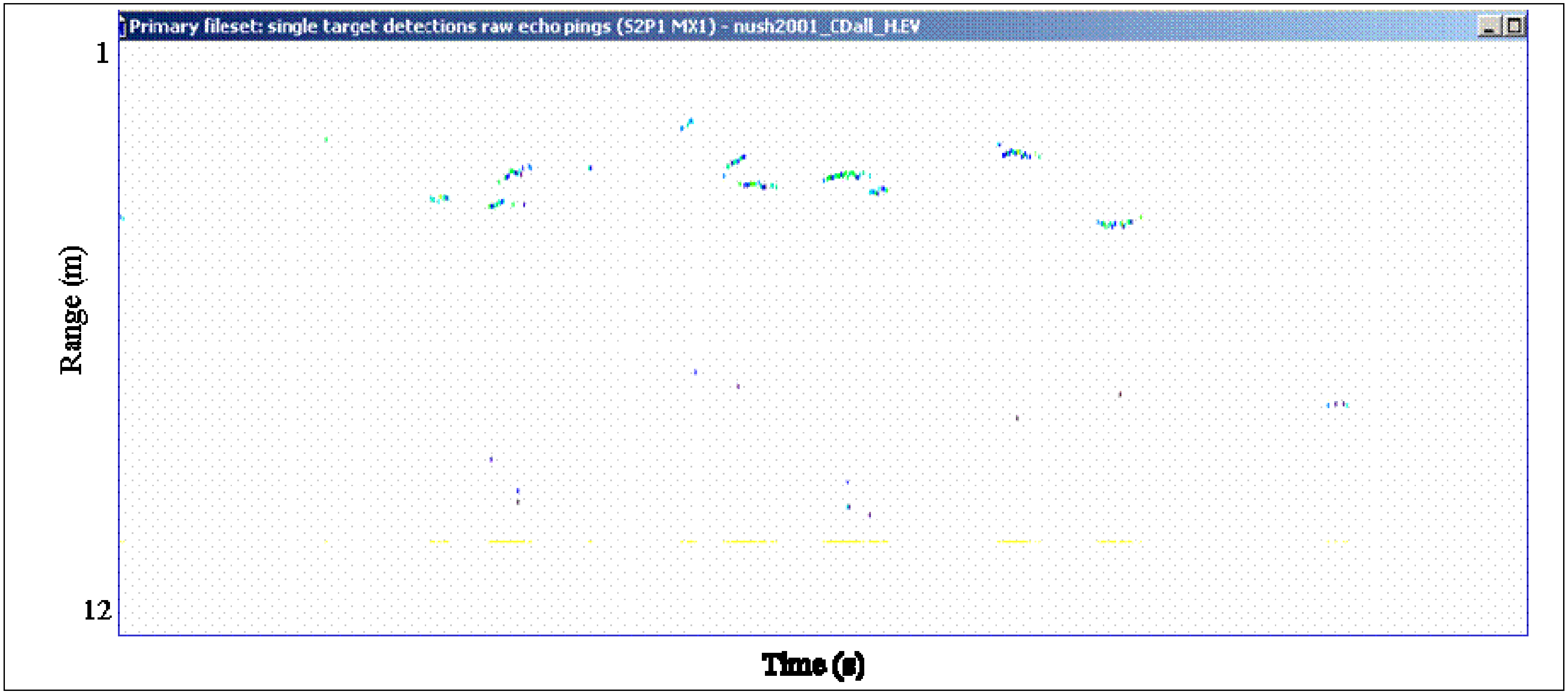

Note: For this aim, there was no interaction with the river bottom within the ensonified range of 12 m.

Figure 27.–An echogram of the nearshore transducer's high aim, July 1, 2001.

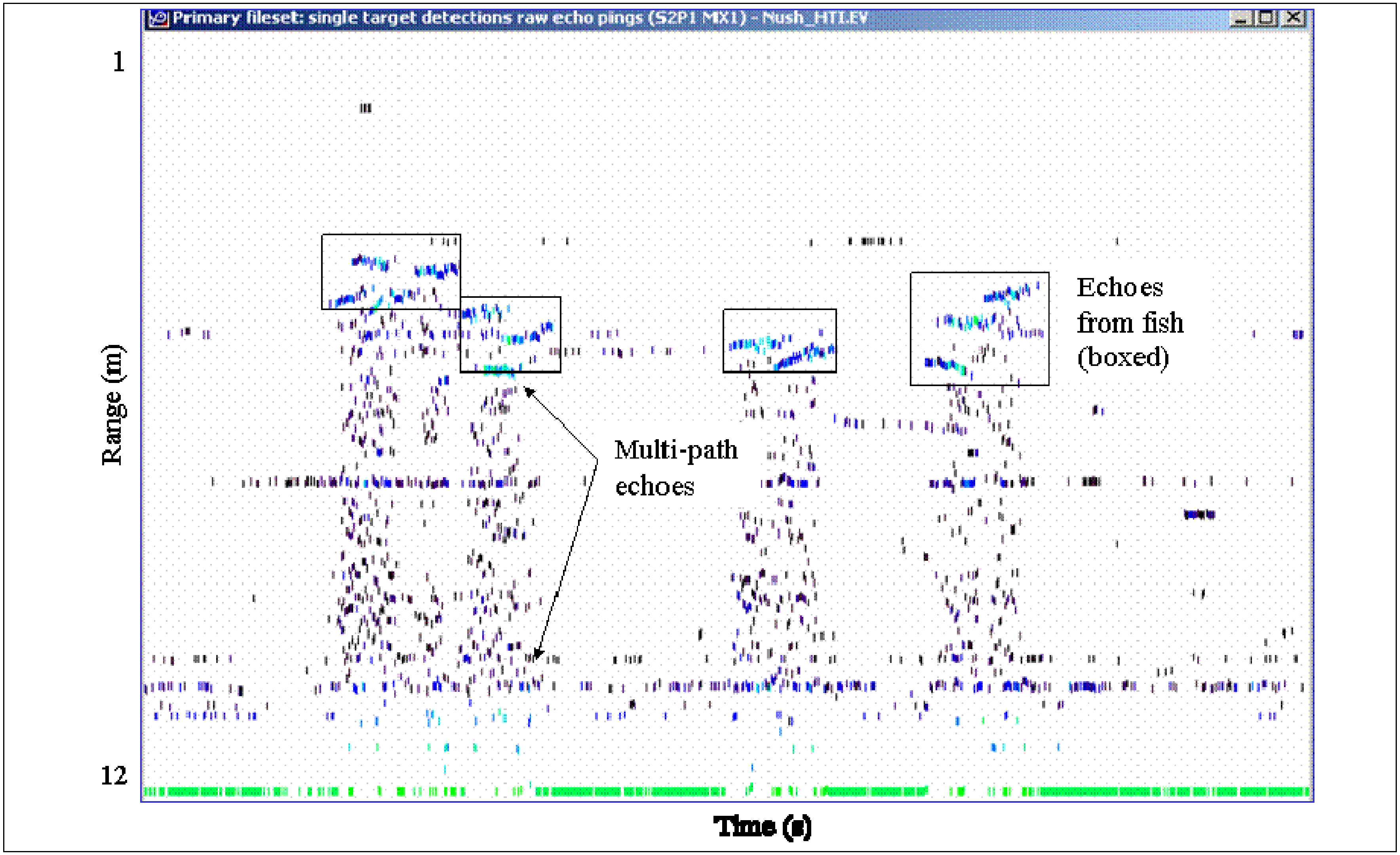

Note: Fish traveling through the beam produced a fountain of echoes reflected off from boundary layers.

Figure 28.–An echogram with an end range of 12 m from the nearshore transducer's low aim, multi-path echoes depend on the depth of the water and the composition of the river bottom, June 21, 2002.

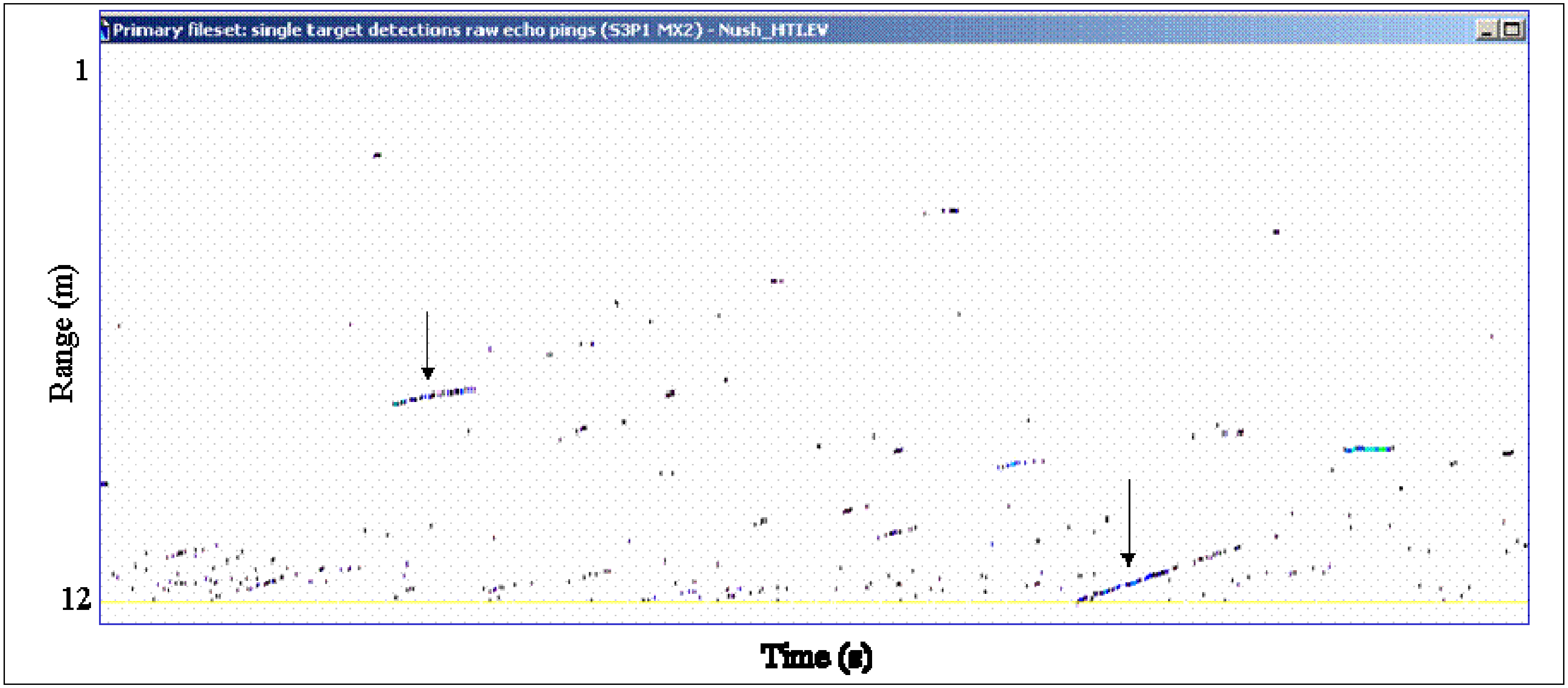

Figure 29.–An echogram from the offshore transducer with arrows pointing to traces from floating plant material, June 30, 2002.

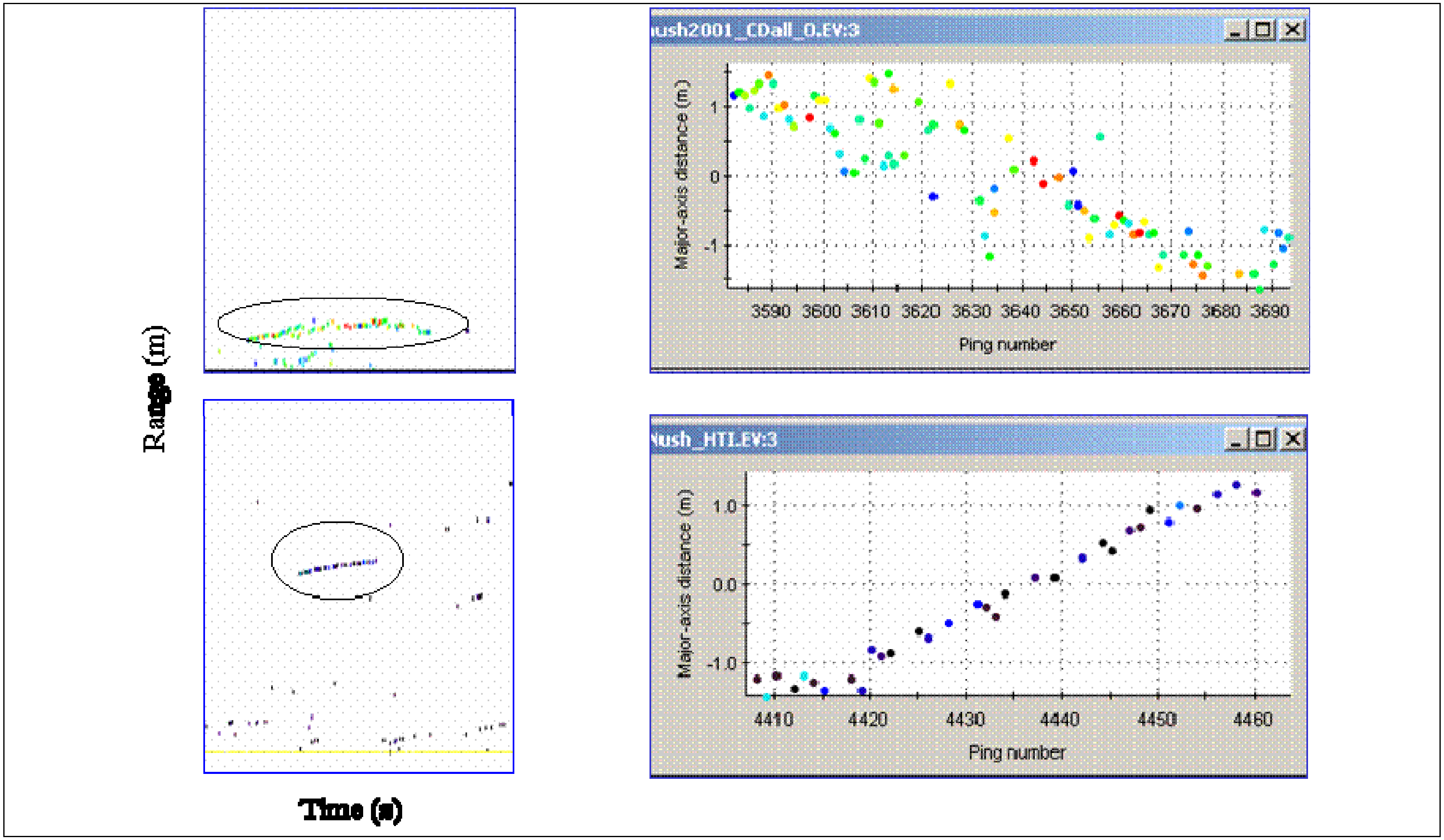

Note: The 2d plot of the fish track contains a great deal more variation in both horizontal and vertical planes compared to the plant material.

Figure 30.–Echograms (left) and 2d plots (right) of a sample fish track (top) and plant material (bottom), June 20, 2002.

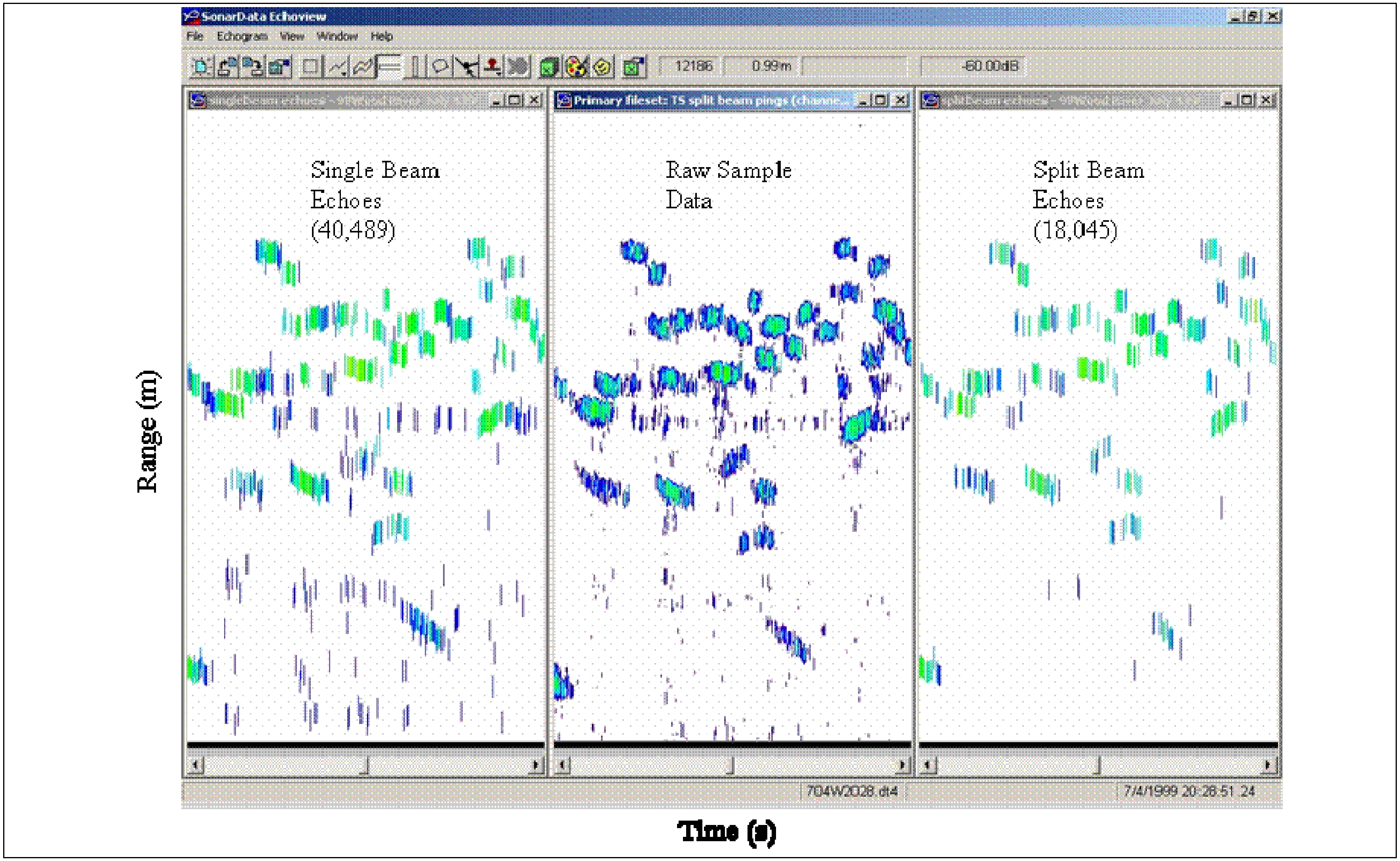

Note: The echo data results in far fewer echoes with the split beam processing when compared to single beam processing. Displayed with SonarData's Echoview software.

Figure 31.–An echogram from the BioSonics' split beam sonar system, showing the raw date (center panel), and the single beam (left) and split beam (right) processed datasets, Nushagak River sonar, 2001.

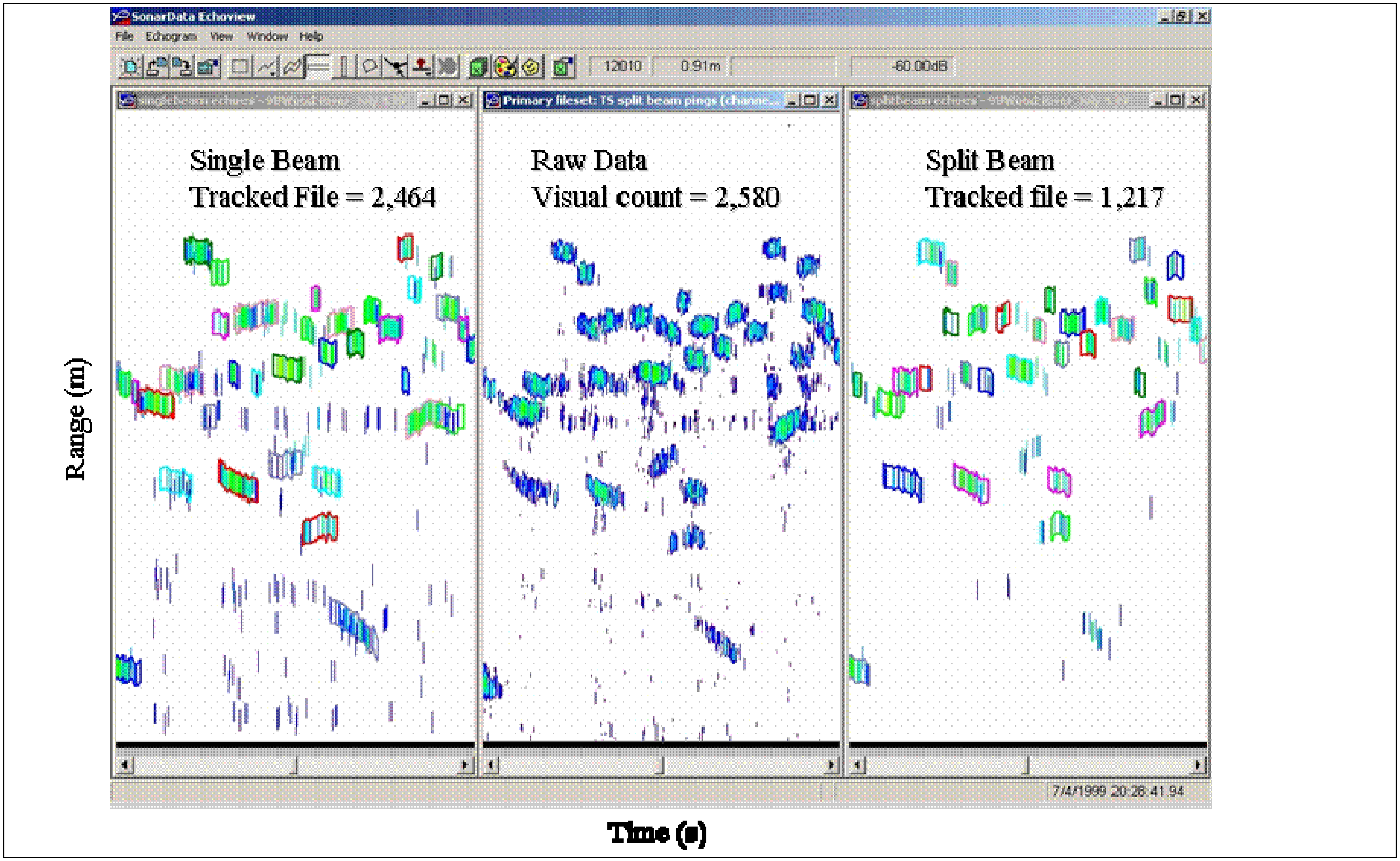

Note: A visual count of the complete data file resulted in 2,580 targets from the raw data, 2,464 targets from the single beam processed data, and 1,217 targets from the split beam processed data.

Figure 32.–Echograms from a BioSonics' sonar showing the raw data (center panel), and the single beam (left) and split beam (right) processed datasets with suspected fish targets tracked (colored outline around the train of echoes).

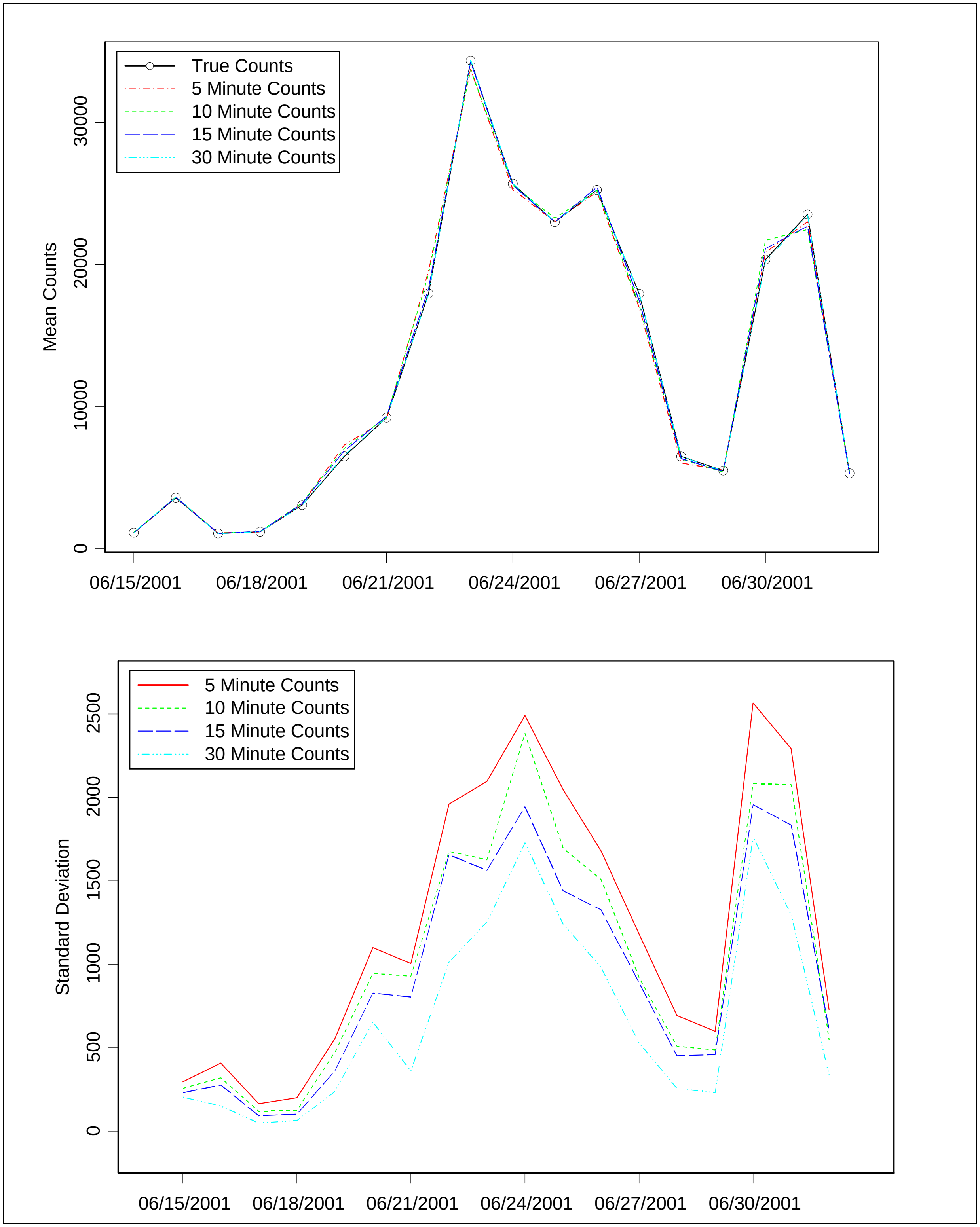

Figure 33.–Estimated mean daily counts (top) and estimated standard deviation (bottom) from simulations with 5-, 10-, 15-, and 30-minute intervals of counting per hour.

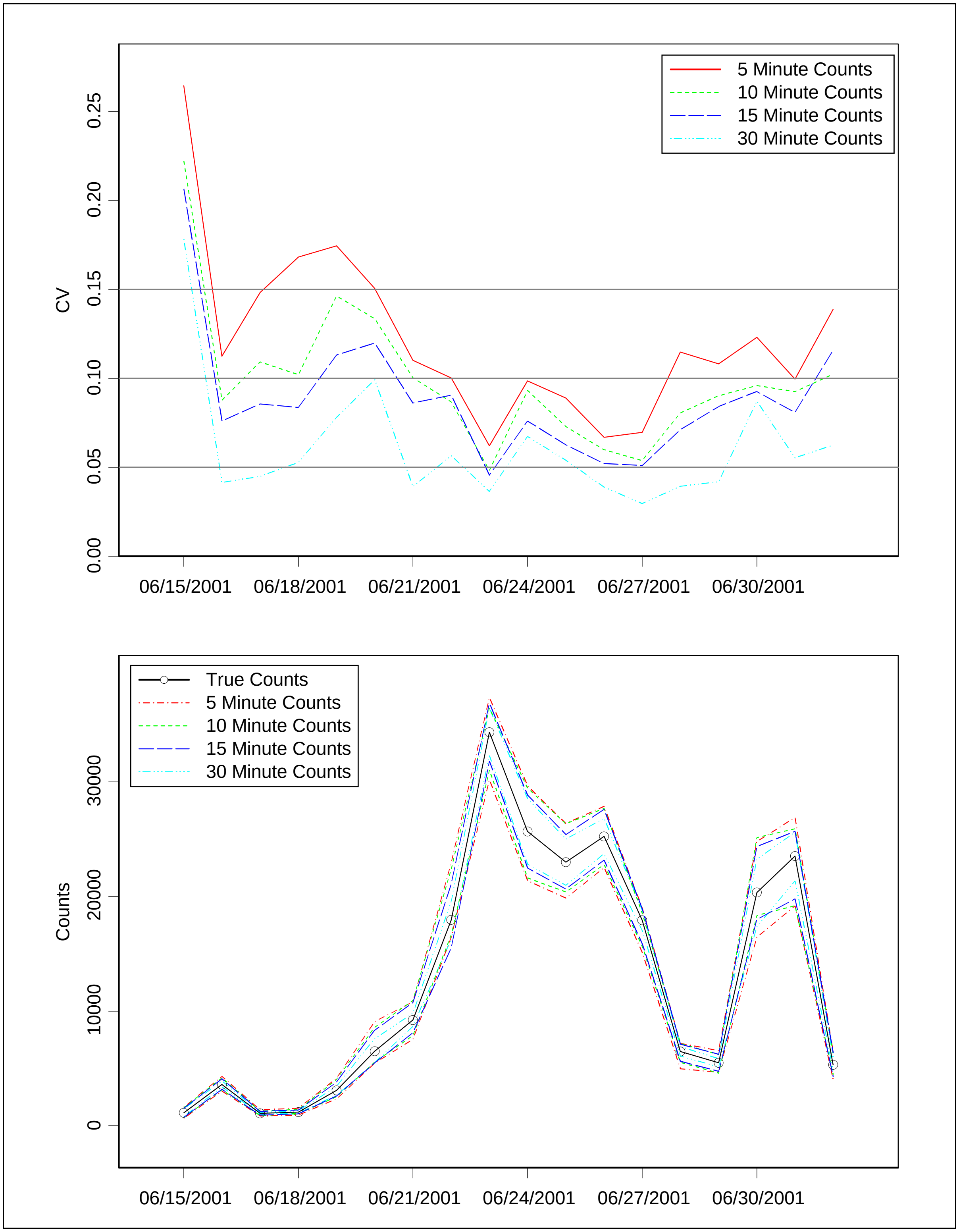

Figure 34.–Estimated coefficient of variation (CV) of estimated daily counts from simulations (top) and true counts with 0.05 and 0.95 quantiles from simulated daily counts (bottom) for 5-, 10-, 15-, and 30-minute intervals of counting per hour.

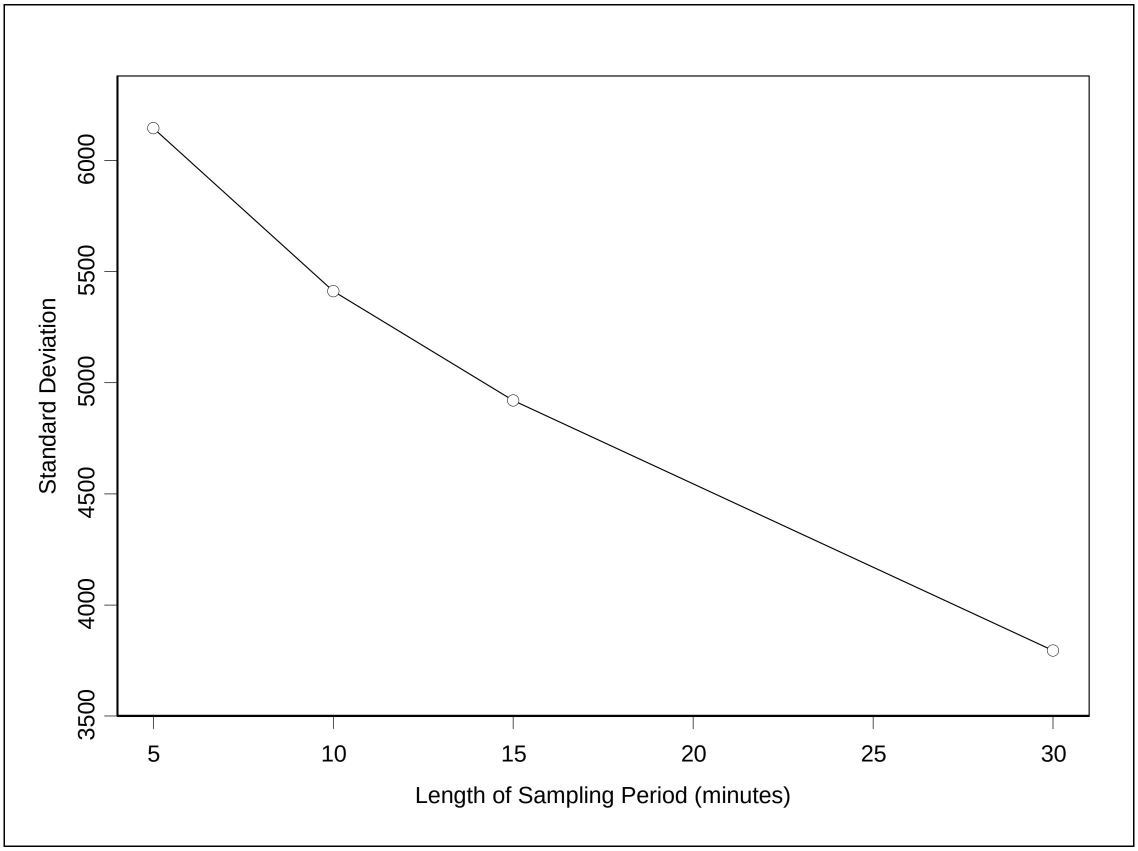

Figure 35.–Standard deviation of cumulative counts plotted against the length of the sampling period.

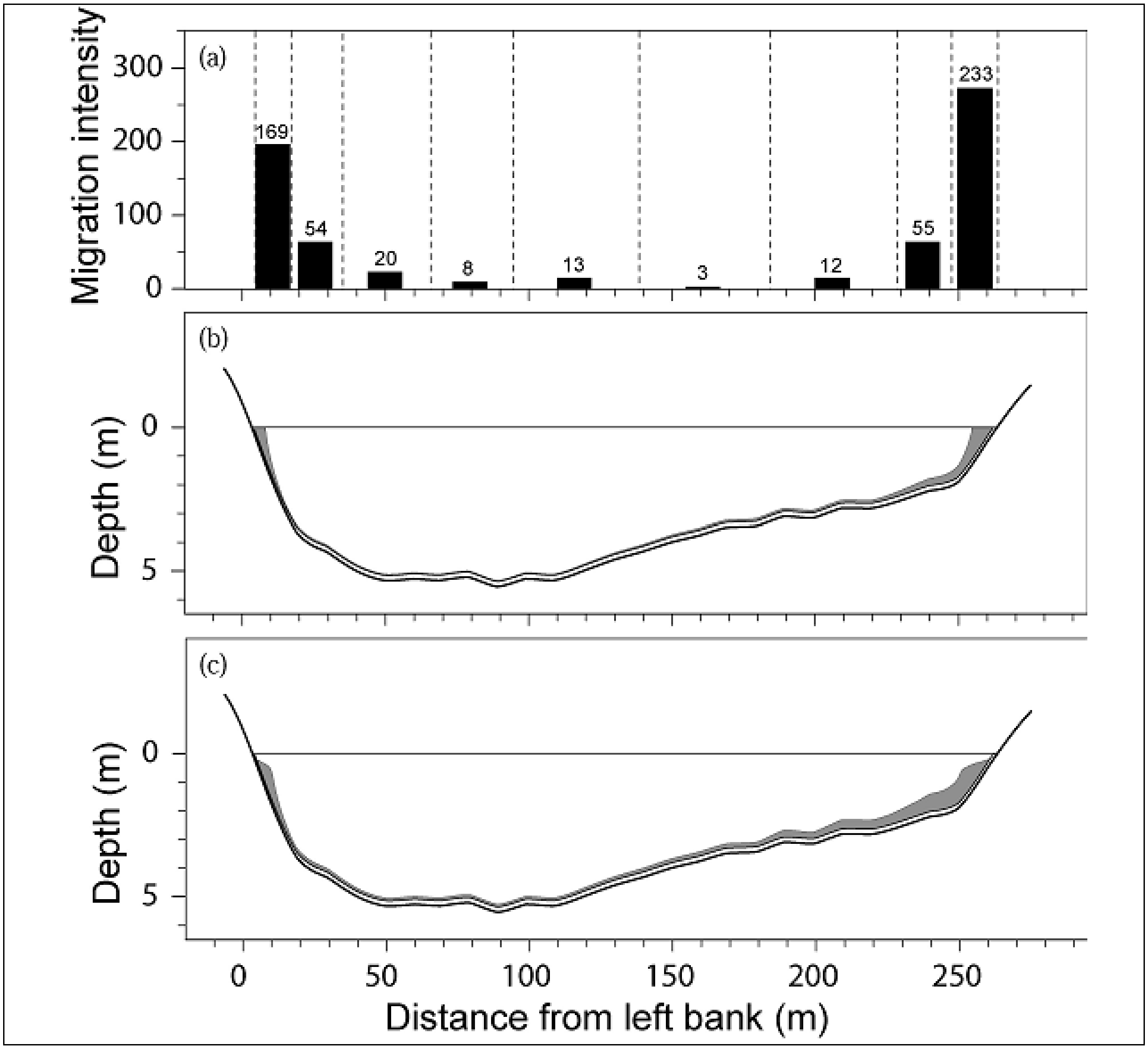

Note: The relative abundance of the salmon are expressed as migration intensity, an estimate of the number of migrants per meter of cross section per 10,000 migrants. The width of the 9 sections varies as shown by the vertical broken lines. Based on the gill-net catch-per-unit-effort data reported by Miller (2000). The shaded area shows that part of the cross-section where the cost-per-unit-distance traveled is no more than twice the minimum cost available to the fish. Reproduced from Hughes (2004) with permission.

Figure 36.–Lateral distribution of sockeye salmon as they migrate past the sonar site on the Nushagak River(a), the predicted cost-minimizing migration corridors under the traditional model (b), and the wave drag model (c).

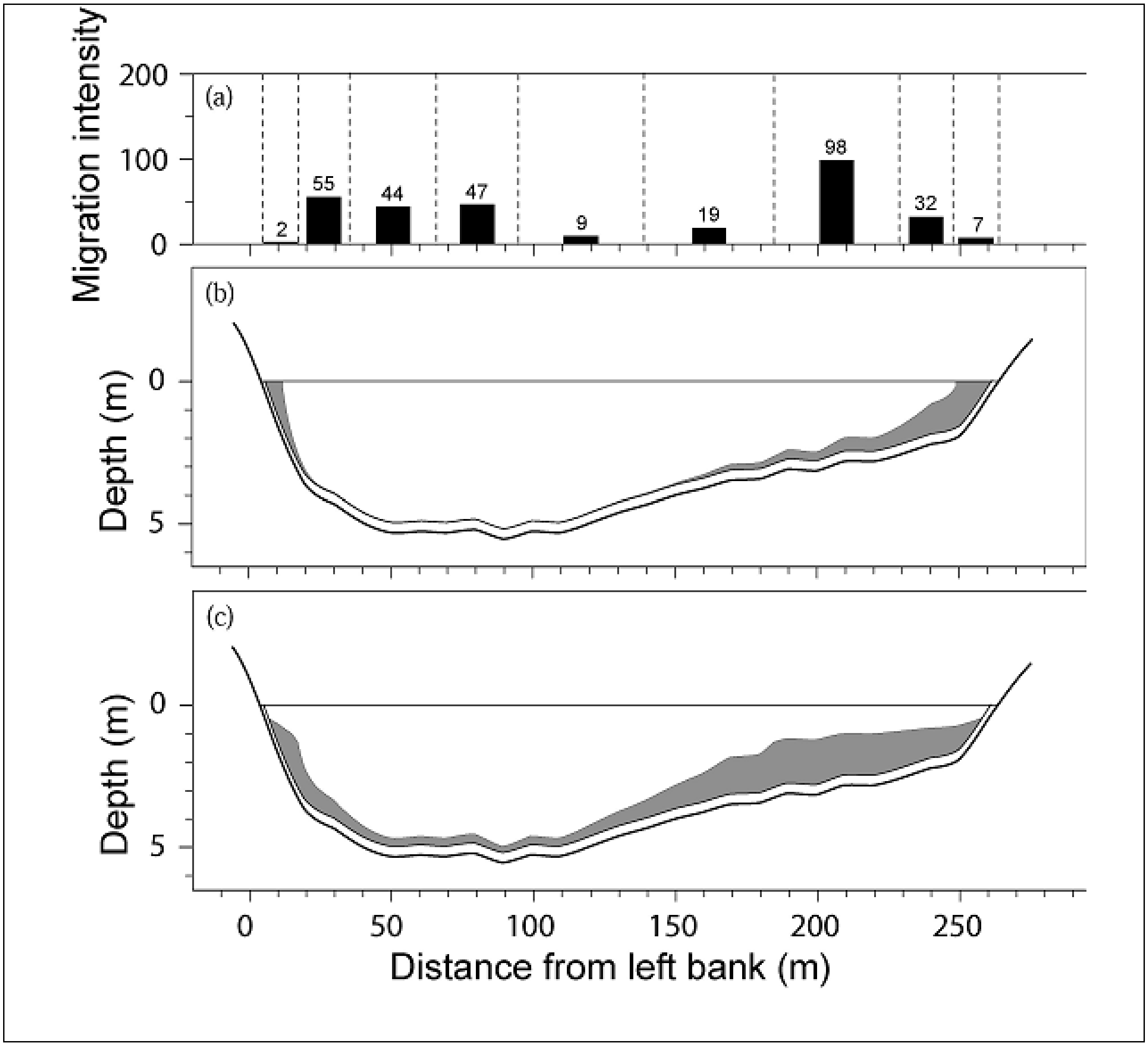

Note: The relative abundance of the salmon are expressed as migration intensity, an estimate of the number of migrants per meter of cross section per 10,000 migrants. The width of the 9 sections varies as shown by the vertical broken lines. Based on the gill-net catch-per-unit-effort data reported by Miller (2000). The shaded area shows that part of the cross-section where the cost-per-unit-distance traveled is no more than twice the minimum cost available to the fish. Reproduced from Hughes (2004) with permission.

Figure 37.–Lateral distribution of Chinook salmon as they migrate past the sonar site on the Nushagak River(a)**,** the predicted cost-minimizing migration corridors under the traditional model (b), and the wave drag model (c).

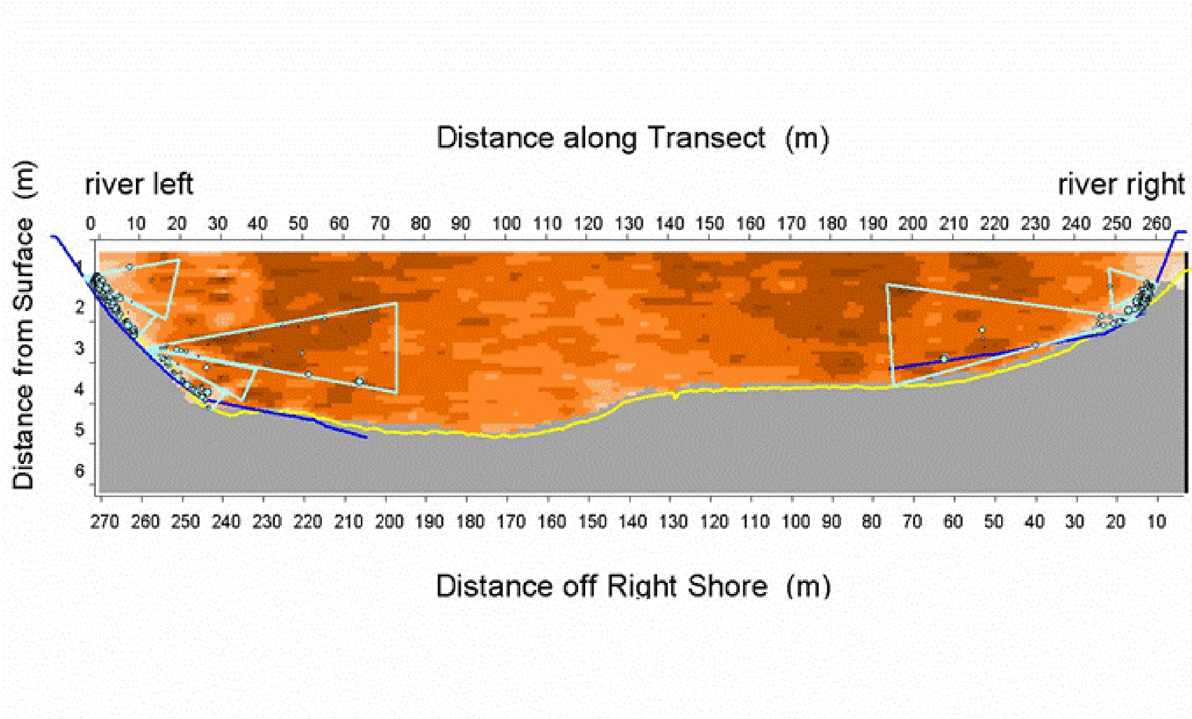

Note: The darker colors indicate faster current.

Figure 38.–Cross river slice of the Nushagak River at the sonar site, transducer beams are drawn in their approximate locations and the fish distribution from 2000 (circles) is shown.

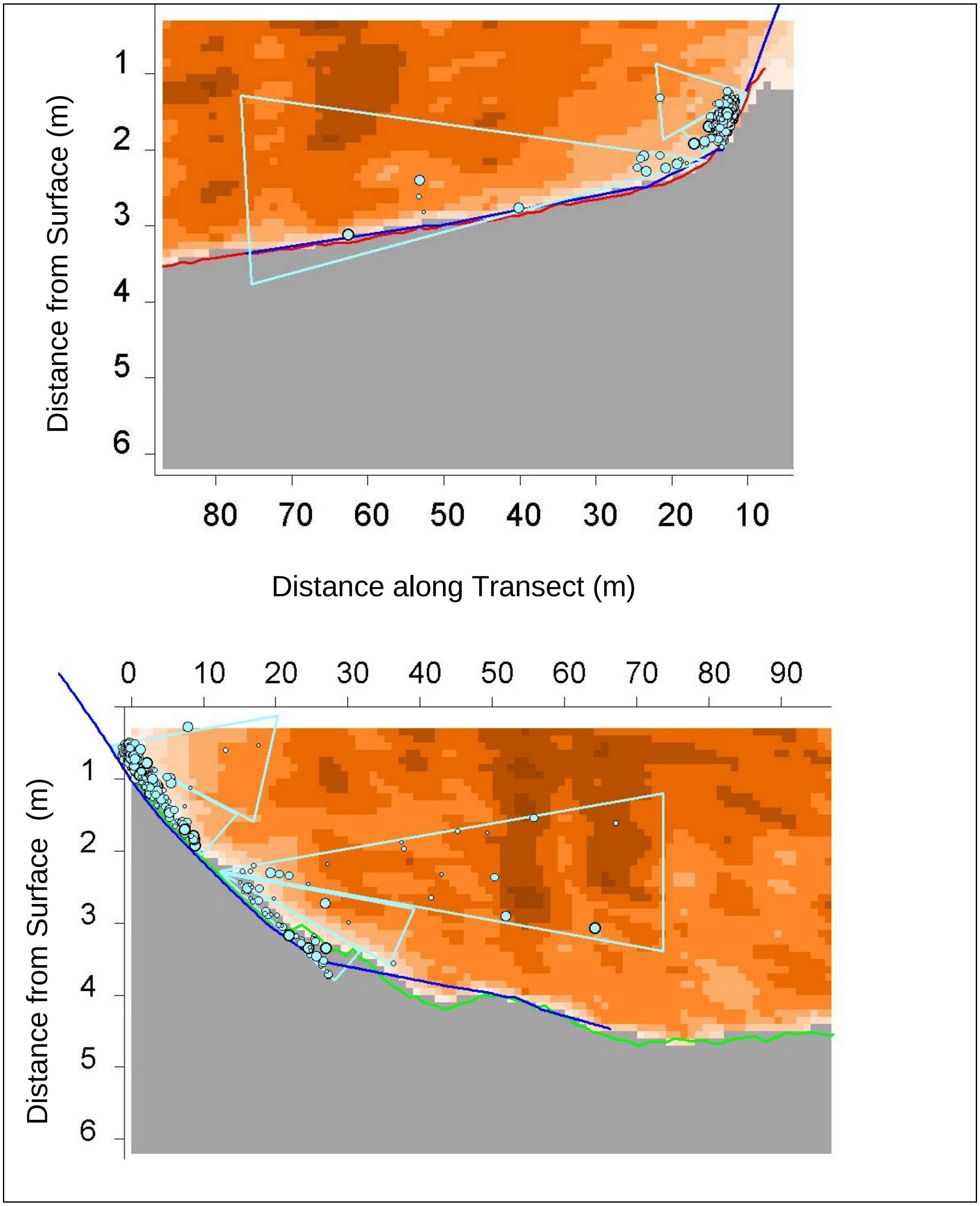

Figure 39.–Fish distribution (circles) and flow along the right bank (top) and left bank (bottom) of the Nushagak River at the location of the HTI split beam transducer with the transducer beams overlaid.

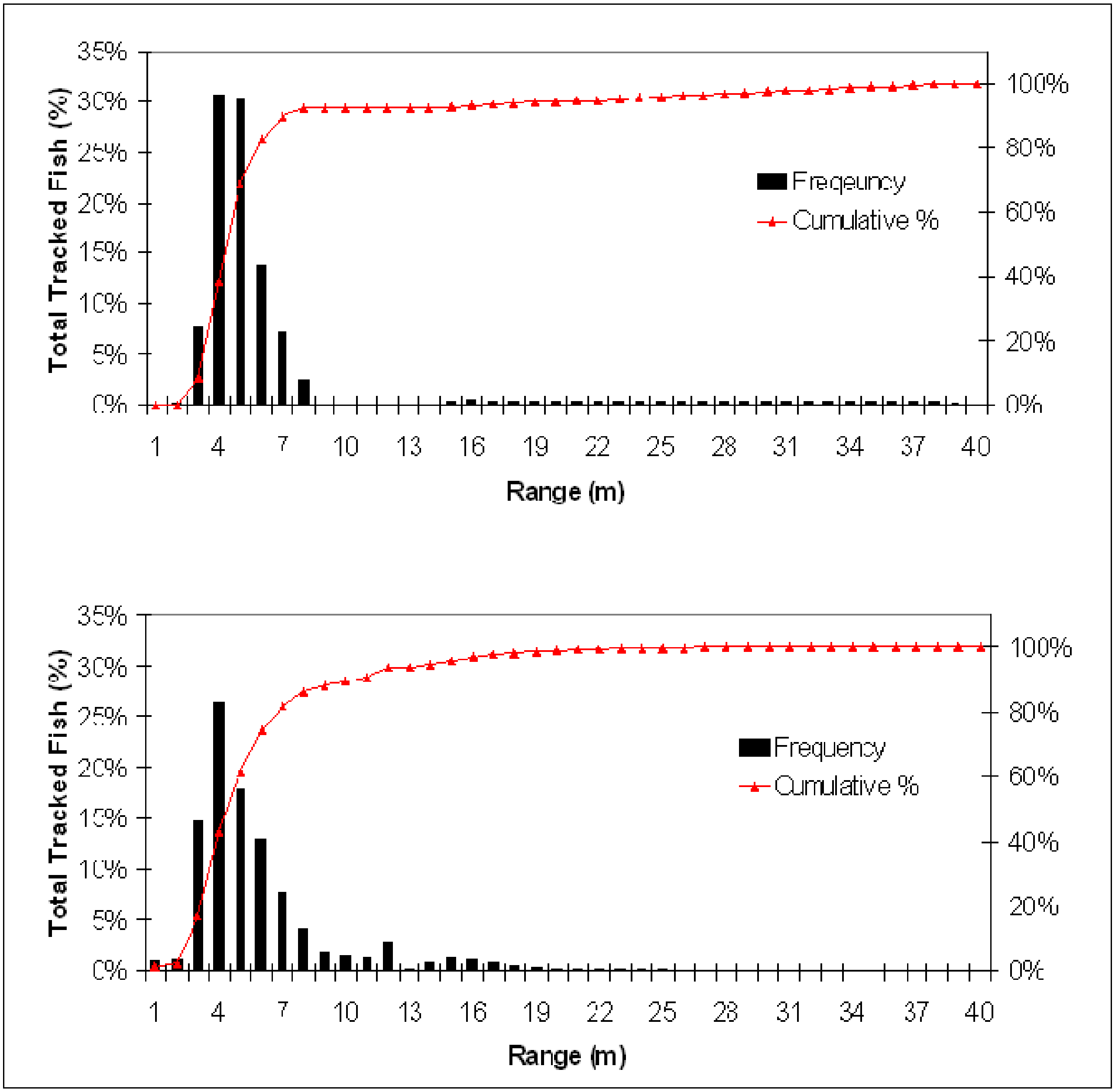

Figure 40.–Range distributions of tracked fish from the HTI system (top) and Bendix (bottom), Nushagak River right bank, 2001.

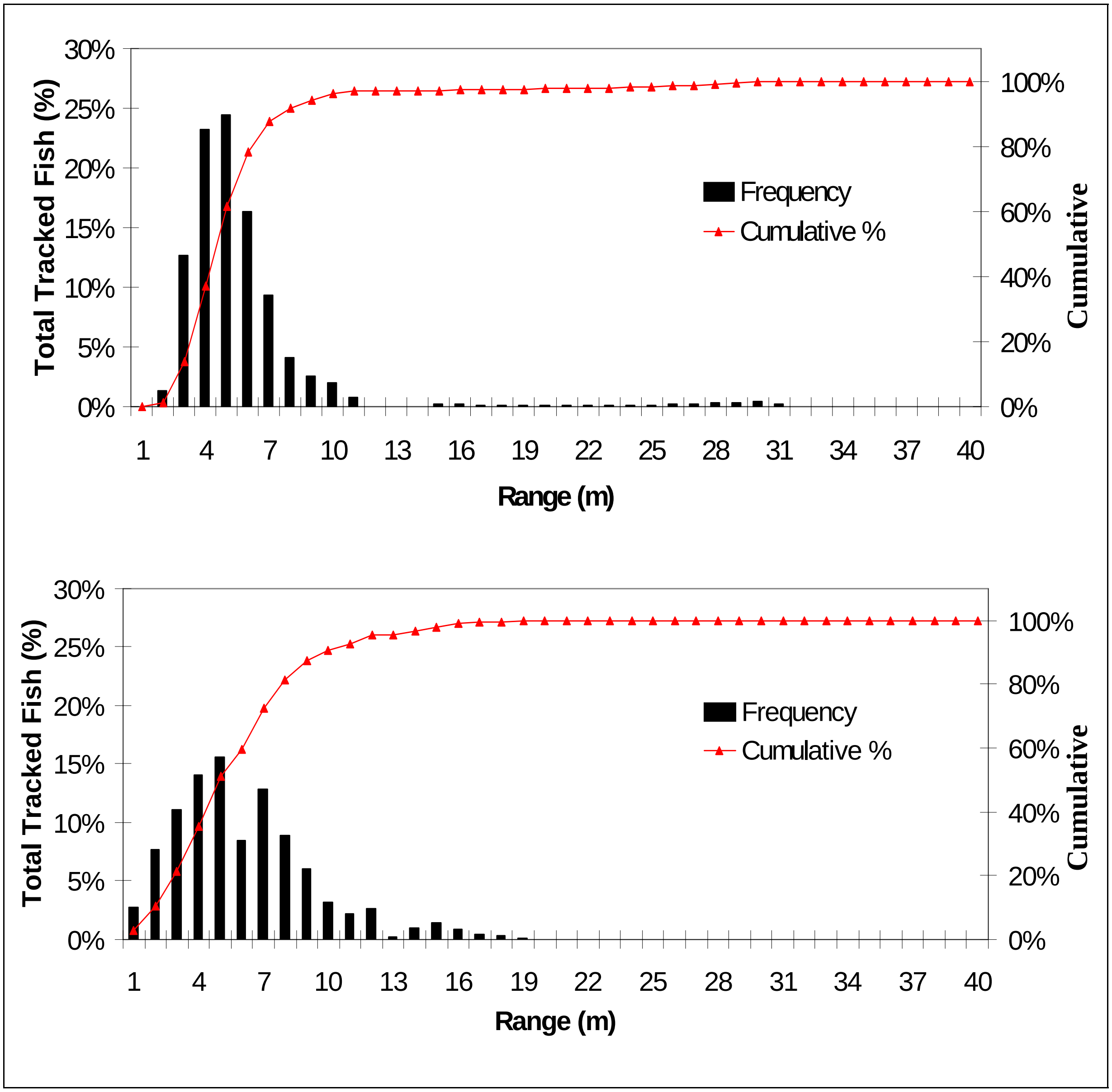

Figure 41.–Range distributions of tracked fish from the HTI system (top) and Bendix (bottom), Nushagak River right bank, 2002.

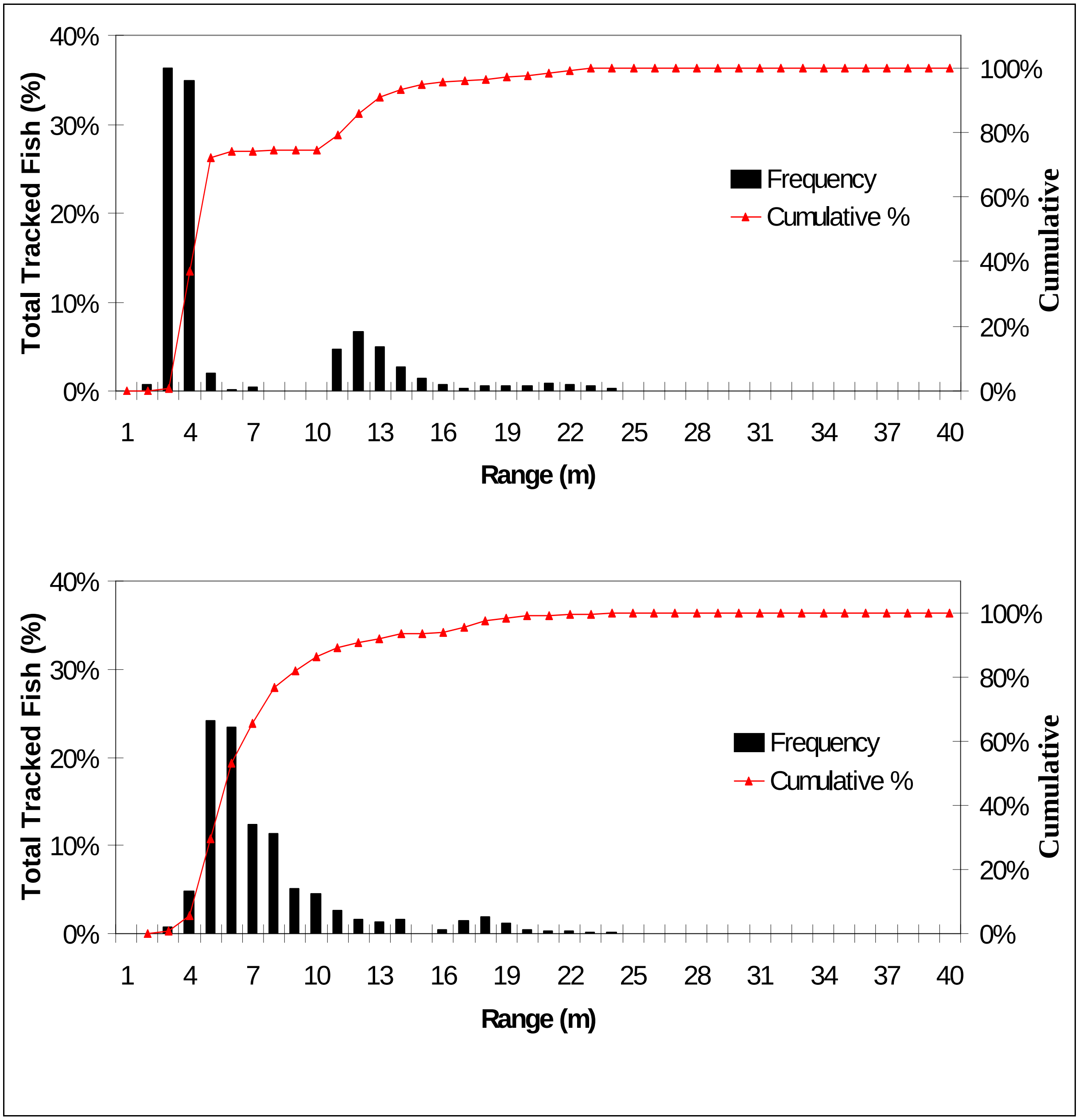

Figure 42.–Range distributions of tracked fish from the HTI system (top) and the Bendix (bottom), Nushagak River right bank, 2003.

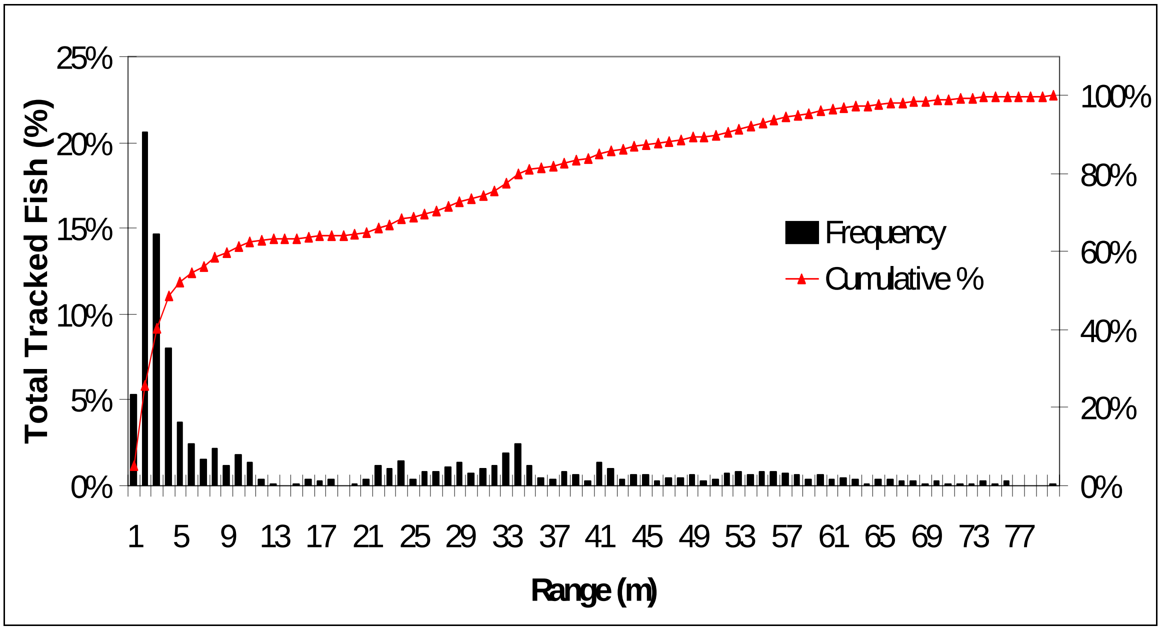

Figure 43.–Range distribution of tracked fish from the HTI system, Nushagak River left bank, July 2, 2000.

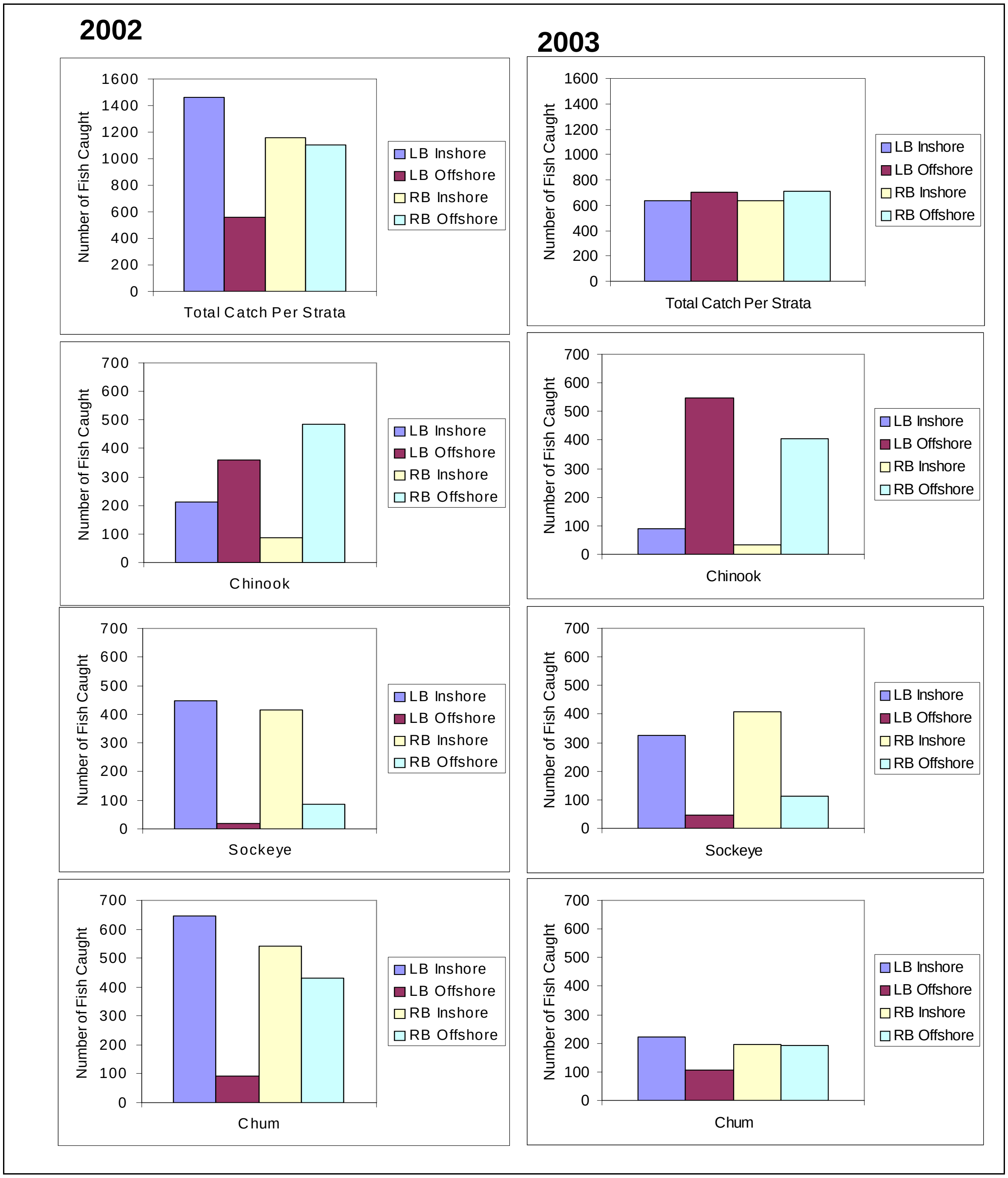

Figure 44.–Distribution of fish by strata for Chinook, sockeye, and chum salmon captured in the drift gillnet test-fishing project at the Nushagak River, 2002 (left) and 2003 (right).

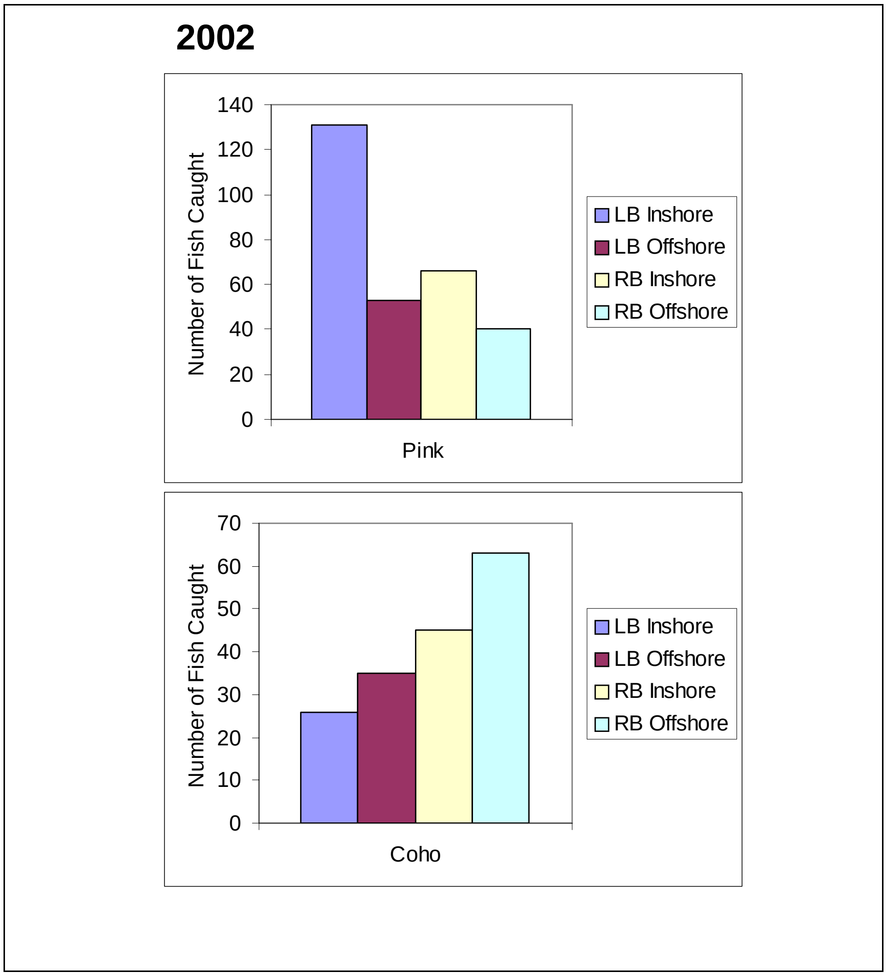

Figure 45.–Distribution of fish by strata for pink and coho salmon captured in the drift gillnet test-fishing project at the Nushagak River, 2002.

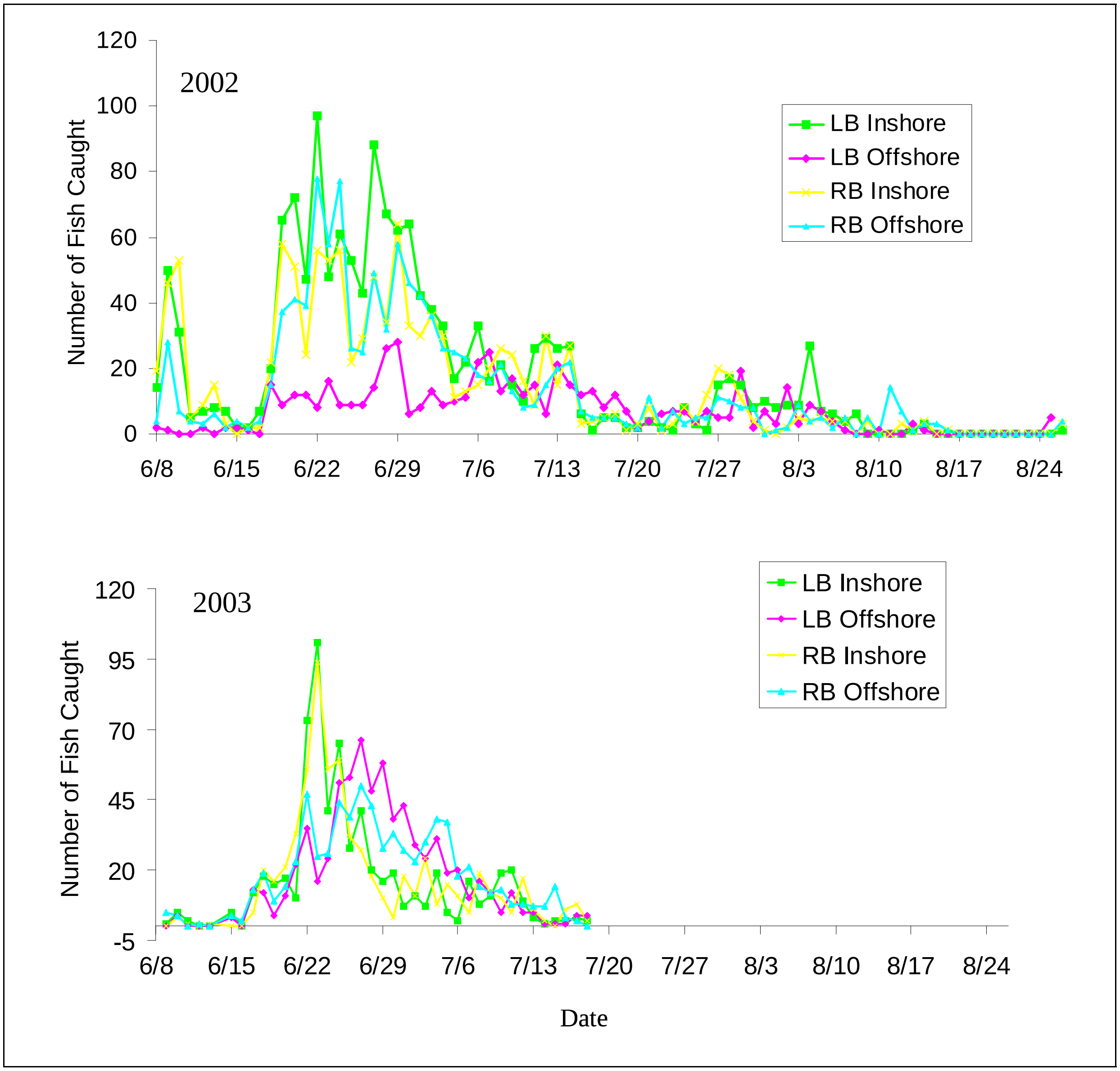

Figure 46.–Daily percentage of fish captured at each of the drift stations in the Nushagak River at the sonar site, 2002 (top) and 2003 (bottom).

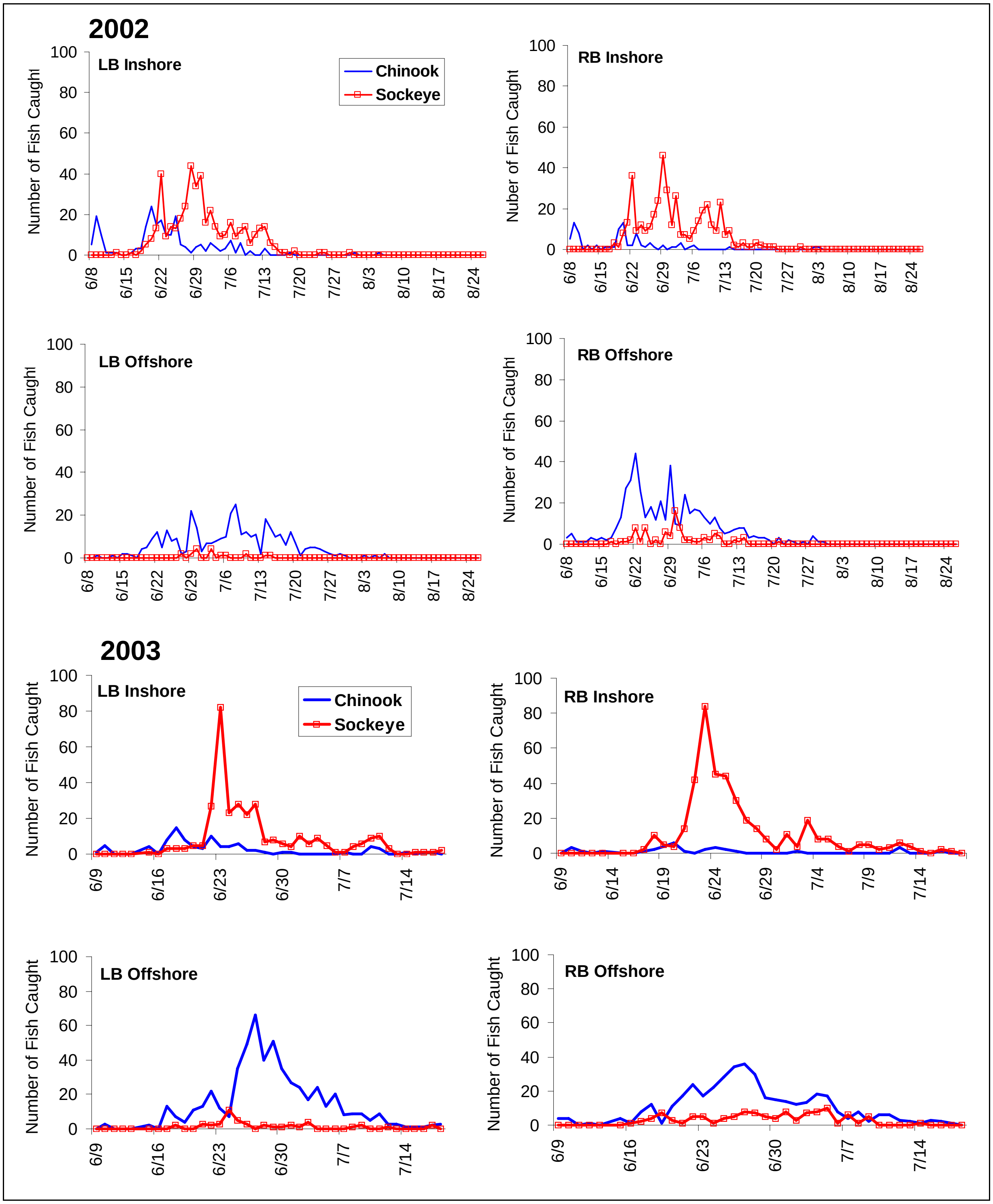

Figure 47.–Daily numbers of sockeye and Chinook salmon captured at each of the drift stations in the Nushagak River at the sonar site, 2002 and 2003.

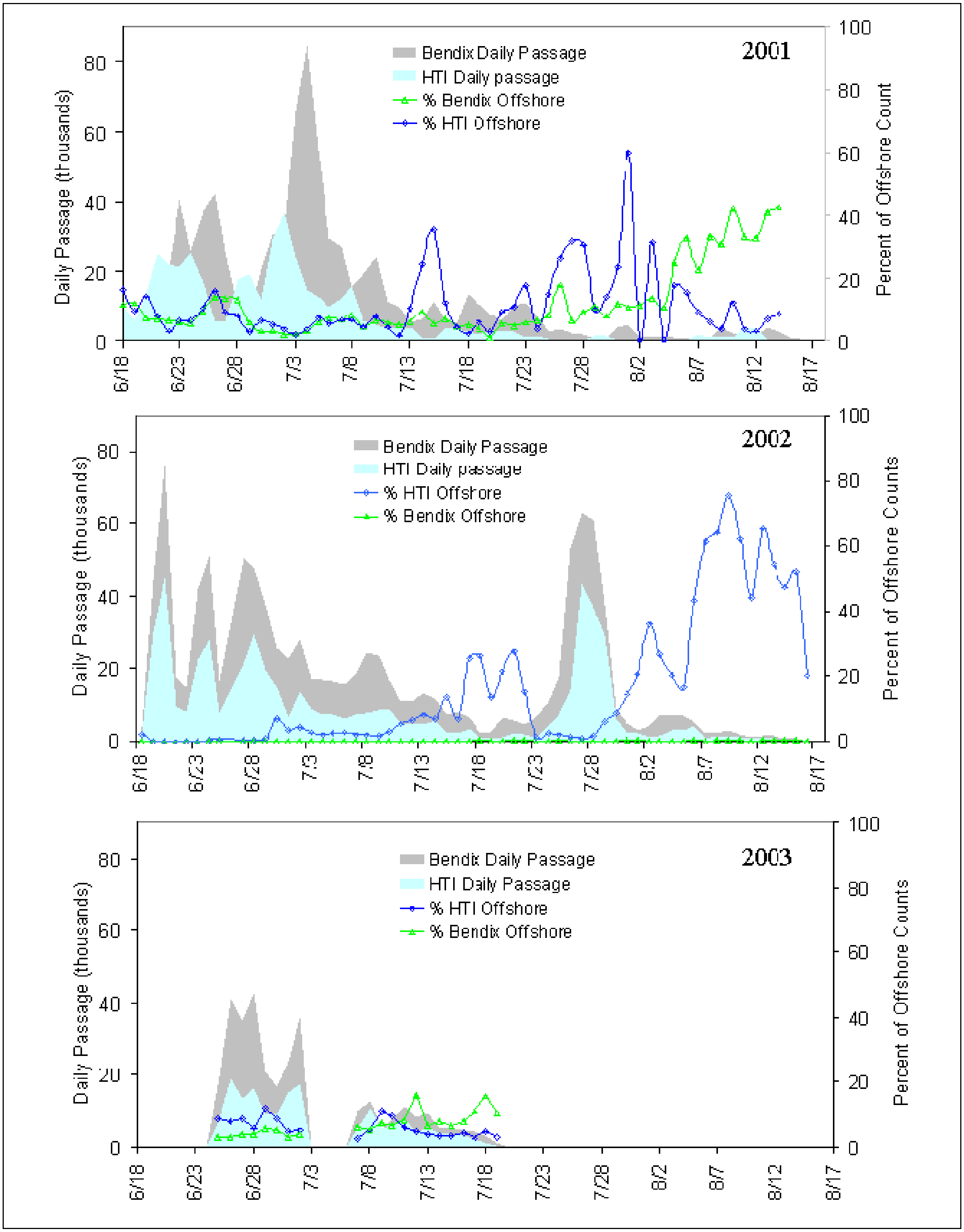

Figure 48.–Daily passage estimates of migrating salmon and the percent of offshore fish from the HTI and Bendix sonars, Nushagak River, 2001–2003.

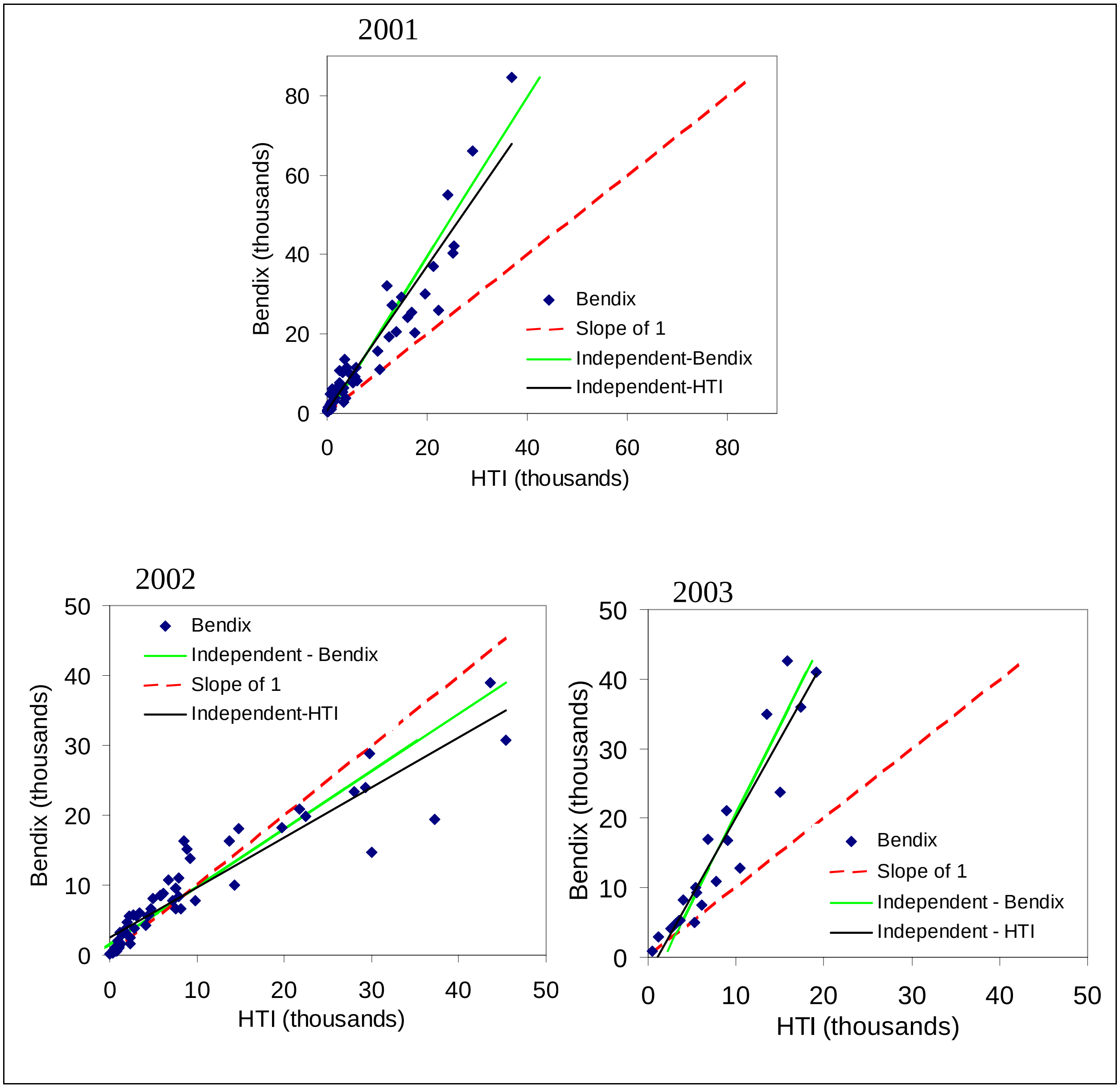

Figure 49.–Daily fish passage regression plots with regression lines using each variable as the independent variable from paired HTI and Bendix datasets collected along the right bank of the Nushagak River, 2001–2003.

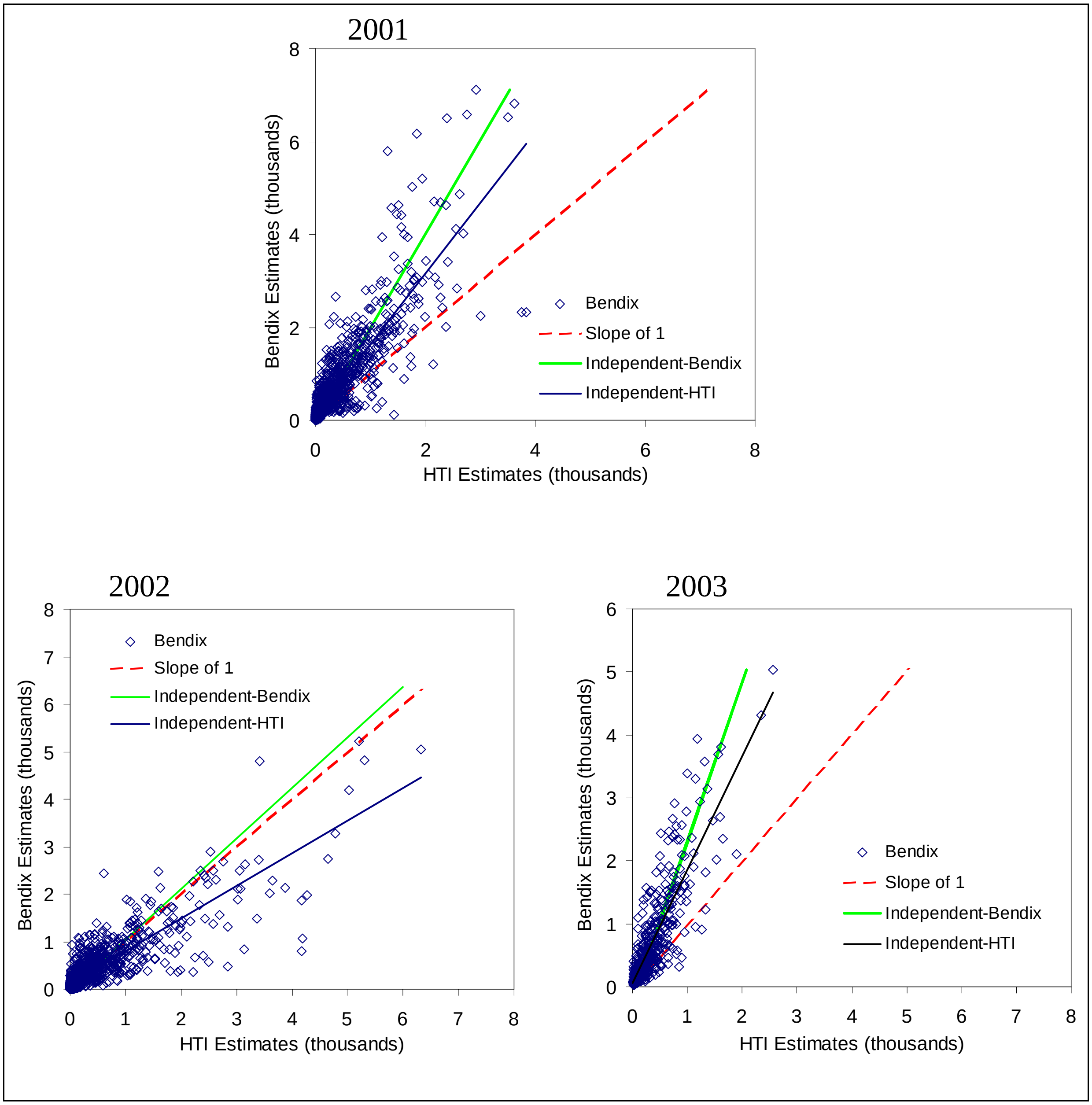

Figure 50.–Hourly passage estimate regression plots with regression lines using each variable as the independent variable, right bank Nushagak River, 2001–2003.

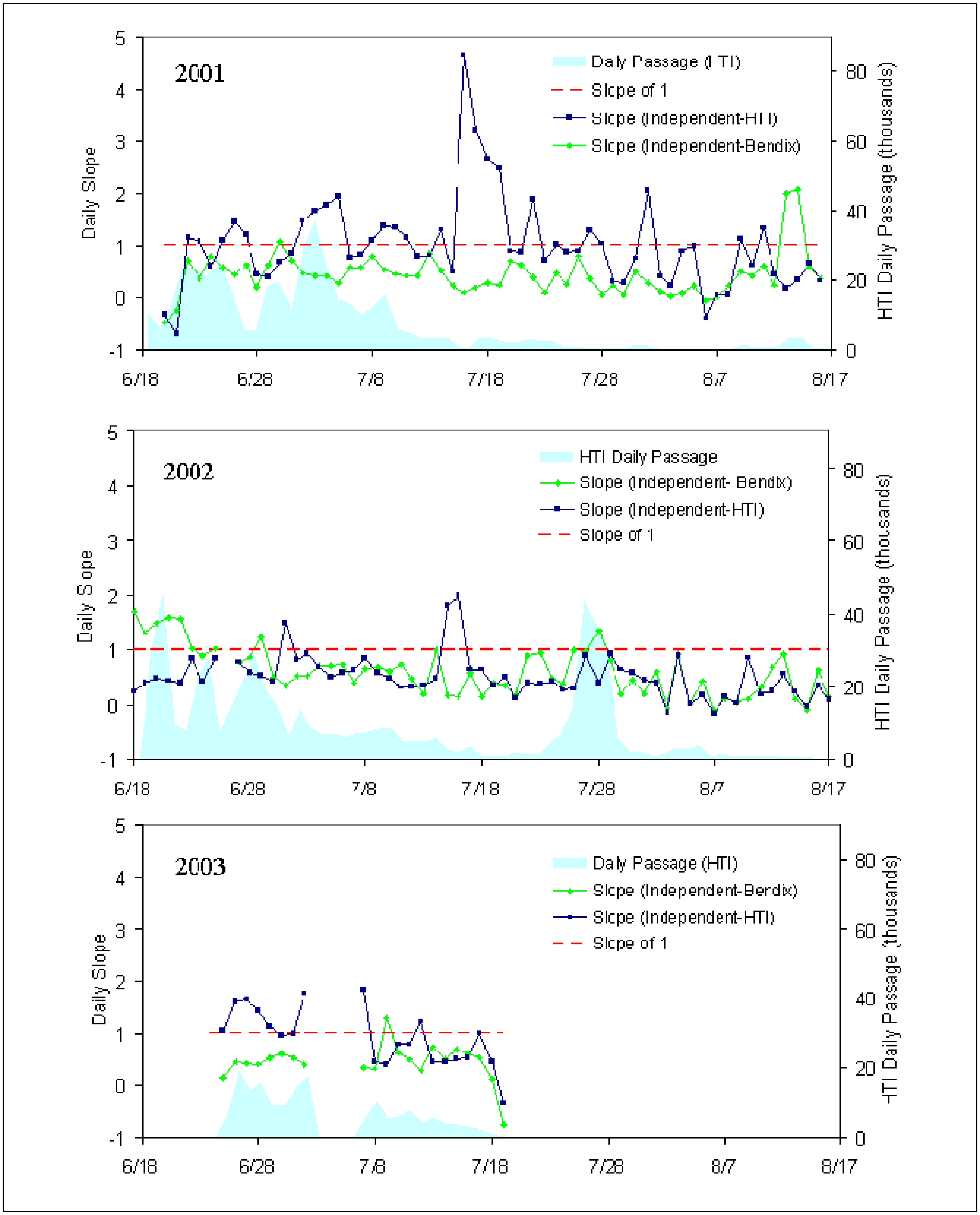

Note: The HTI daily passage estimates are shown for reference purposes.

Figure 51.–Slope values from daily regressions of the hourly HTI and Bendix sonar data with each variable used as the independent variable, Nushagak River right bank, 2001–2003.

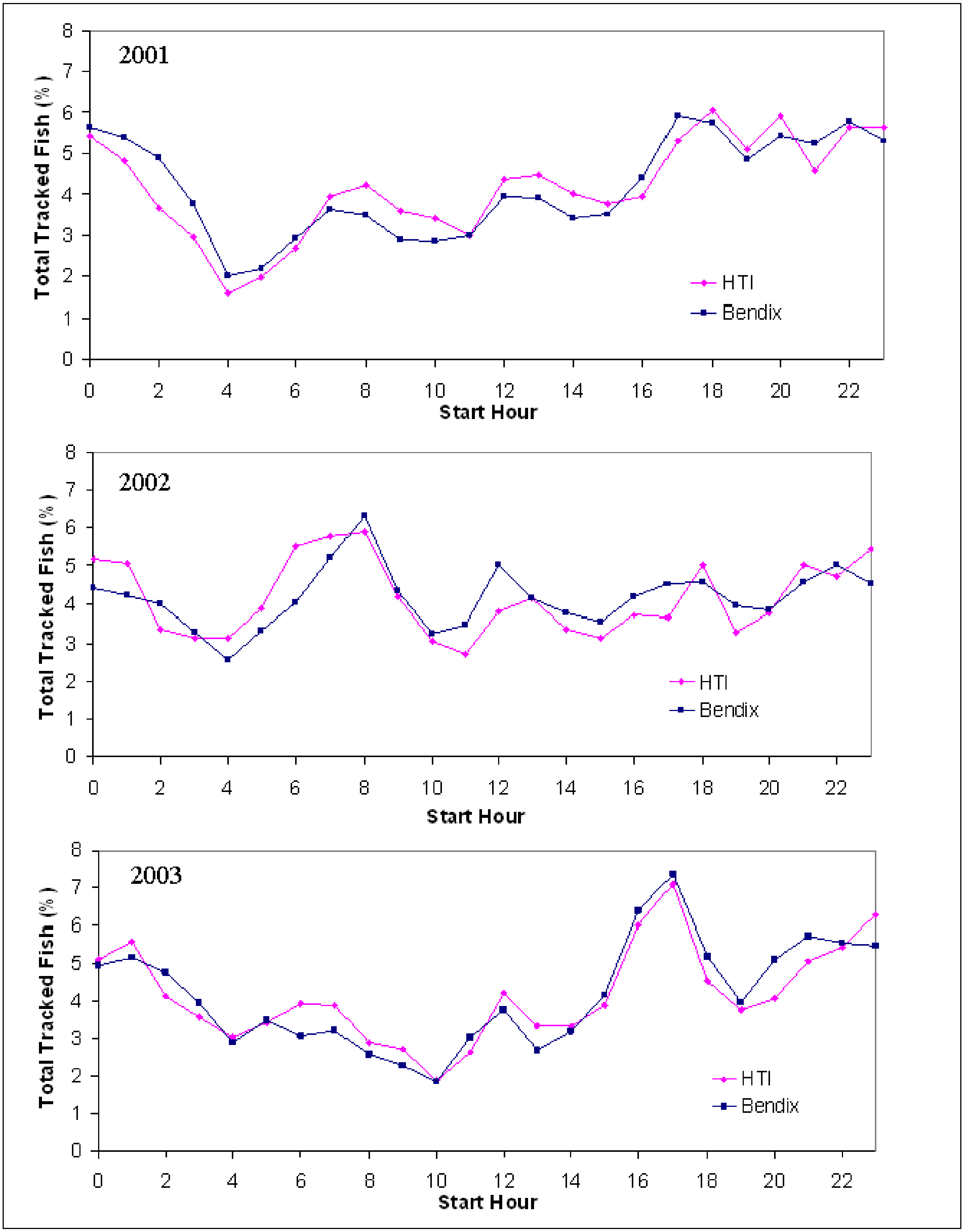

Figure 52.–HTI and Bendix estimated fish passage summed per hour across the field season along the right bank of the Nushagak River, 2001–2003.

APPENDIX A.

Appendix A1.–Laboratory calibrations for the split-beam sonar.

Hydroacoustic Technology, Inc.

ADF&G MAXWELL
TRANSDUCER CALIBRATION FOR
MODEL 241 SPLIT-BEAM SYSTEM
NUSHAGAK
MAY 30, 2002

Hydroacoustic Technology, Inc.
715 NE Northlake Way
Seattle, WA 98105
USA
(206) 633-3383
(206) 633-5912 fax
e-mail: consulting@HTIsonar.com

023-0044-9A Calibration Cover Sheet

-continued-

200 KHz – 2X10 Degree –400ft

S/N 1014819

-continued-

Hydroacoustic Technology Inc.

HTI

Standard Sphere Calibration

		Freq	200 KHz
Customer	ADFG MAXWELL	Transducer S/N	1014819
Project Name	NUSHAGAK	Beam Width	~~4X10~~ Deg 2X10
Calibration Location	HTI-Impulse	Echo Sounder S/N	1320758
Customer Contact	SUSIE MAXWELL	Model #	241
Calibrated by	BK, GH	Calibration Date	14-Nov-01
		Calibration File	819S758 .xls
Sphere Type	38.1 mm Tungsten-carbide	Cable Length	400 Feet

FILE NAME RAW / MDB	RX Gain dB	TVG Gain dB	TX Pwr dBW	PW ms	Pulse Type	Chirp BW KHz	Range m	Echoes #	TS dB	Std. DEV dB
S3181409	-6	0	20	0.40	NORM	0.0	6.08	648	-38.71	0.63
S3181412	-6	0	20	5.00	CHIRP	10.0	6.05	142	-40.58	0.52
S3181413	-6	0	20	2.50	CHIRP	10.0	6.05	322	-40.06	0.53
S3181415	-6	0	20	1.25	CHIRP	10.0	6.03	552	-39.42	0.53

-continued-

Hydroacoustic Technology, Inc.

HTI

Hydroacoustic System Calibration

		Frequency (kHz)	200
Customer	ADF&G	Transducer S/N	1014819
Project Name	Nushagak	Beam Width	2X10
Calibration Location	HTI-Impulse	Echo Sounder S/N	1320758
Customer Contact	Susie Maxwell	Model #	241
Calibrated by	BK, GH	Calibration Date	14-Nov-01
		G1+SL20 =	48.00 dB

Echo Sounder

Arguments to: TVG	1 2 0 42 0 3 1	Arguments to: RX	0
Arguments to: TRIG	00/10	Arguments to: REP	100 10
Arguments to: TX	1-2 to 1-20	Arguments to: MUX	1
Arguments to:FILTER	3	Arguments to:	

Frequency	200	kHz	Band Width	n/a	kHz
Receiver Gain (Rg)	0	dB	Pulse Width	0.5	msec
TVG Full Range	n/a	m	Blanking Control	3	
TVG Crossover	11.22	m	Blanking Min	1	m
TVG Cal Rng (Rcal)	11.22	m	Blanking Max	2	m
Alpha (a)	0	dB/km	Rel Noise (wet)	-34.8	dBV
RCAL @ T 0 42 TX 1 20	not measured	Vdet40		(T 0 82 .. CWFILT 4)	

Cable

Cable S/N	1302026+030	Cable Length	400	ft
Cable Type	Split-beam	Mux Port	2	

Standard Transducer

Type	ITC-5323	Ts =	124.1	dBuPa/V
S/N	007	Ss =	-223.84	dBv/uPa
Last Calibration	Nov 25, 2000 PAS			
		Preamp Gain 20=	13.39	dB
LP Filter	100 x 1k	Equiv. Ss20 =	-210.45	dBv/uPa
HP Filter	300 x 1k			
		Preamp Gain 40=	33.34	dB
		Equiv. Ss40 =	-190.5	dBv/uPa

Air and Water Parameters

Air Temperature	62	°F	Calibration Depth	4.57	m
Water Temperature	51.8	°F	Separation (Rs)	6.1	m

Filename: 819S758.xls

Page 1

-continued-

Hydroacoustic Technology, Inc.

HTI

Hydroacoustic System Calibration

		Frequency (kHz)	200
Customer	ADF&G	Transducer S/N	1014819
Project Name	Nushagak	Beam Width	2X10
Calibration Location	HTI-Impulse	Echo Sounder S/N	1320758
Customer Contact	Susie Maxwell	Model #	241
Calibrated by	BK, GH	Calibration Date	14-Nov-01
		G1+SL20 =	48.00 dB

Echo Sounder

Arguments to: TVG	1 2 0 42 0 3 1	Arguments to: RX	0
Arguments to: TRIG	00/10	Arguments to: REP	100 10
Arguments to: TX	1-2 to 1-20	Arguments to: MUX	1
Arguments to:FILTER	3	Arguments to:	

Frequency	200	kHz	Band Width	n/a	kHz
Receiver Gain (Rg)	0	dB	Pulse Width	0.5	msec
TVG Full Range	n/a	m	Blanking Control	3	
TVG Crossover	11.22	m	Blanking Min	1	m
TVG Cal Rng (Rcal)	11.22	m	Blanking Max	2	m
Alpha (a)	0	dB/km	Rel Noise (wet)	-34.8	dBV
RCAL @ T 0 42 TX 1 20	not measured	Vdet40		(T 0 82 .. CWFILT 4)	

Cable

Cable S/N	1302026+030	Cable Length	400	ft
Cable Type	Split-beam	Mux Port	2	

Standard Transducer

Type	ITC-5323	Ts =	124.1	dBuPa/V
S/N	007	Ss =	-223.84	dBv/uPa
Last Calibration	Nov 25, 2000 PAS			
		Preamp Gain 20=	13.39	dB
LP Filter	100 x 1k	Equiv. Ss20 =	-210.45	dBv/uPa
HP Filter	300 x 1k			
		Preamp Gain 40=	33.34	dB
		Equiv. Ss40 =	-190.5	dBv/uPa

Air and Water Parameters

Air Temperature	62	°F	Calibration Depth	4.57	m
Water Temperature	51.8	°F	Separation (Rs)	6.1	m

Filename: 819S758.xls

Page 1

-continued-

Hydroacoustic Technology, Inc.

HTI

Receiving Sensitivity

Transducer S/N	1014819
Sounder S/N	1320758

Voltage Into Standard Vs (Generator at 23 dBm)

Vs= 6.22 *volts (rms)*

Vs= 15.87 dBVrms

Transmission Loss TL = 20 log Rs + aRs

TL = 15.71 dB

Acoustic Level L = Ts + Vs - TL

L = 124.26 dB/uPa

Sum Channel Detected 12 kHz Output

Calibration Readings

v12kHz = 0.391 *volts (rms)*

Vdet = -5.15 dB Vdet

TVG Gain G(40) = (40 log Rcal + 2a Rcal)

G(40) = 42.00 dB

Vdet = V12kHz + 3.01 dB

Sensitivity at Rcal Gx = Vdet - L

Gx = -129.41 dB/uPa@Rcal

Sensitivity at 1 m G1 = Gx - G(40) - Rg

G1 = -171.41 dB/uPa @ 1m

Up Channel Detected 12 kHz Output

Calibration Readings

v12kHz = 0.205 *volts (rms)*

Vdet = -10.75 dB Vdet

TVG Gain G(40) = (40 log Rcal + 2a Rcal)

G(40) = 42.00

Sensitivity at Rcal Gx = Vdet - L

Gx = -135.02 dB/uPa@Rcal

Sensitivity at 1 m G1 = Gx - G(40) - Rg

G1 = -177.02 dB/uPa @ 1m

Left Channel Detected 12 kHz Output

Calibration Readings

v12kHz = 0.198 *volts (rms)*

Vdet = -11.06 dB Vdet

TVG Gain G(40) = (40 log Rcal + 2a Rcal)

G(40) = 42.00 dB

Sensitivity at Rcal Gx = Vdet - L

Gx = -135.32 dB/uPa@Rcal

Sensitivity at 1 m G1 = Gx - G(40) - Rg

G1 = -177.32 dB/uPa @ 1m

20 Log R Channel Detected Output

Calibration Readings

vdet = 0.562 *volts (peak)*

Vdet = -5.01 dBV (det)

TVG Gain G(20) = (20 log Rcal + 2a Rcal)

G(20) = 21.00 dB

Sensitivity at Rcal Gx = Vdet - L

Gx = -129.27 dB/uPa@Rcal

Sensitivity at 1 m G1 = Gx - G(20) - Rg

G1 = -150.27 dB/uPa @ 1m

Transmission Loss TL = 20 log Rs + aR

TL = 15.71 dB

Source Level SL = Vso - Ss + TL-Pre-Amp

Transmit Power (dB)	Standard Transducer Vso (FFT) dBV (+20)	Standard Transducer Vso (FFT) dBV (+40)	Source Level (dBuPa @ 1 m)
20.0	-6.75		219.41
14.0	-12.69		213.47
8.0		1.25	207.46
2.0		4.81	211.02

Filename: 819S758.xls

Page 2

-continued-

Sum Detected Voltage vs Power and Gain

Hydroacoustic Technology, Inc.

HTI

Transducer S/N 1014819

Sounder S/N 1320758

Power Level 20		Vdet = SL + TS + G1 + Rg						
		Target Strength (dB)						
		-65	-60	-55	-50	-45	-40	-35
Receiver Gain (dB)	-18	0.018	0.032	0.056	0.100	0.178	0.316	0.562
	-12	0.035	0.063	0.112	0.199	0.355	0.631	1.122
	-6	0.071	0.126	0.224	0.398	0.708	1.259	2.238
	0	0.141	0.251	0.447	0.794	1.412	2.511	4.466
	6	0.282	0.501	0.891	1.585	2.818	5.011	8.911
	12	0.562	1.000	1.778	3.162	5.622	9.998	>
	18	1.122	1.995	3.547	6.308	>	>	>
	24	2.238	3.980	7.078	>	>	>	>

Power Level 14		Vdet = SL + TS + G1 + Rg						
		Target Strength (dB)						
		-65	-60	-55	-50	-45	-40	-35
Receiver Gain (dB)	-18	0.009	0.016	0.028	0.050	0.090	0.160	0.284
	-12	0.018	0.032	0.057	0.101	0.179	0.318	0.566
	-6	0.036	0.064	0.113	0.201	0.357	0.635	1.130
	0	0.071	0.127	0.225	0.401	0.713	1.267	2.254
	6	0.142	0.253	0.450	0.800	1.422	2.529	4.497
	12	0.284	0.505	0.897	1.596	2.837	5.046	8.972
	18	0.566	1.007	1.790	3.184	5.661	>	>
	24	1.130	2.009	3.572	6.352	>	>	>

Power Level 8		Vdet = SL + TS + G1 + Rg						
		Target Strength (dB)						
		-65	-60	-55	-50	-45	-40	-35
Receiver Gain (dB)	-18	0.004	0.008	0.014	0.025	0.045	0.080	0.142
	-12	0.009	0.016	0.028	0.050	0.090	0.159	0.283
	-6	0.018	0.032	0.057	0.101	0.179	0.318	0.565
	0	0.036	0.063	0.113	0.201	0.357	0.634	1.128
	6	0.071	0.127	0.225	0.400	0.712	1.266	2.251
	12	0.142	0.253	0.449	0.799	1.420	2.526	4.492
	18	0.283	0.504	0.896	1.594	2.834	5.040	8.962
	24	0.565	1.006	1.788	3.180	5.655	>	>

Power Level 2		Vdet = SL + TS + G1 + Rg						
		Target Strength (dB)						
		-65	-60	-55	-50	-45	-40	-35
Receiver Gain (dB)	-18	0.007	0.012	0.021	0.038	0.068	0.120	0.214
	-12	0.014	0.024	0.043	0.076	0.135	0.240	0.427
	-6	0.027	0.048	0.085	0.152	0.269	0.479	0.852
	0	0.054	0.096	0.170	0.302	0.538	0.956	1.700
	6	0.107	0.191	0.339	0.603	1.073	1.908	3.392
	12	0.214	0.381	0.677	1.204	2.140	3.806	6.769
	18	0.427	0.759	1.351	2.402	4.271	7.595	>
	24	0.852	1.515	2.695	4.792	8.521	>	>

Filename: 819S758.xls

Page 3

-continued-

Hydroacoustic Technology Inc.

Collected By: BK, GH
Date November 14, 2001
Time 14:21:4
Sounder S/N 1320758 241
Transducer S/N 1014819 2x10
Cable S/N 1302026+030 400'

Depth 4.57 m
Sep. Dist. 6.1 m
Water Temp 51.8 F
Bandwidth N/A Hz

-3dB Beamwidth = 9.80 Deg
BoreSite = 12.97 dBv @ 184.88 RAM Deg
Largest Left Side Lobe = -25.05 dB @ -67.72 Deg
Largest Right Side Lobe = -32.43 dB @ 69.60 Deg

Processes: Clip=C Smooth=S Boresite=B Normalize=N
Performed: C,C,S,S,N,N,B,B,B,

Comments: PLOT-90 IS LEFT: 819A00P

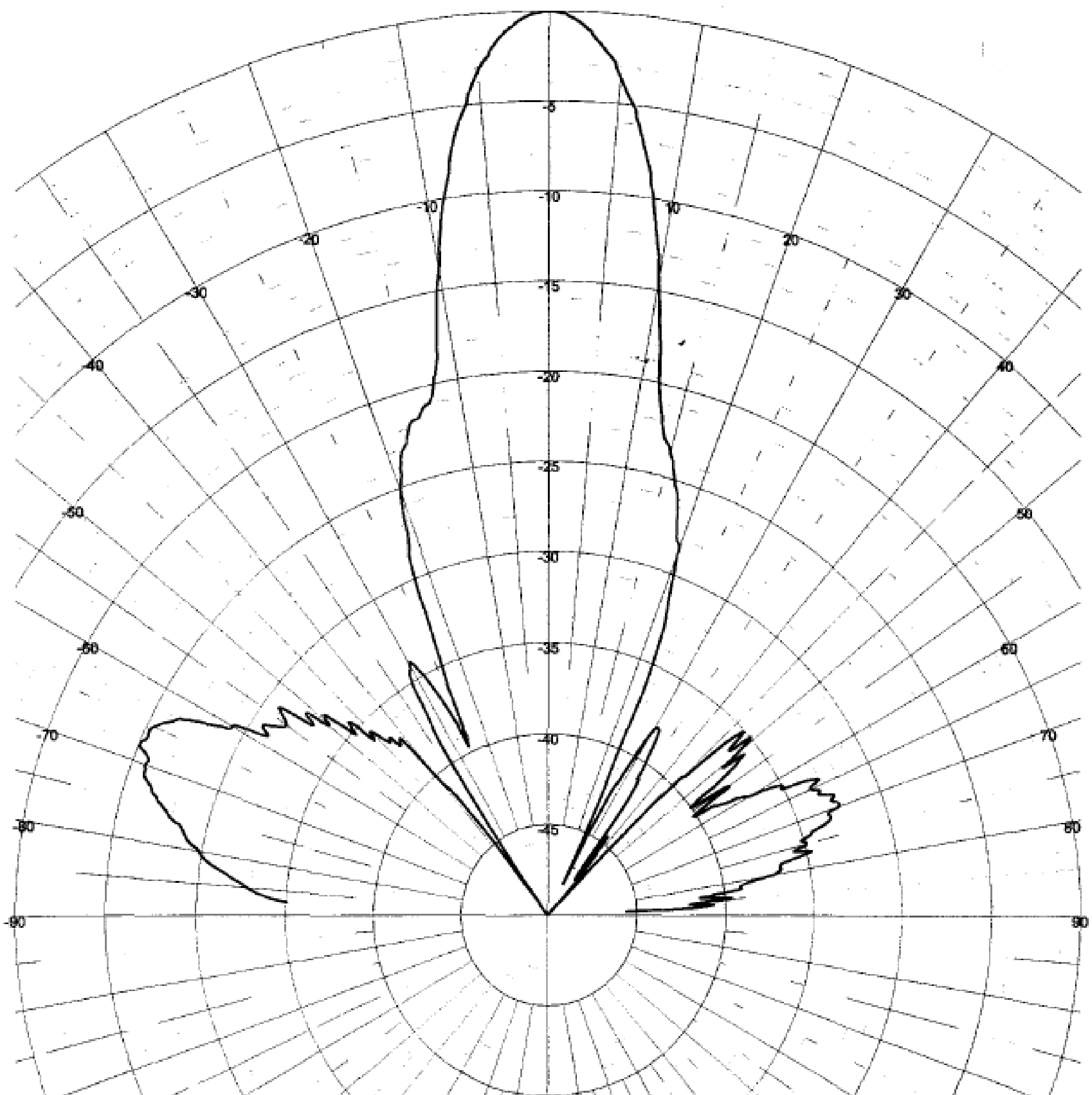

Printed: November 14, 2001 @ 14:22:49

-continued-

Left-Right Stiffness.

HTI Copyright © 1996

Collected By: BK, GH
Date November 14, 2001
Time 14:21:4
Sounder S/N 1320758 241
Transducer S/N 1014819 2x10
Cable S/N 1302026+030 400'
Comments: PLOT-90 IS LEFT: 819A00P

Depth 4.57 m
Sep. Dist. 6.1 m
Water Temp 51.8 F
Bandwidth N/A Hz

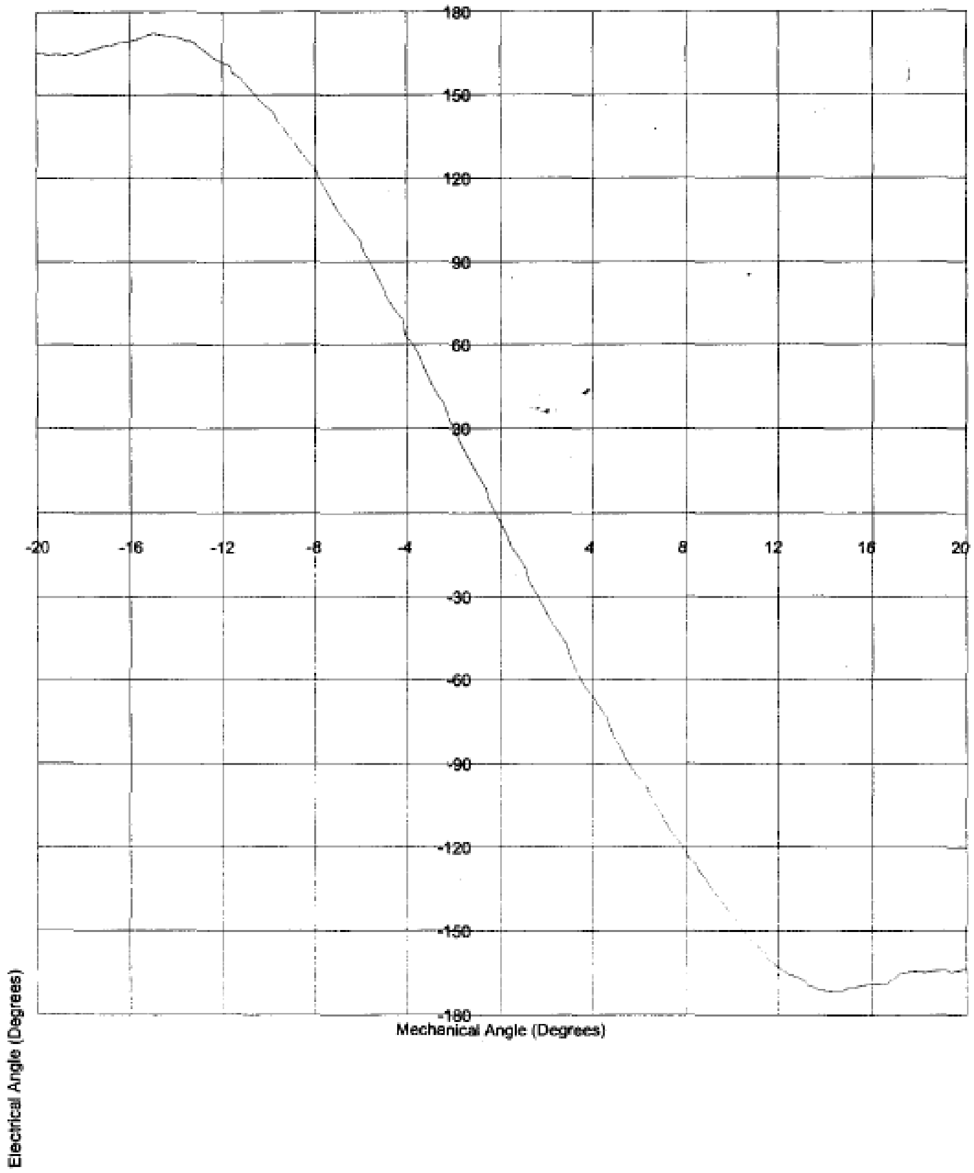

-continued-

Transducer S/N 1014819 2x10 Left/Sum Stiffness processed Nov 14, 2001 14:23:
Comments: PLOT-90 IS LEFT: 819A00P
Calibrated on HTI Impulse: Date November 14, 2001 Time 14:21:4

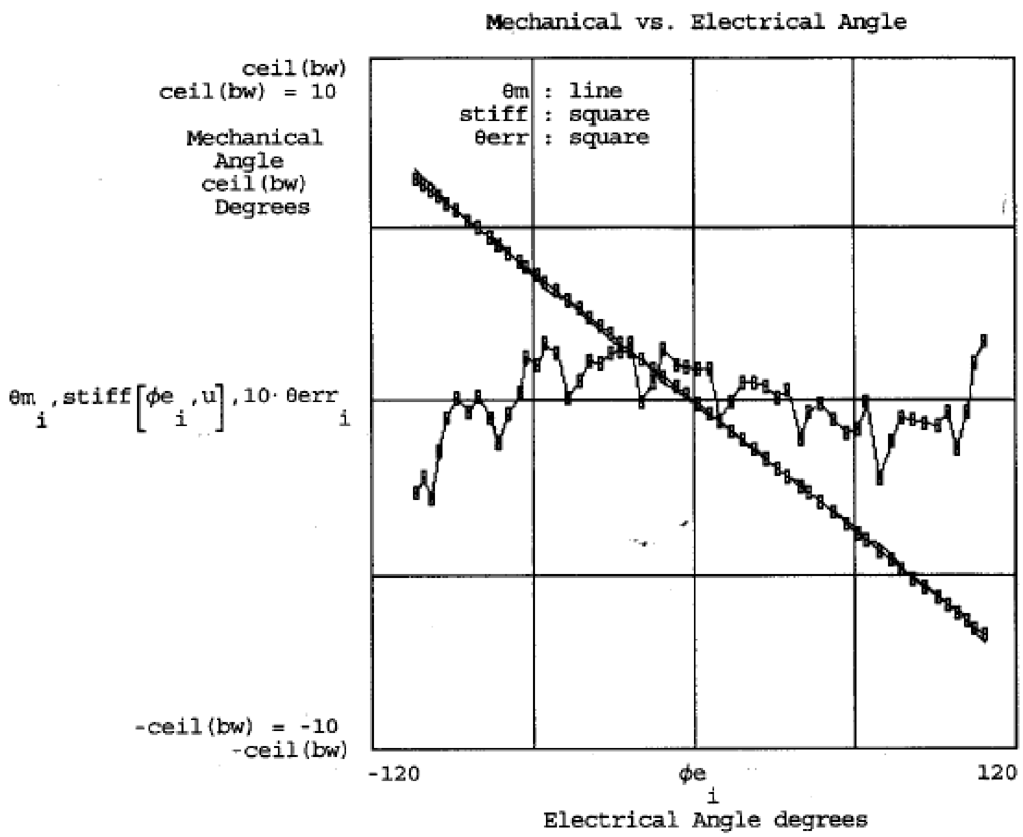

Stiffness constant: U = -16.105346

-continued-

```
Transducer S/N 1014819   2x10 Left/Sum Stiffness processed Nov 14, 2001   14:23:
Comments: PLOT-90 IS LEFT: 819A00P
Calibrated on HTI Impulse:                      Date November 14, 2001 Time 14:21:4
```

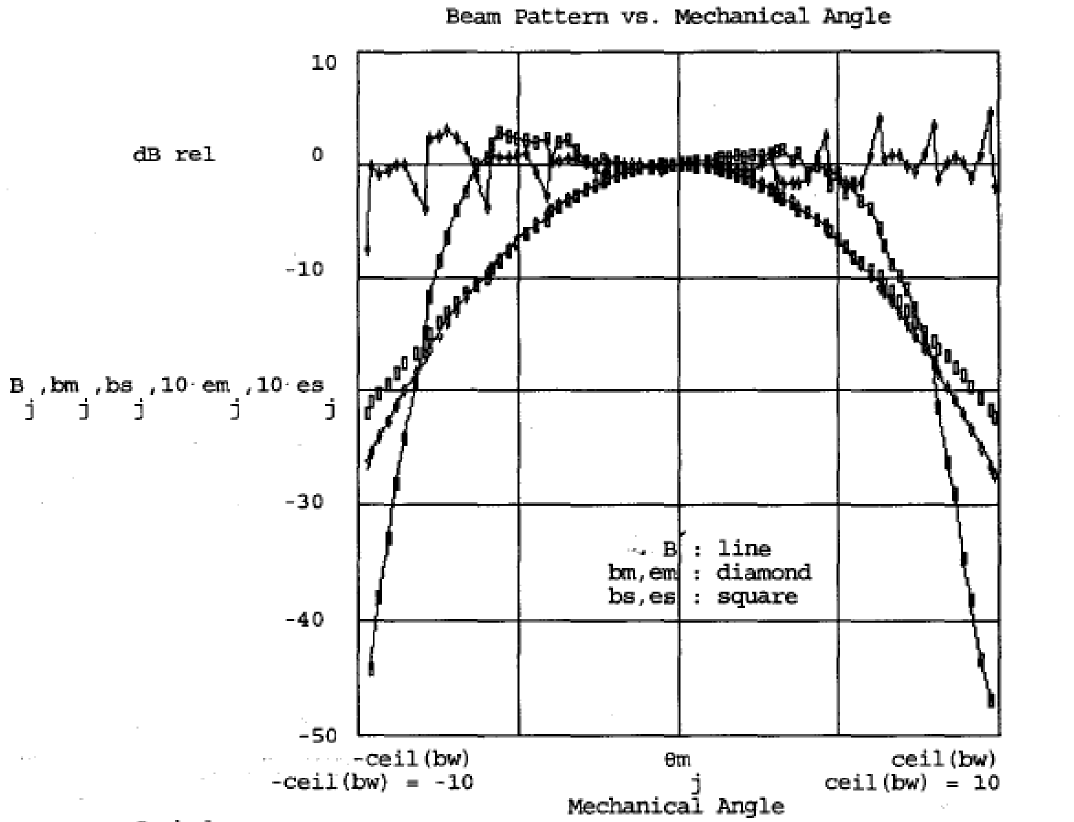

Symbols:
- B beam pattern factor
- θm mechanical angle
- ϕe electrical angle

Beam pattern fit plot:
- B: pattern plotted against mechanical angle, θm
- bm: fit of pattern, θm -> bm
- bs: pattern predicted from stiffness, ϕe -> θm' -> bm

Beam fit coefficients: Measured beamwidth: bw = 9.536
Beamwidth from fit: bw_fit = 9.504

$$c = \begin{array}{cc} \begin{bmatrix} 0 \\ 0.000048 \\ -0.262894 \\ -0.00021 \\ -0.000164 \end{bmatrix} & \begin{array}{c} a \\ b \\ c \\ d \\ e \end{array} \end{array}$$

-continued-

Up-Down Stiffness

Collected By: BK, GH
Date November 14, 2001
Time 14:21:4
Sounder S/N 1320758 241
Transducer S/N 1014819 2x10
Cable S/N 1302026+030 400'
Comments: PLOT-90 IS LEFT: 819A00P

Depth 4.57 m
Sep. Dist. 6.1 m
Water Temp 51.8 F
Bandwidth N/A Hz

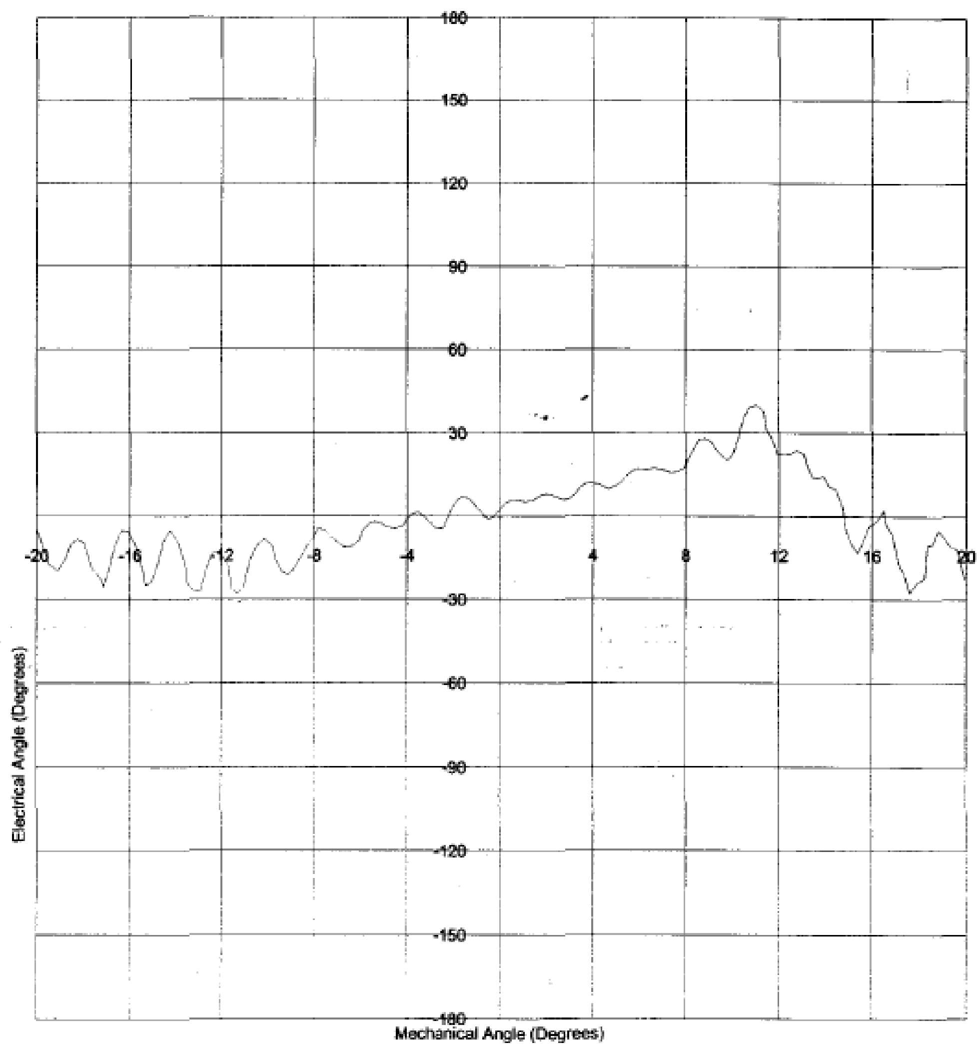

-continued-

Hydroacoustic Technology Inc. Copyright © 1996

Collected By: BK, GH	Depth 4.57 m	-3dB Beamwidth = 2.09 Deg
Date November 14, 2001	Sep. Dist. 6.1 m	BoreSite = 12.66 dBv @ 185.33 RAM Deg
Time 14:28:23	Water Temp 51.8 F	Largest Left Side Lobe = -22.06 dB @ -10.83 Deg
Sounder S/N 1320758 241	Bandwidth N/A Hz	Largest Right Side Lobe = -20.97 dB @ 10.86 Deg
Transducer S/N 1014819 2X10		
Cable S/N 1302026+030 400'	Processes: Clip=C Smooth=S Boresite=B Normalize=N Performed: C,C,S,S,N,N,B,B,	

Comments: PLOT-90 IS UP: 819A90N

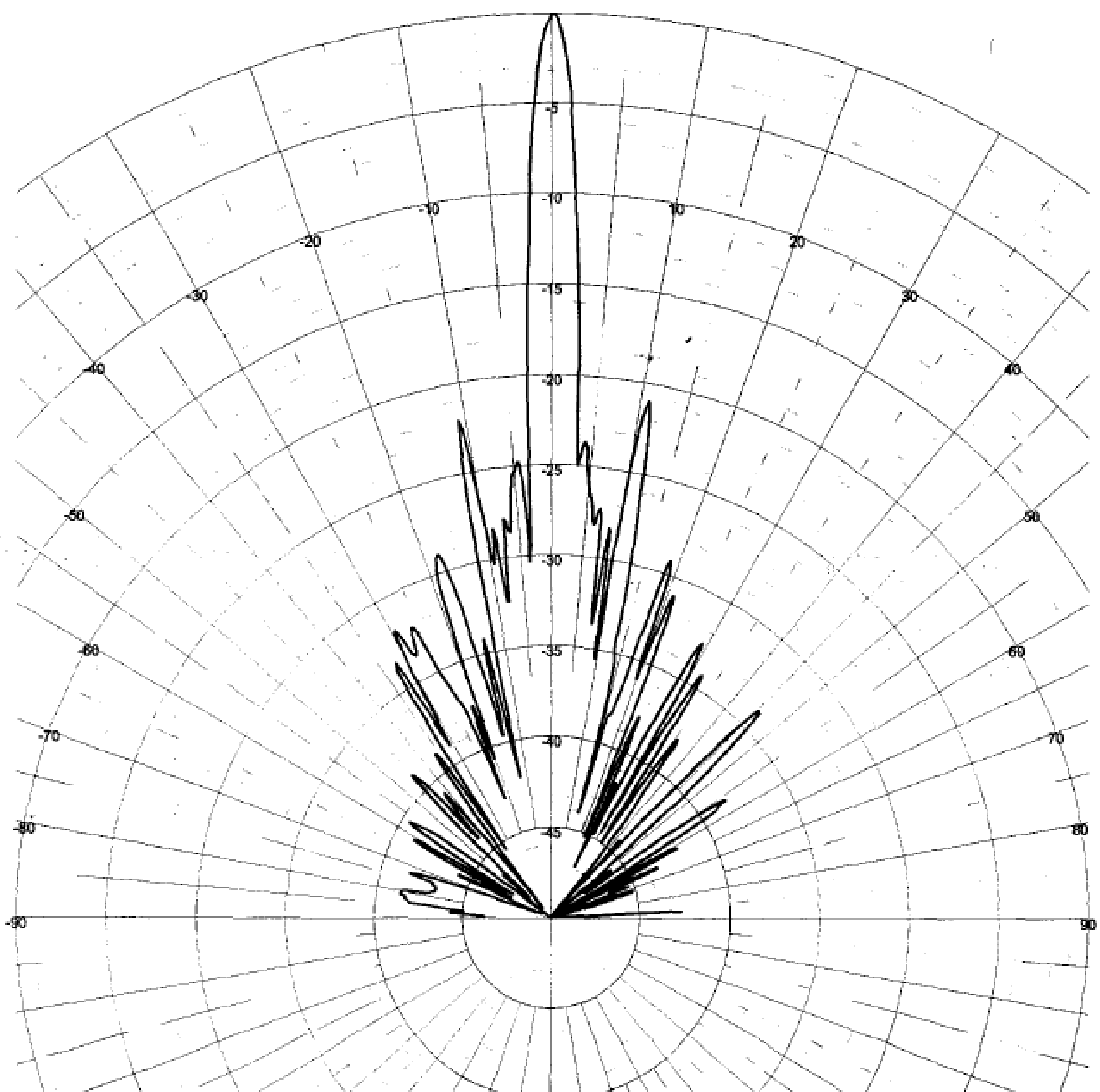

Printed: November 14, 2001 @ 14:28:53

-continued-

Left-Right Stiffness.

Collected By: BK, GH
Date November 14, 2001
Time 14:28:23
Sounder S/N 1320758 241
Transducer S/N 1014819 2X10
Cable S/N 1302026+030 400'
Comments: PLOT-90 IS UP: 819A90N

Depth 4.57 m
Sep. Dist. 6.1 m
Water Temp 51.8 F
Bandwidth N/A Hz

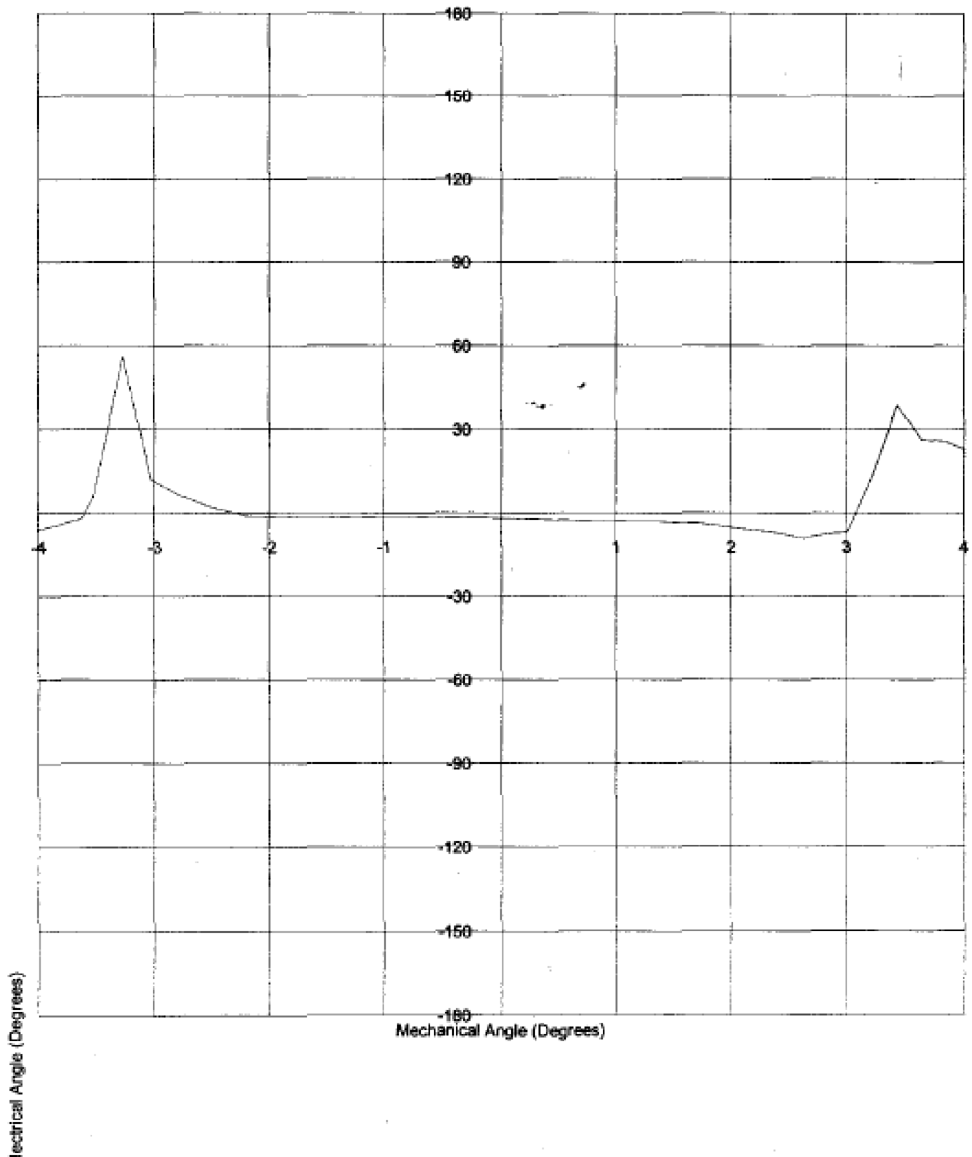

-continued-

HTI Copyright © 1996

Up-Down Stiffness

Collected By: BK, GH
Date November 14, 2001
Time 14:28:23
Sounder S/N 1320758 241
Transducer S/N 1014819 2X10
Cable S/N 1302026+030 400'
Comments: PLOT-90 IS UP: 819A90N

Depth 4.57 m
Sep. Dist. 6.1 m
Water Temp 51.8 F
Bandwidth N/A Hz

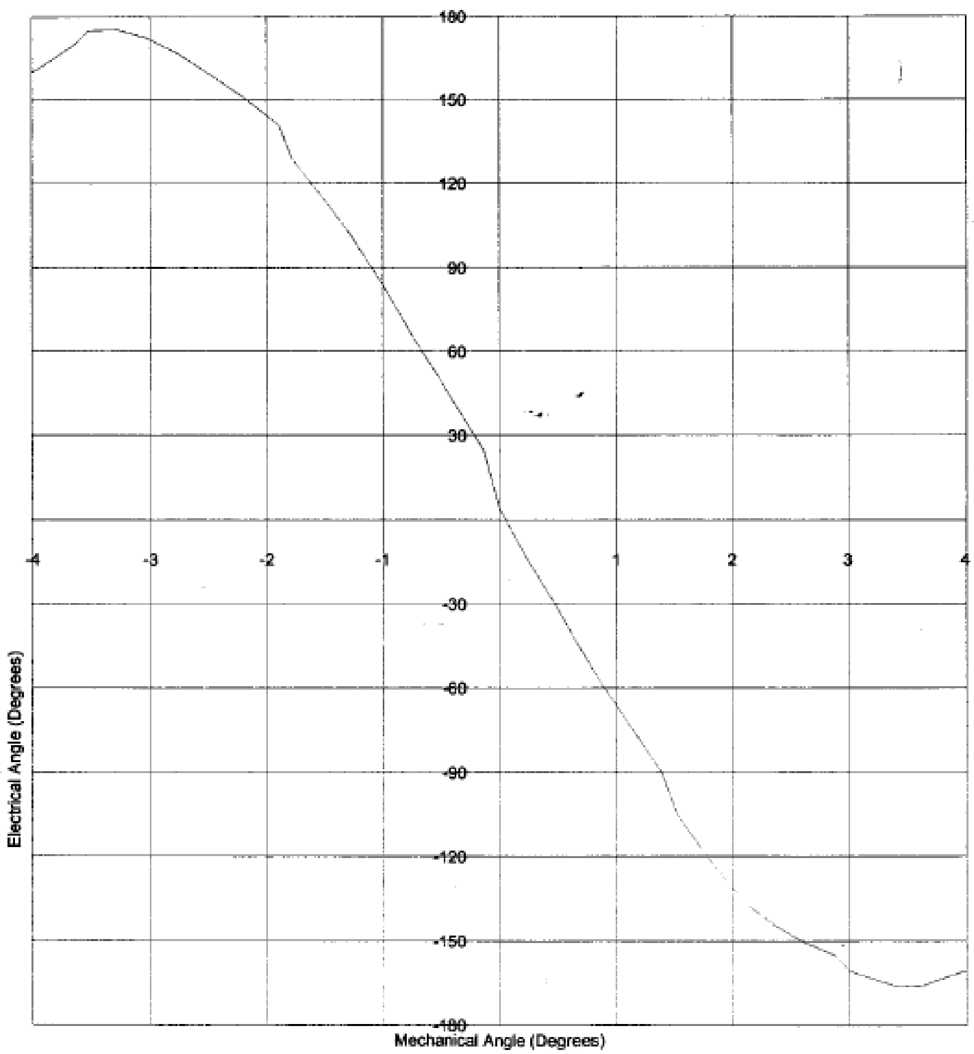

-continued-

Transducer S/N 1014819 2X10 Up/Sum Stiffness processed Nov 14, 2001 14:31:07
Comments: PLOT-90 IS UP: 819A90N
Calibrated on HTI Impulse: Date November 14, 2001 Time 14:28:23

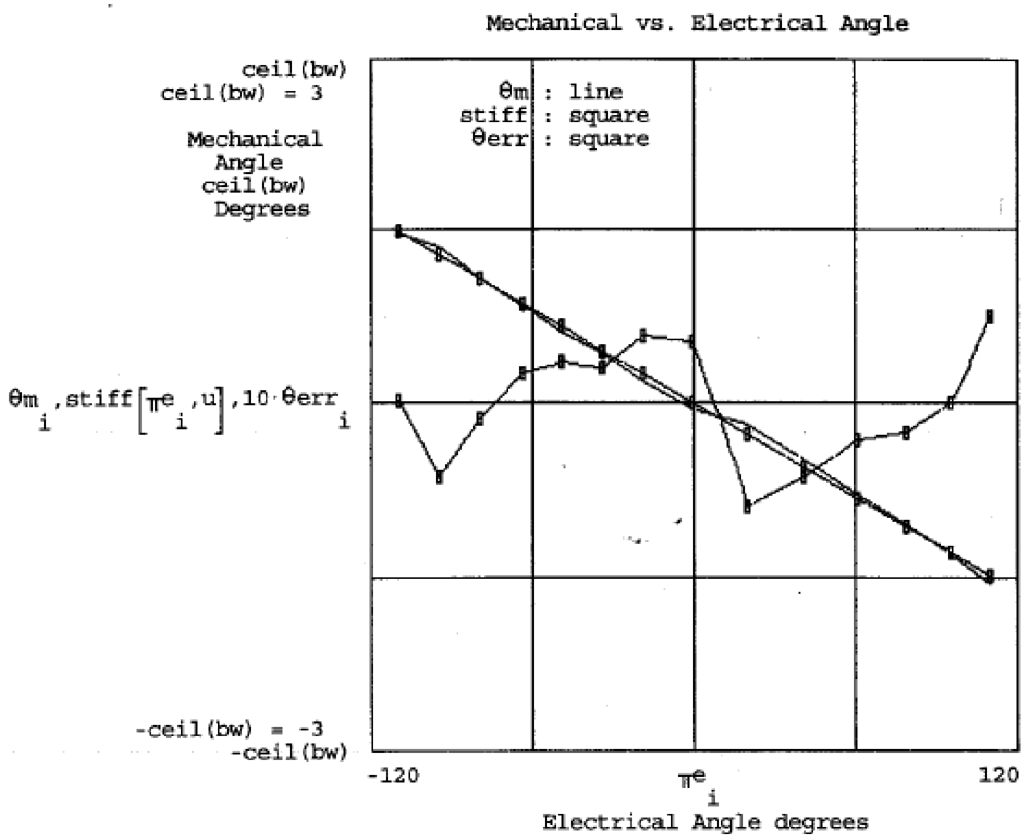

Stiffness constant: U = -74.039123

-continued-

```
Transducer S/N 1014819 2X10 Up/Sum Stiffness processed Nov 14, 2001  14:31:07
Comments: PLOT-90 IS UP: 819A90N
Calibrated on HTI Impulse:                      Date November 14, 2001 Time 14:28:23
```

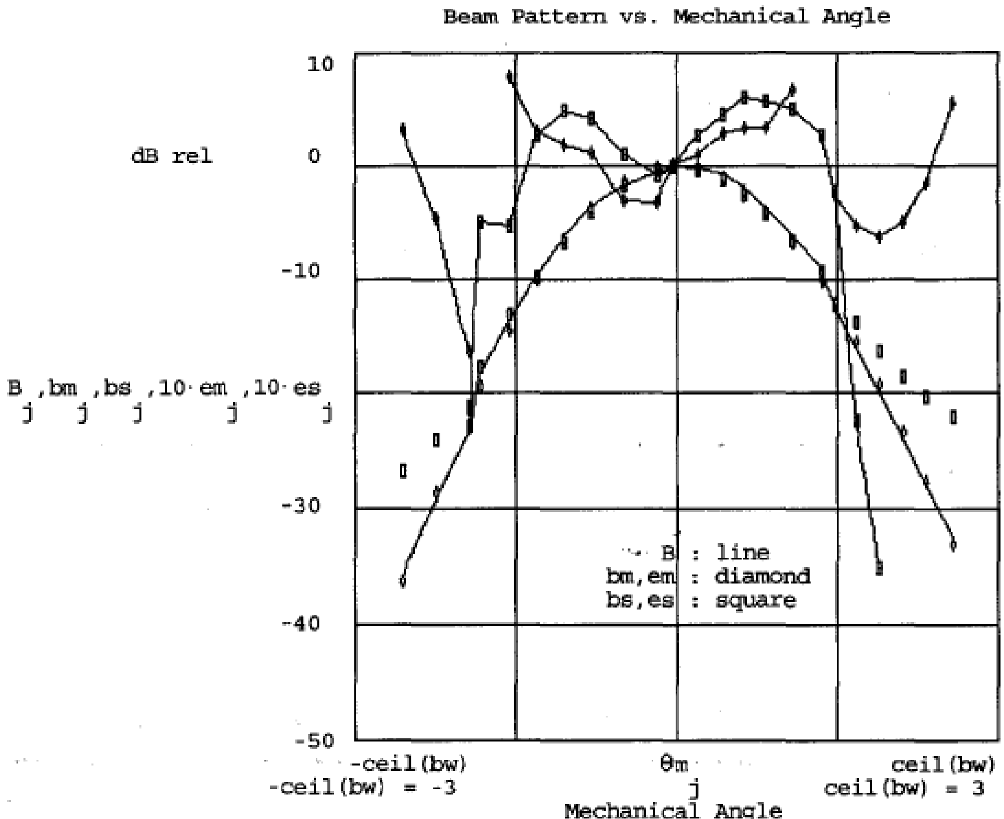

Symbols:
- B beam pattern factor
- θm mechanical angle
- πe electrical angle

Beam pattern fit plot:
- B: pattern plotted against mechanical angle, θm
- bm: fit of pattern, θm -> bm
- bs: pattern predicted from stiffness, πe -> θm' -> bm

Beam fit coefficients:

Measured beamwidth: bw = 2.091
Beamwidth from fit: bw_fit = 2.023

$$c = \begin{array}{cc} \begin{bmatrix} 0 \\ 0.006153 \\ -6.002329 \\ 0.119906 \\ 0.114977 \end{bmatrix} & \begin{array}{c} a \\ b \\ c \\ d \\ e \end{array} \end{array}$$

-continued-

Squared Beam Pattern Factor Calculation for Rectangular Transducer Element

For XD: **1014819** **200 KhZ, 2 x 10**

Actual 3dB beamwidth from beamfit - using coefficients

Vertical Plane:	2.02 °	7.987905 Ly/Lambda
Horizontal Plane:	9.50 °	1.70215 Lx/Lambda

Find squared beam pattern factor (b^2(theta,phi)):

Where:

Lx = transducer element size (wavelengths) in one plane
lambda = wavelength
BW = 3 dB one-way beamwidfth
constant1 = 0.1410112 is empirically determined

First find Lx/lambda and Ly/lambda:

Lx / lambda = constant / sin(BW/2)
10Log(b^2(theta,phi)) = 10Log((1/(Lx/lambda)) * (1/(Ly/lambda))) - 11.572

b^2(theta,phi) = Squared Beam Pattern Factor
constant2 = -11.572 is empirically derived

10Log(b^2(theta,phi)) = -22.9063

b^2(theta,phi) = **0.005121**

These equations were developed by J. Ehrenberg,
after those expressed in Urick, 1963

-continued-

200 KHz – 4X10 Degree –400ft

S/N 1210518

-continued-

Hydroacoustic Technology Inc.

HTI

Standard Sphere Calibration

		Freq	200 KHz
Customer	ADFG MAXWELL	Transducer S/N	1210518
Project Name	NUSHAGAK	Beam Width	4X10 Deg
Calibration Location	HTI-Impulse	Echo Sounder S/N	1320758
Customer Contact	SUSIE MAXWELL	Model #	241
Calibrated by	BK, GH	Calibration Date	14-Nov-01
		Calibration File	518S758 .xls
Sphere Type	38.1 mm Tungsten-carbide	Cable Length	400 Feet

FILE NAME RAW / MDB	RX Gain dB	TVG Gain dB	TX Pwr dBW	PW ms	Pulse Type	Chirp BW KHz	Range m	Echoes #	TS dB	Std. DEV dB
S3181242	-6	0	20	0.40	NORM	0.0	6.16	260	-39.38	0.45
S3181243	-6	0	20	5.00	CHIRP	10.0	6.09	142	-40.55	0.41
S3181244	-6	0	20	2.50	CHIRP	10.0	6.09	276	-39.83	0.35
S3181245	-6	0	20	1.25	CHIRP	10.0	6.08	305	-39.14	0.30

-continued-

Hydroacoustic Technology, Inc.

HTI

Hydroacoustic System Calibration

		Frequency (kHz)	200
Customer	ADF&G	Transducer S/N	1210518
Project Name	Nushagak	Beam Width	4X10
Calibration Location	HTI-Impulse	Echo Sounder S/N	1320758
Customer Contact	Susie Maxwell	Model #	241
Calibrated by	BK, GH	Calibration Date	14-Nov-01
		G1+SL20 =	46.31 dB

Echo Sounder

Arguments to: TVG	1 2 0 42 0 3 1	Arguments to: RX	0
Arguments to: TRIG	00/10	Arguments to: REP	100 10
Arguments to: TX	1-2 to 1-20	Arguments to: MUX	1
Arguments to:FILTER	3	Arguments to:	

Frequency	200	kHz	Band Width	n/a	kHz
Receiver Gain (Rg)	0	dB	Pulse Width	0.5	msec
TVG Full Range	n/a	m	Blanking Control	3	
TVG Crossover	11.22	m	Blanking Min	1	m
TVG Cal Rng (Rcal)	11.22	m	Blanking Max	2	m
Alpha (a)	0	dB/km	Rel Noise (wet)	-32.2	dBV
RCAL @ T 0 42 TX 1 20	not measured	Vdet40		(T 0 82 .. CWFILT 4)	

Cable

Cable S/N	1302026+030	Cable Length	400	ft
Cable Type	Split-beam	Mux Port	1	

Standard Transducer

Type	ITC-5323	Ts =	124.1	dBuPa/V
S/N	007	Ss =	-223.84	dBv/uPa
Last Calibration	Nov 25, 2000 PAS			
		Preamp Gain 20=	13.39	dB
LP Filter	100 x 1k	Equiv. Ss20 =	-210.45	dBv/uPa
HP Filter	300 x 1k			
		Preamp Gain 40=	33.34	dB
		Equiv. Ss40 =	-190.5	dBv/uPa

Air and Water Parameters

Air Temperature	62	°F	Calibration Depth	4.57	m
Water Temperature	51.8	°F	Separation (Rs)	6.1	m

Filename: 518S758.xls

Page 1

-continued-

Hydroacoustic Technology, Inc.

HTI

Receiving Sensitivity	Transducer S/N	1210518	
	Sounder S/N	1320758	

Voltage Into Standard Vs (Generator at 23 dBm)

Vs= 6.26 *volts (rms)*

Vs= 15.93 dBVrms

Transmission Loss TL = 20 log Rs + aRs

TL = 15.71 dB

Acoustic Level L = Ts + Vs - TL

L = 124.33 dB/uPa

Sum Channel Detected 12 kHz Output

Calibration Readings

v12kHz = *0.422* *volts (rms)*

Vdet = -4.48 dB Vdet

TVG Gain G(40) = (40 log Rcal + 2a Rcal)

G(40) = 42.00 dB

Vdet = V12kHz + 3.01 dB

Sensitivity at Rcal Gx = Vdet - L

Gx = -128.81 dB/uPa@Rcal

Sensitivity at 1 m G1 = Gx - G(40) - Rg

G1 = -170.81 dB/uPa @ 1m

Up Channel Detected 12 kHz Output

Calibration Readings

v12kHz = *0.216* *volts (rms)*

Vdet = -10.30 dB Vdet

TVG Gain G(40) = (40 log Rcal + 2a Rcal)

G(40) = 42.00

Sensitivity at Rcal Gx = Vdet - L

Gx = -134.63 dB/uPa@Rcal

Sensitivity at 1 m G1 = Gx - G(40) - Rg

G1 = -176.63 dB/uPa @ 1m

Left Channel Detected 12 kHz Output

Calibration Readings

v12kHz = *0.215* *volts (rms)*

Vdet = -10.34 dB Vdet

TVG Gain G(40) = (40 log Rcal + 2a Rcal)

G(40) = 42.00 dB

Sensitivity at Rcal Gx = Vdet - L

Gx = -134.67 dB/uPa@Rcal

Sensitivity at 1 m G1 = Gx - G(40) - Rg

G1 = -176.67 dB/uPa @ 1m

20 Log R Channel Detected Output

Calibration Readings

vdet = *0.600* *volts (peak)*

Vdet = -4.44 dBV (det)

TVG Gain G(20) = (20 log Rcal + 2a Rcal)

G(20) = 21.00 dB

Sensitivity at Rcal Gx = Vdet - L

Gx = -128.76 dB/uPa@Rcal

Sensitivity at 1 m G1 = Gx - G(20) - Rg

G1 = -149.76 dB/uPa @ 1m

Transmission Loss TL = 20 log Rs + aR

TL = 15.71 dB

Source Level SL = Vso - Ss + TL-Pre-Amp

Transmit Power (dB)	Standard Transducer Vso (FFT) dBV (+20)	Vso (FFT) dBV (+40)	Source Level (dBuPa @ 1 m)
20.0	-9.03		217.13
14.0	-14.72		211.44
8.0		-0.50	205.71
2.0		-6.44	199.77

Filename: 518S758.xls

Page 2

-continued-

Sum Detected Voltage vs Power and Gain

Hydroacoustic Technology, Inc.

HTI

Transducer S/N 1210518

Sounder S/N 1320758

Power Level 20		Vdet = SL + TS + G1 + Rg						
		Target Strength (dB)						
		-65	-60	-55	-50	-45	-40	-35
Receiver Gain (dB)	-18	0.015	0.026	0.046	0.082	0.146	0.260	0.463
	-12	0.029	0.052	0.092	0.164	0.292	0.520	0.924
	-6	0.058	0.104	0.184	0.328	0.583	1.037	1.844
	0	0.116	0.207	0.368	0.654	1.163	2.069	3.679
	6	0.232	0.413	0.734	1.305	2.321	4.128	7.340
	12	0.463	0.824	1.465	2.604	4.632	8.236	>
	18	0.924	1.643	2.922	5.197	9.241	>	>
	24	1.844	3.279	5.831	>	>	>	>

Power Level 14		Vdet = SL + TS + G1 + Rg						
		Target Strength (dB)						
		-65	-60	-55	-50	-45	-40	-35
Receiver Gain (dB)	-18	0.008	0.014	0.024	0.043	0.076	0.135	0.241
	-12	0.015	0.027	0.048	0.085	0.152	0.270	0.480
	-6	0.030	0.054	0.096	0.170	0.303	0.539	0.958
	0	0.060	0.107	0.191	0.340	0.604	1.075	1.911
	6	0.121	0.214	0.381	0.678	1.206	2.144	3.813
	12	0.241	0.428	0.761	1.353	2.406	4.278	7.608
	18	0.480	0.854	1.518	2.699	4.800	8.536	>
	24	0.958	1.703	3.029	5.386	9.578	>	>

Power Level 8		Vdet = SL + TS + G1 + Rg						
		Target Strength (dB)						
		-65	-60	-55	-50	-45	-40	-35
Receiver Gain (dB)	-18	0.004	0.007	0.012	0.022	0.039	0.070	0.124
	-12	0.008	0.014	0.025	0.044	0.078	0.140	0.248
	-6	0.016	0.028	0.050	0.088	0.157	0.278	0.495
	0	0.031	0.056	0.099	0.176	0.312	0.556	0.988
	6	0.062	0.111	0.197	0.351	0.623	1.109	1.971
	12	0.124	0.221	0.393	0.699	1.244	2.212	3.933
	18	0.248	0.441	0.785	1.396	2.482	4.413	7.848
	24	0.495	0.881	1.566	2.785	4.952	8.806	>

Power Level 2		Vdet = SL + TS + G1 + Rg						
		Target Strength (dB)						
		-65	-60	-55	-50	-45	-40	-35
Receiver Gain (dB)	-18	0.002	0.004	0.006	0.011	0.020	0.035	0.063
	-12	0.004	0.007	0.013	0.022	0.040	0.070	0.125
	-6	0.008	0.014	0.025	0.044	0.079	0.141	0.250
	0	0.016	0.028	0.050	0.089	0.158	0.280	0.499
	6	0.031	0.056	0.100	0.177	0.315	0.560	0.995
	12	0.063	0.112	0.199	0.353	0.628	1.117	1.986
	18	0.125	0.223	0.396	0.704	1.253	2.228	3.962
	24	0.250	0.445	0.790	1.406	2.500	4.445	7.904

Filename: 518S758.xls

Page 3

-continued-

Hydroacoustic Technology Inc. Copyright © 1996

Collected By: BK, GH
Date November 14, 2001
Time 13:23:10
Sounder S/N 1320758 241
Transducer S/N 1210518 4x10
Cable S/N 1302026+030 400'

Depth 4.57 m
Sep. Dist. 6.1 m
Water Temp 51.8 F
Bandwidth N/A Hz

-3dB Beamwidth = 9.76 Deg
BoreSite = 13.55 dBv @ 185.10 RAM Deg
Largest Left Side Lobe = -25.16 dB @ -70.86 Deg
Largest Right Side Lobe = -26.61 dB @ 72.02 Deg

Processes: Clip=C Smooth=S Boresite=B Normalize=N
Performed: C,C,S,S,N,N,B,B,

Comments: PLOT-90 IS LEFT: 518A00P

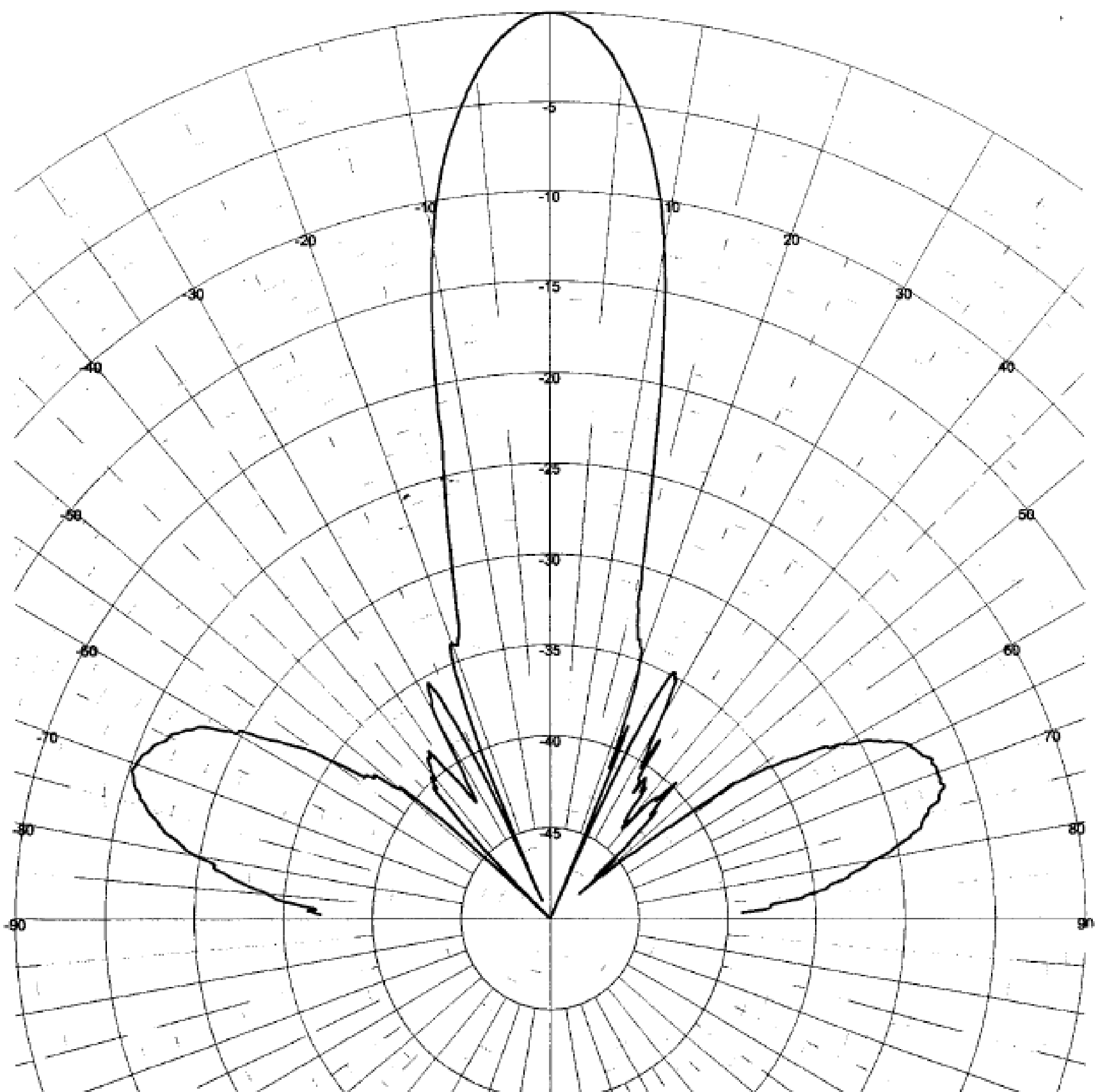

Printed: November 14, 2001 @ 13:23:45

-continued-

Left-Right Stiffness.

HTI Copyright © 1996

Collected By: BK, GH
Date November 14, 2001
Time 13:23:10
Sounder S/N 1320758 241
Transducer S/N 1210518 4x10
Cable S/N 1302026+030 400'
Comments: PLOT-90 IS LEFT: 518A00P

Depth 4.57 m
Sep. Dist. 6.1 m
Water Temp 51.8 F
Bandwidth N/A Hz

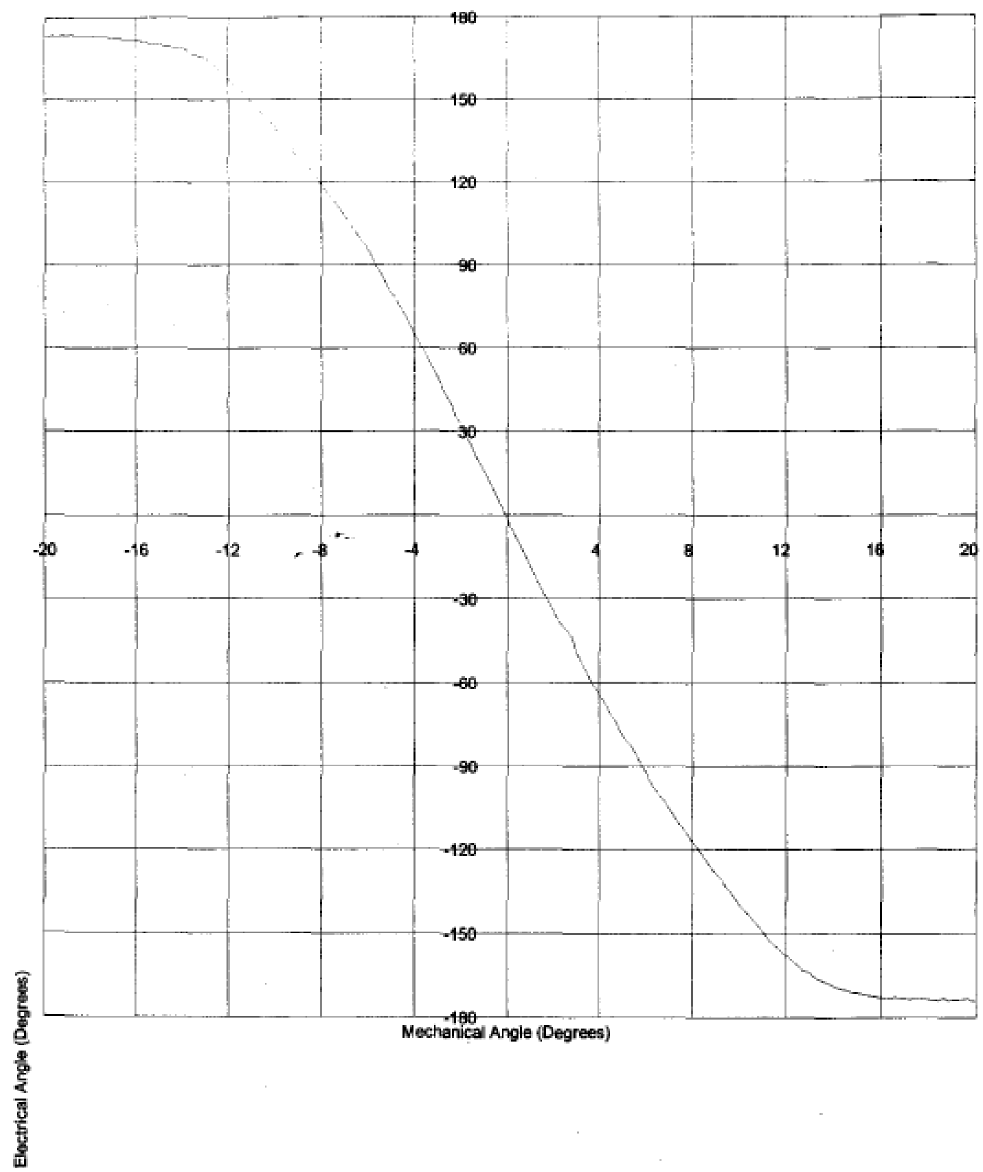

-continued-

```
Transducer S/N 1210518  4x10 Left/Sum Stiffness processed Nov 14, 2001  13:24:
Comments: PLOT-90 IS LEFT: 518A00P
Calibrated on HTI Impulse:                    Date November 14, 2001 Time 13:23:10
```

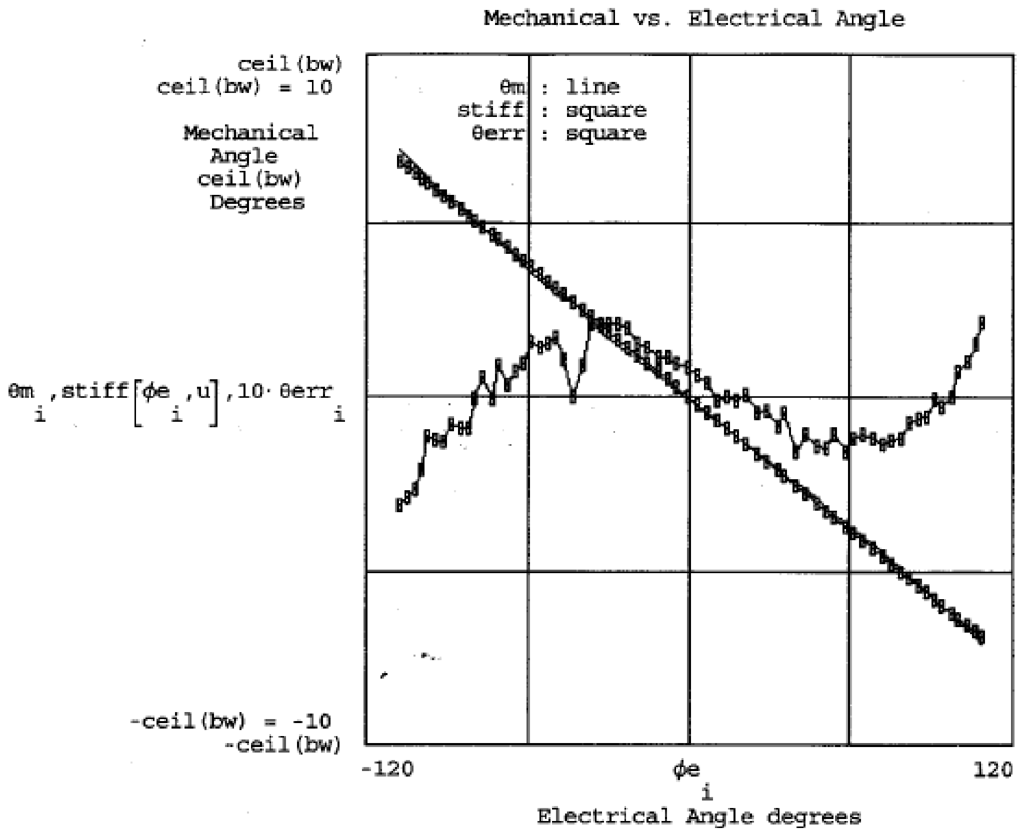

Stiffness constant: U = -15.781457

-continued-

Transducer S/N 1210518 4x10 Left/Sum Stiffness processed Nov 14, 2001 13:24:
Comments: PLOT-90 IS LEFT: 518A00P
Calibrated on HTI Impulse: Date November 14, 2001 Time 13:23:10

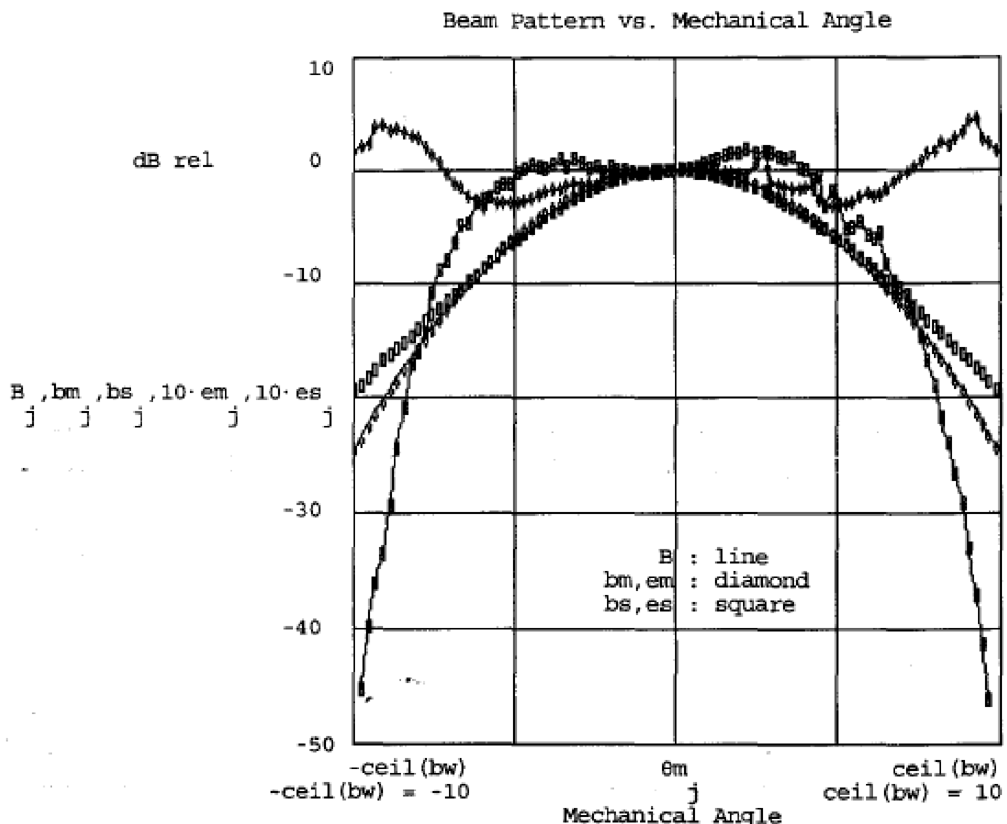

Symbols:
- B beam pattern factor
- θm mechanical angle
- ϕe electrical angle

Beam pattern fit plot:
- B: pattern plotted against mechanical angle, θm
- bm: fit of pattern, θm -> bm
- bs: pattern predicted from stiffness, ϕe -> θm' -> bm

Beam fit coefficients: Measured beamwidth: bw = 9.675
Beamwidth from fit: bw_fit = 9.935

$$c = \begin{array}{cc} \left[\begin{array}{r} 0 \\ 0.000108 \\ -0.242064 \\ -0.000151 \\ -0.000077 \end{array}\right] & \begin{array}{c} a \\ b \\ c \\ d \\ e \end{array} \end{array}$$

-continued-

Hydroacoustic Technology Inc. Copyright © 1996

Collected By: BK, GH	Depth 4.57 m	-3dB Beamwidth = 4.03 Deg
Date November 14, 2001	Sep. Dist. 6.1 m	BoreSite = 13.49 dBv @ 184.86 RAM Deg
Time 13:26:31	Water Temp 51.8 F	Largest Left Side Lobe = -21.86 dB @ -22.54 Deg
Sounder S/N 1320758 241	Bandwidth N/A Hz	Largest Right Side Lobe = -21.33 dB @ 22.46 Deg
Transducer S/N 1210518 4x10		
Cable S/N 1302026+030 400'	Processes: Clip=C Smooth=S Boresite=B Normalize=N Performed: C,C,S,S,N,N,B,B,B,B,	

Comments: PLOT-90 IS UP: 518A90N

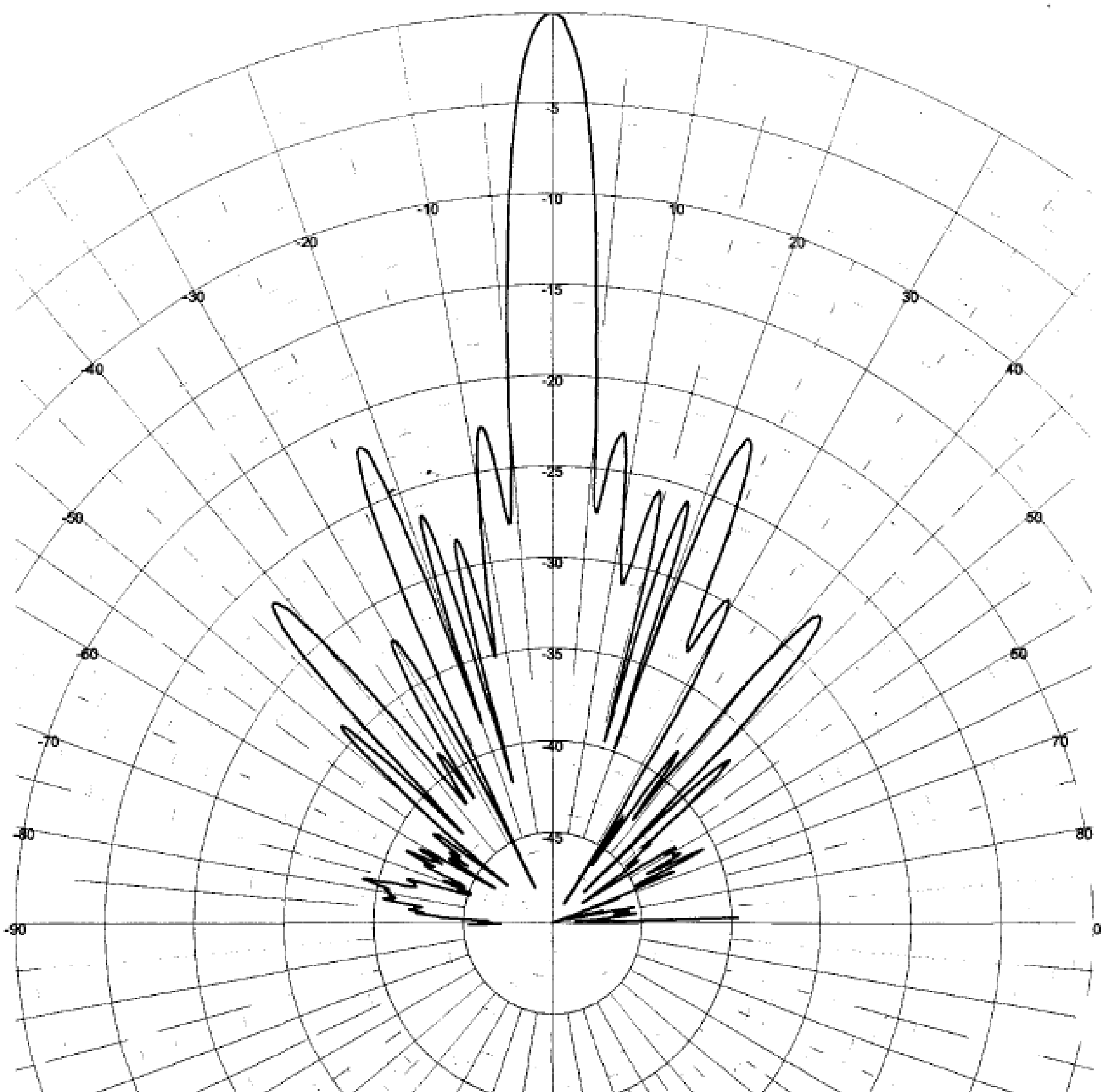

Printed: November 14, 2001 @ 13:27:53

-continued-

Up-Down Stiffness

Collected By: BK, GH
Date November 14, 2001
Time 13:26:31
Sounder S/N 1320758 241
Transducer S/N 1210518 4x10
Cable S/N 1302026+030 400'
Comments: PLOT-90 IS UP: 518A90N

Depth 4.57 m
Sep. Dist. 6.1 m
Water Temp 51.8 F
Bandwidth N/A Hz

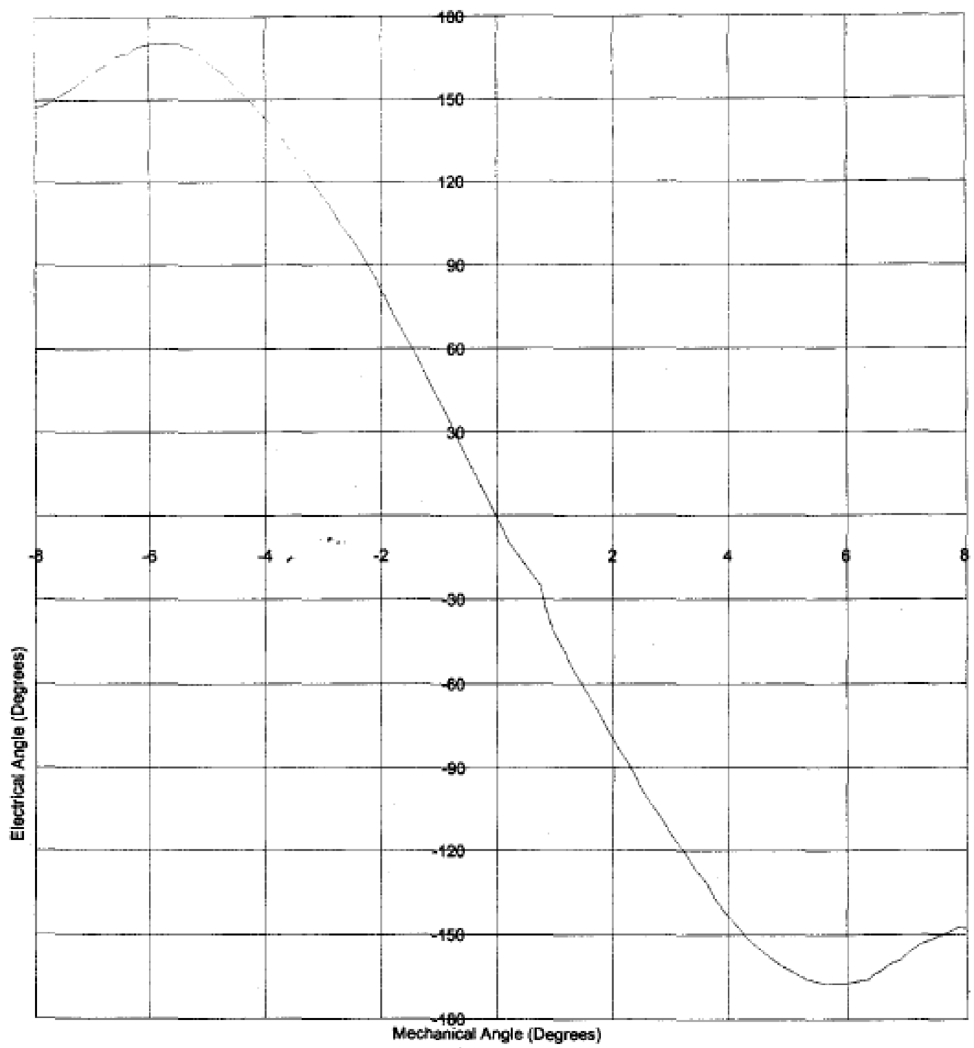

-continued-

Transducer S/N 1210518 4x10 Up/Sum Stiffness processed Nov 14, 2001 13:28:29
Comments: PLOT-90 IS UP: 518A90N
Calibrated on HTI Impulse: Date November 14, 2001 Time 13:26:31

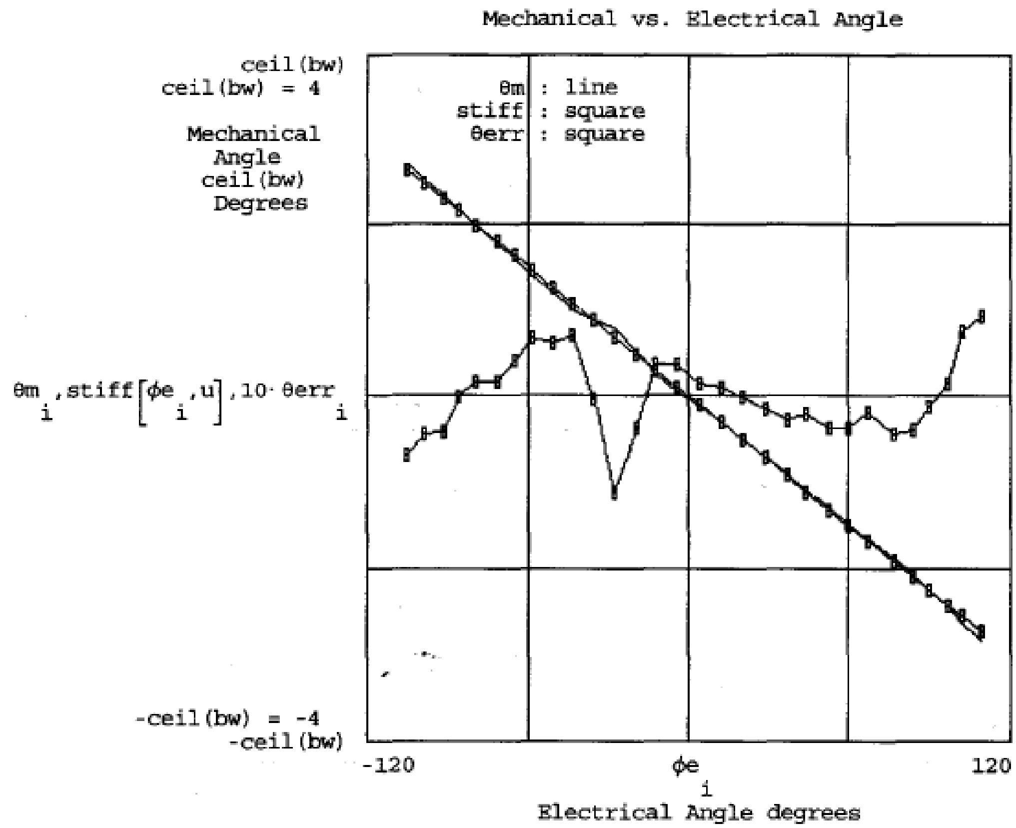

Stiffness constant: U = -39.796064

Transducer S/N 1210518 4x10 Up/Sum Stiffness processed Nov 14, 2001 13:28:29
Comments: PLOT-90 IS UP: 518A90N
Calibrated on HTI Impulse: Date November 14, 2001 Time 13:26:31

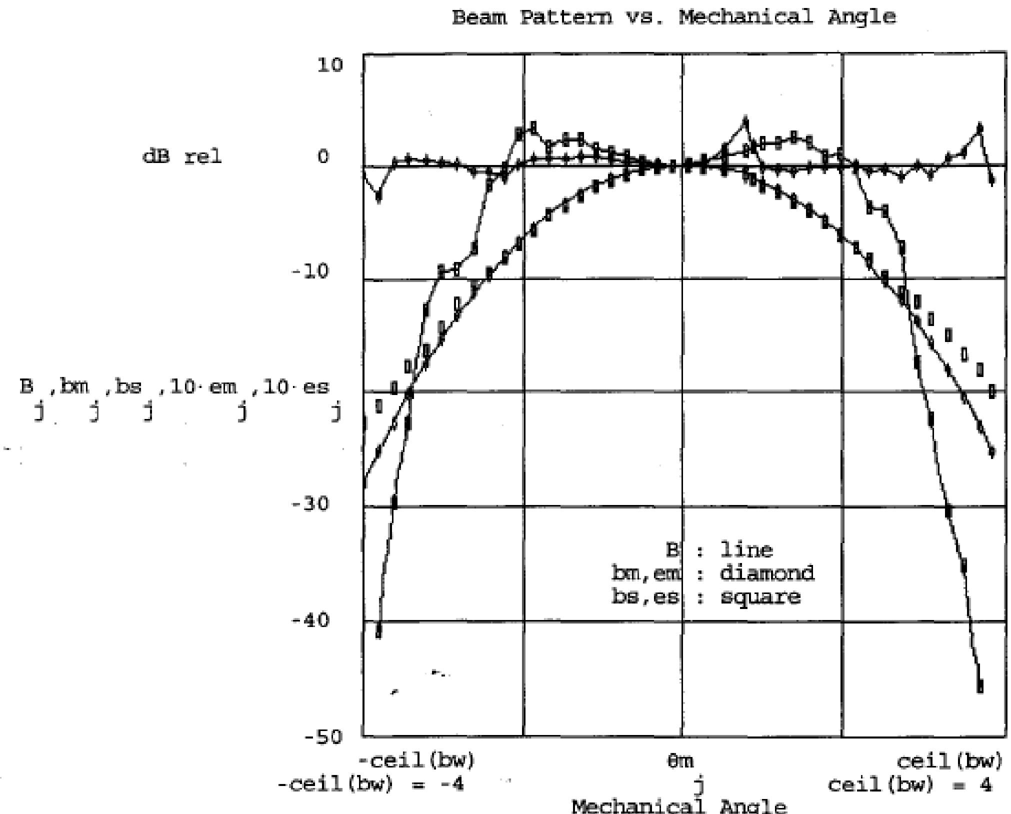

Symbols:
- B beam pattern factor
- θm mechanical angle
- φe electrical angle

Beam pattern fit plot:
- B: pattern plotted against mechanical angle, θm
- bm: fit of pattern, θm -> bm
- bs: pattern predicted from stiffness, φe -> θm' -> bm

Beam fit coefficients:

Measured beamwidth: bw = 3.91
Beamwidth from fit: bw_fit = 3.907

$$c = \begin{bmatrix} 0 \\ 0.000013 \\ -1.525745 \\ 0.003905 \\ -0.013496 \end{bmatrix} \begin{array}{l} a \\ b \\ c \\ d \\ e \end{array}$$

-continued-

Squared Beam Pattern Factor Calculation for Rectangular Transducer Element

For XD:	**s/n 1210518**	**200 KhZ, 4 x 10**

Actual 3dB beamwidth from beamfit - using coefficients

Vertical Plane:	**3.91** °	4.136633	Ly/Lambda
Horizontal Plane:	**9.94** °	1.628481	Lx/Lambda

Find squared beam pattern factor (b^2(theta,phi)):

Where:

Lx = transducer element size (wavelengths) in one plane
lambda = wavelength
BW = 3 dB one-way beamwidfth
constant1 = 0.1410112 is empirically determined

First find Lx/lambda and Ly/lambda:

Lx / lambda = constant / sin(BW/2)
10Log(b^2(theta,phi)) = 10Log((1/(Lx/lambda)) * (1/(Ly/lambda))) - 11.572

b^2(theta,phi) = Squared Beam Pattern Factor
constant2 = -11.572 is empirically derived

10Log(b^2(theta,phi)) = -19.8563

b^2(theta,phi) = 0.010336

These equations were develeped by J. Ehrenberg,
after those expressed in Urick, 1963

-continued-

200 KHz – 6X10 Degree –400ft

S/N 926451

-continued-

Hydroacoustic Technology Inc.

HTI

Standard Sphere Calibration

Customer	ADFG MAXWELL	Freq	200 KHz
Project Name	NUSHAGAK	Transducer S/N	926451
Calibration Location	HTI-Impulse	Beam Width	6X10 Deg
Customer Contact	SUSIE MAXWELL	Echo Sounder S/N	1320758
Calibrated by	BK, GH, MA	Model #	241
		Calibration Date	06/05/02
		Calibration File	451S758 .xls
Sphere Type	38.1 mm Tungsten-carbide	Cable Length	400 Feet

FILE NAME RAW / MDB	RX Gain dB	TVG Gain dB	TX Pwr dBW	PW ms	Pulse Type	Chirp BW KHz	Range m	Echoes #	TS dB	Std. DEV dB
S1560733	-6	0	14	0.40	NORM	0.0	6.09	516	-38.80	0.92
S1560735	-6	0	14	5.00	CHIRP	10.0	6.06	198	-40.12	0.82
S1560736	-6	0	14	2.50	CHIRP	10.0	6.05	296	-39.39	0.50
S1560738	-6	0	14	1.25	CHIRP	10.0	6.05	296	-39.04	0.62

-continued-

Hydroacoustic Technology, Inc.

HTI

Hydroacoustic System Calibration

		Frequency (kHz)	200
Customer	ADF&G	Transducer S/N	926451
Project Name	Nushagak	Beam Width	6X10
Calibration Location	HTI-Impulse	Echo Sounder S/N	1320758
Customer Contact	Susie Maxwell	Model #	241
Calibrated by	BK, GH	Calibration Date	04-Jun-02
		G1+SL20 =	44.71 dB

Echo Sounder

Arguments to: TVG	1 2 0 42 0 3 1	Arguments to: RX	0
Arguments to: TRIG	00/10	Arguments to: REP	100 10
Arguments to: TX	1-2 to 1-20	Arguments to: MUX	1
Arguments to:FILTER	3	Arguments to:	

Frequency	200	kHz	Band Width	n/a	kHz
Receiver Gain (Rg)	0	dB	Pulse Width	0.5	msec
TVG Full Range	n/a	m	Blanking Control	3	
TVG Crossover	11.22	m	Blanking Min	1	m
TVG Cal Rng (Rcal)	11.22	m	Blanking Max	2	m
Alpha (a)	0	dB/km	Rel Noise (wet)	-30.1	dBV
RCAL @ T 0 42 TX 1 20	not measured	Vdet40		(T 0 82 .. CWFILT 4)	

Cable

Cable S/N	1302026+030	Cable Length	400	ft
Cable Type	Split-beam	Mux Port	1	

Standard Transducer

Type	ITC-5323	Ts =	124.1	dBuPa/V
S/N	007	Ss =	-223.84	dBv/uPa
Last Calibration	Nov 25, 2000 PAS			
		Preamp Gain 20=	13.39	dB
LP Filter	100 x 1k	Equiv. Ss20 =	-210.45	dBv/uPa
HP Filter	300 x 1k			
		Preamp Gain 40=	33.34	dB
		Equiv. Ss40 =	-190.5	dBv/uPa

Air and Water Parameters

Air Temperature	62	°F	Calibration Depth	4.57	m
Water Temperature	55	°F	Separation (Rs)	6.1	m

Filename: 451S758.xls Page 1

-continued-

Hydroacoustic Technology, Inc.

HTI

Receiving Sensitivity

Transducer S/N 926451

Sounder S/N 1320758

Voltage Into Standard Vs (Generator at 23 dBm)

Vs= 6.24 *volts (rms)*

Vs= 15.91 dBVrms

Transmission Loss TL = 20 log Rs + aRs

TL = 15.71 dB

Acoustic Level L = Ts + Vs - TL

L = 124.30 dB/uPa

Sum Channel Detected 12 kHz Output

Calibration Readings

v12kHz = 0.420 *volts (rms)*

Vdet = -4.53 dB Vdet

TVG Gain G(40) = (40 log Rcal + 2a Rcal)

G(40) = 42.00 dB

Vdet = V12kHz + 3.01 dB

Sensitivity at Rcal Gx = Vdet - L

Gx = -128.83 dB/uPa@Rcal

Sensitivity at 1 m G1 = Gx - G(40) - Rg

G1 = -170.83 dB/uPa @ 1m

Up Channel Detected 12 kHz Output

Calibration Readings

v12kHz = 0.218 *volts (rms)*

Vdet = -10.22 dB Vdet

TVG Gain G(40) = (40 log Rcal + 2a Rcal)

G(40) = 42.00

Sensitivity at Rcal Gx = Vdet - L

Gx = -134.52 dB/uPa@Rcal

Sensitivity at 1 m G1 = Gx - G(40) - Rg

G1 = -176.52 dB/uPa @ 1m

Left Channel Detected 12 kHz Output

Calibration Readings

v12kHz = 0.222 *volts (rms)*

Vdet = -10.06 dB Vdet

TVG Gain G(40) = (40 log Rcal + 2a Rcal)

G(40) = 42.00 dB

Sensitivity at Rcal Gx = Vdet - L

Gx = -134.36 dB/uPa@Rcal

Sensitivity at 1 m G1 = Gx - G(40) - Rg

G1 = -176.36 dB/uPa @ 1m

20 Log R Channel Detected Output

Calibration Readings

vdet = 0.612 *volts (peak)*

Vdet = -4.26 dBV (det)

TVG Gain G(20) = (20 log Rcal + 2a Rcal)

G(20) = 21.00 dB

Sensitivity at Rcal Gx = Vdet - L

Gx = -128.57 dB/uPa@Rcal

Sensitivity at 1 m G1 = Gx - G(20) - Rg

G1 = -149.57 dB/uPa @ 1m

Transmission Loss TL = 20 log Rs + aR

TL = 15.71 dB

Source Level SL = Vso - Ss + TL-Pre-Amp

Transmit Power (dB)	Standard Transducer Vso (FFT) dBV (+20)	Vso (FFT) dBV (+40)	Source Level (dBuPa @ 1 m)
20.0	-10.62		215.54
14.0	-16.25		209.91
8.0		-2.19	204.02
2.0		-8.13	198.08

Filename: 451S758.xls

Page 2

-continued-

Sum Detected Voltage vs Power and Gain

Hydroacoustic Technology, Inc.

HTI

Transducer S/N 926451

Sounder S/N 1320758

Power Level 20 — Vdet = SL + TS + G1 + Rg

Receiver Gain (dB)	TS -65	TS -60	TS -55	TS -50	TS -45	TS -40	TS -35
-18	0.012	0.022	0.039	0.068	0.122	0.217	0.385
-12	0.024	0.043	0.077	0.137	0.243	0.432	0.768
-6	0.048	0.086	0.153	0.273	0.485	0.862	1.533
0	0.097	0.172	0.306	0.544	0.967	1.720	3.059
6	0.193	0.343	0.610	1.085	1.930	3.432	6.103
12	0.385	0.685	1.218	2.165	3.851	6.847	>
18	0.768	1.366	2.430	4.320	7.683	>	>
24	1.533	2.726	4.848	8.620	>	>	>

Power Level 14 — Vdet = SL + TS + G1 + Rg

Receiver Gain (dB)	TS -65	TS -60	TS -55	TS -50	TS -45	TS -40	TS -35
-18	0.006	0.011	0.020	0.036	0.064	0.113	0.201
-12	0.013	0.023	0.040	0.071	0.127	0.226	0.402
-6	0.025	0.045	0.080	0.143	0.254	0.451	0.802
0	0.051	0.090	0.160	0.284	0.506	0.900	1.600
6	0.101	0.179	0.319	0.568	1.009	1.795	3.192
12	0.201	0.358	0.637	1.132	2.014	3.581	6.368
18	0.402	0.715	1.271	2.260	4.018	7.145	>
24	0.802	1.426	2.535	4.508	8.017	>	>

Power Level 8 — Vdet = SL + TS + G1 + Rg

Receiver Gain (dB)	TS -65	TS -60	TS -55	TS -50	TS -45	TS -40	TS -35
-18	0.003	0.006	0.010	0.018	0.032	0.057	0.102
-12	0.006	0.011	0.020	0.036	0.065	0.115	0.204
-6	0.013	0.023	0.041	0.072	0.129	0.229	0.407
0	0.026	0.046	0.081	0.144	0.257	0.457	0.812
6	0.051	0.091	0.162	0.288	0.512	0.911	1.620
12	0.102	0.182	0.323	0.575	1.022	1.818	3.233
18	0.204	0.363	0.645	1.147	2.040	3.628	6.451
24	0.407	0.724	1.287	2.289	4.070	7.238	>

Power Level 2 — Vdet = SL + TS + G1 + Rg

Receiver Gain (dB)	TS -65	TS -60	TS -55	TS -50	TS -45	TS -40	TS -35
-18	0.002	0.003	0.005	0.009	0.016	0.029	0.052
-12	0.003	0.006	0.010	0.018	0.033	0.058	0.103
-6	0.006	0.012	0.021	0.037	0.065	0.116	0.205
0	0.013	0.023	0.041	0.073	0.130	0.231	0.410
6	0.026	0.046	0.082	0.145	0.259	0.460	0.818
12	0.052	0.092	0.163	0.290	0.516	0.918	1.632
18	0.103	0.183	0.326	0.579	1.030	1.831	3.257
24	0.205	0.365	0.650	1.156	2.055	3.654	6.498

Filename: 451S758.xls

Page 3

-continued-

Hydroacoustic Technology Inc. Copyright © 1996

Collected By: BK, GH	Depth 4.57 m	-3dB Beamwidth = 9.56 Deg
Date June 05, 2002	Sep. Dist. 6.1 m	BoreSite = 13.77 dBv @ 186.54 RAM Deg
Time 7:9:46	Water Temp 55 F	Largest Left Side Lobe = -23.79 dB @ -66.25 Deg
Sounder S/N 1320758 241	Bandwidth N/A Hz	Largest Right Side Lobe = -25.28 dB @ 65.86 Deg
Transducer S/N 926451 6x10		
Cable S/N 1302026+030 400'	Processes: Clip=C Smooth=S Boresite=B Normalize=N	
	Performed: C,C,S,S,N,N,B,B,	

Comments: PLOT-90 IS LEFT: 451A00P

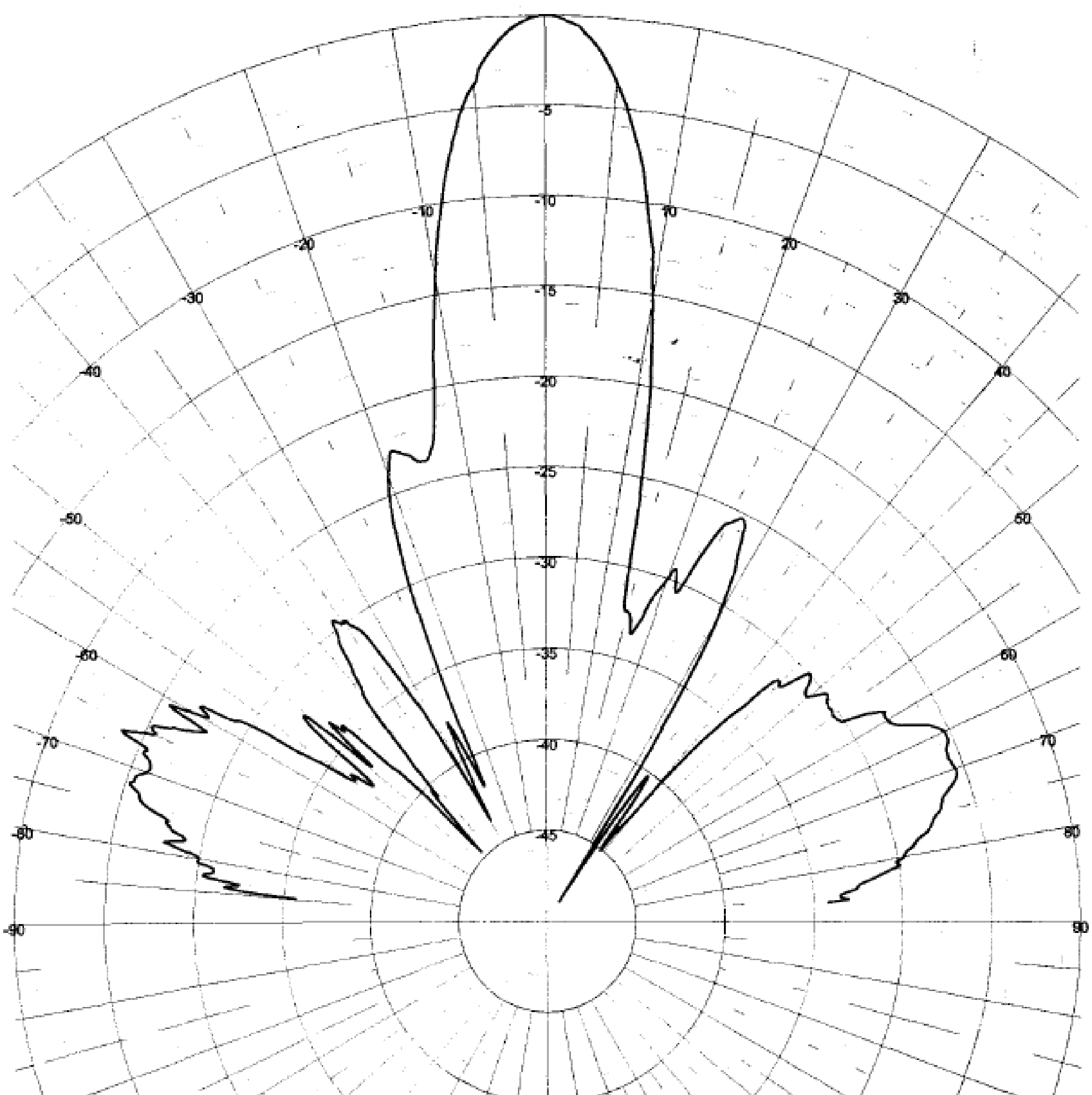

Printed: June 05, 2002 @ 7:12:22

-continued-

Up-Down Stiffness

Collected By: BK, GH
Date June 05, 2002
Time 7:9:46
Sounder S/N 1320758 241
Transducer S/N 926451 6x10
Cable S/N 1302026+030 400'
Comments: PLOT-90 IS LEFT: 451A00P

Depth 4.57 m
Sep. Dist. 6.1 m
Water Temp 55 F
Bandwidth N/A Hz

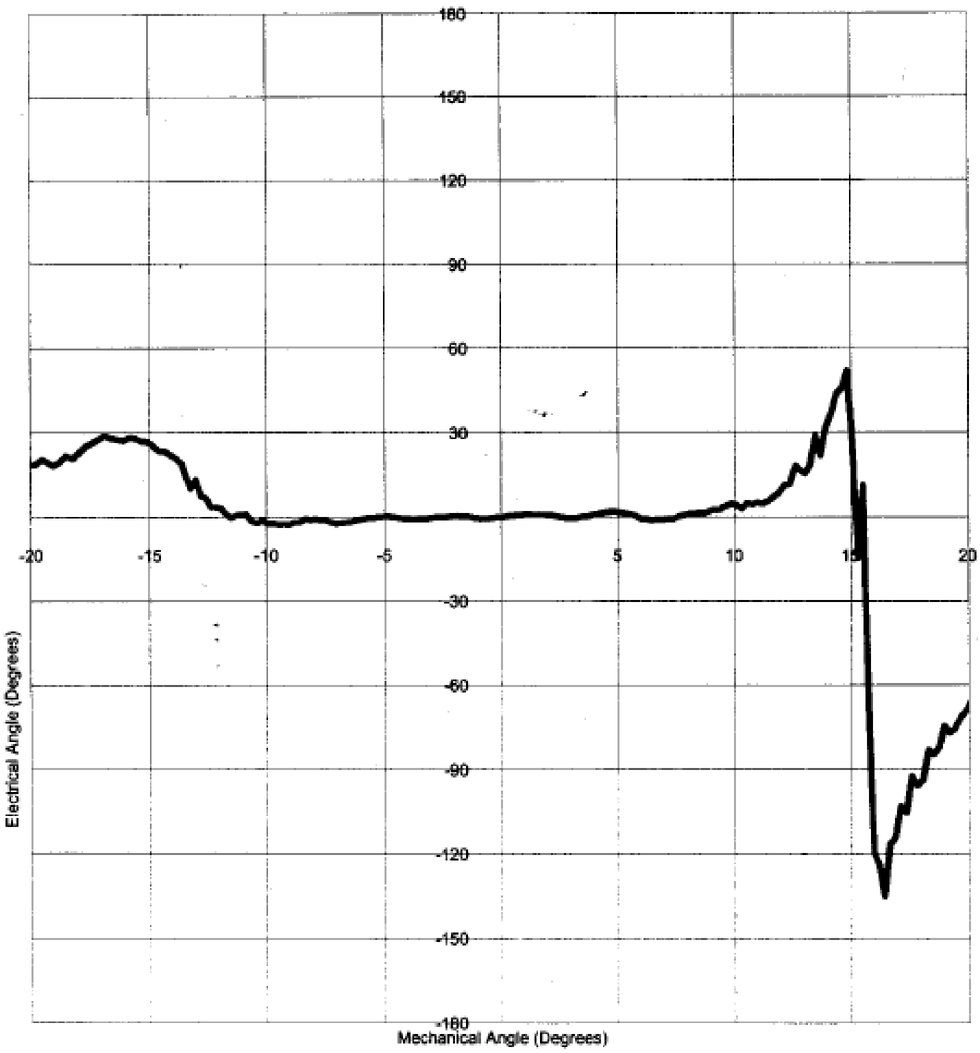

-continued-

```
Transducer S/N 926451  6x10 Left/Sum Stiffness processed Jun 05, 2002  07:13:1
Comments: PLOT-90 IS LEFT: 451A00P
Calibrated on HTI Impulse:                  Date June 05, 2002 Time 7:9:46
```

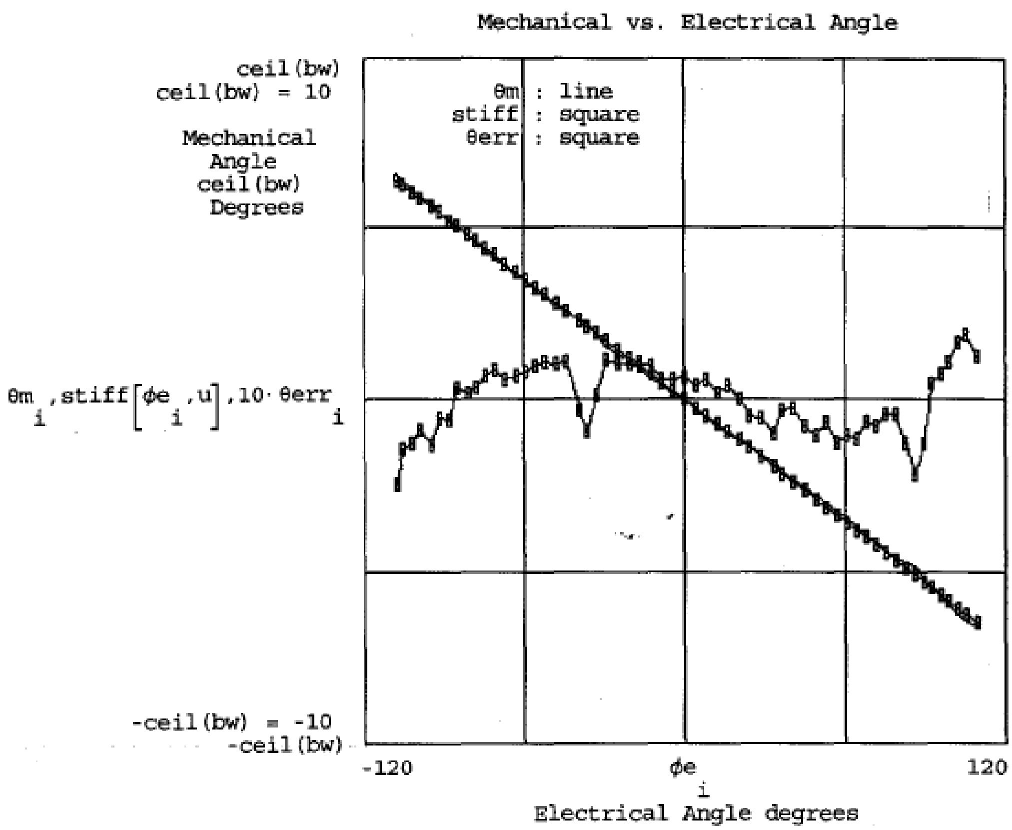

Stiffness constant: U = -16.926347

-continued-

Transducer S/N 926451 6x10 Left/Sum Stiffness processed Jun 05, 2002 07:13:1
Comments: PLOT-90 IS LEFT: 451A00P
Calibrated on HTI Impulse: Date June 05, 2002 Time 7:9:46

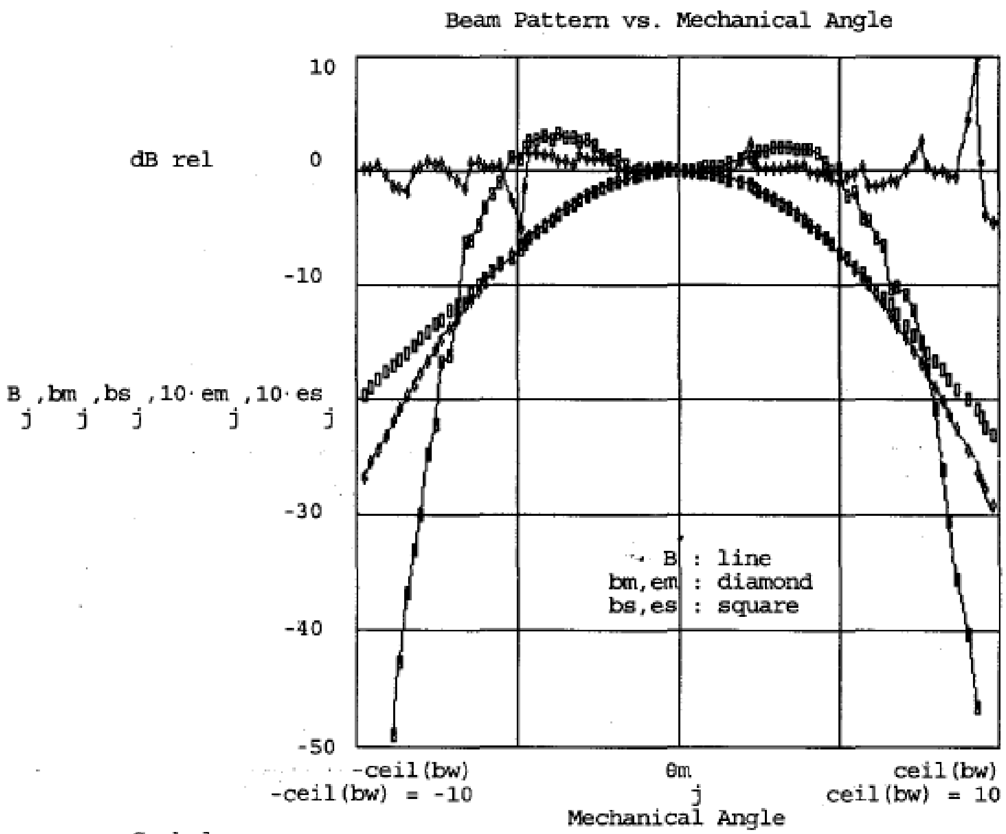

Symbols:
- B beam pattern factor
- θm mechanical angle
- ϕe electrical angle

Beam pattern fit plot:
- B: pattern plotted against mechanical angle, θm
- bm: fit of pattern, θm -> bm
- bs: pattern predicted from stiffness, ϕe -> θm' -> bm

Beam fit coefficients: Measured beamwidth: bw = 9.288
Beamwidth from fit: bw_fit = 9.301

$$c = \begin{bmatrix} 0 \\ -0.000058 \\ -0.27492 \\ -0.001202 \\ -0.000166 \end{bmatrix} \begin{array}{l} a \\ b \\ c \\ d \\ e \end{array}$$

-continued-

Left-Right Stiffness.

HTI Copyright © 1996

Collected By: BK, GH
Date June 05, 2002
Time 7:9:46
Sounder S/N 1320758 241
Transducer S/N 926451 6x10
Cable S/N 1302026+030 400'
Comments: PLOT-90 IS LEFT: 451A00P

Depth 4.57 m
Sep. Dist. 6.1 m
Water Temp 55 F
Bandwidth N/A Hz

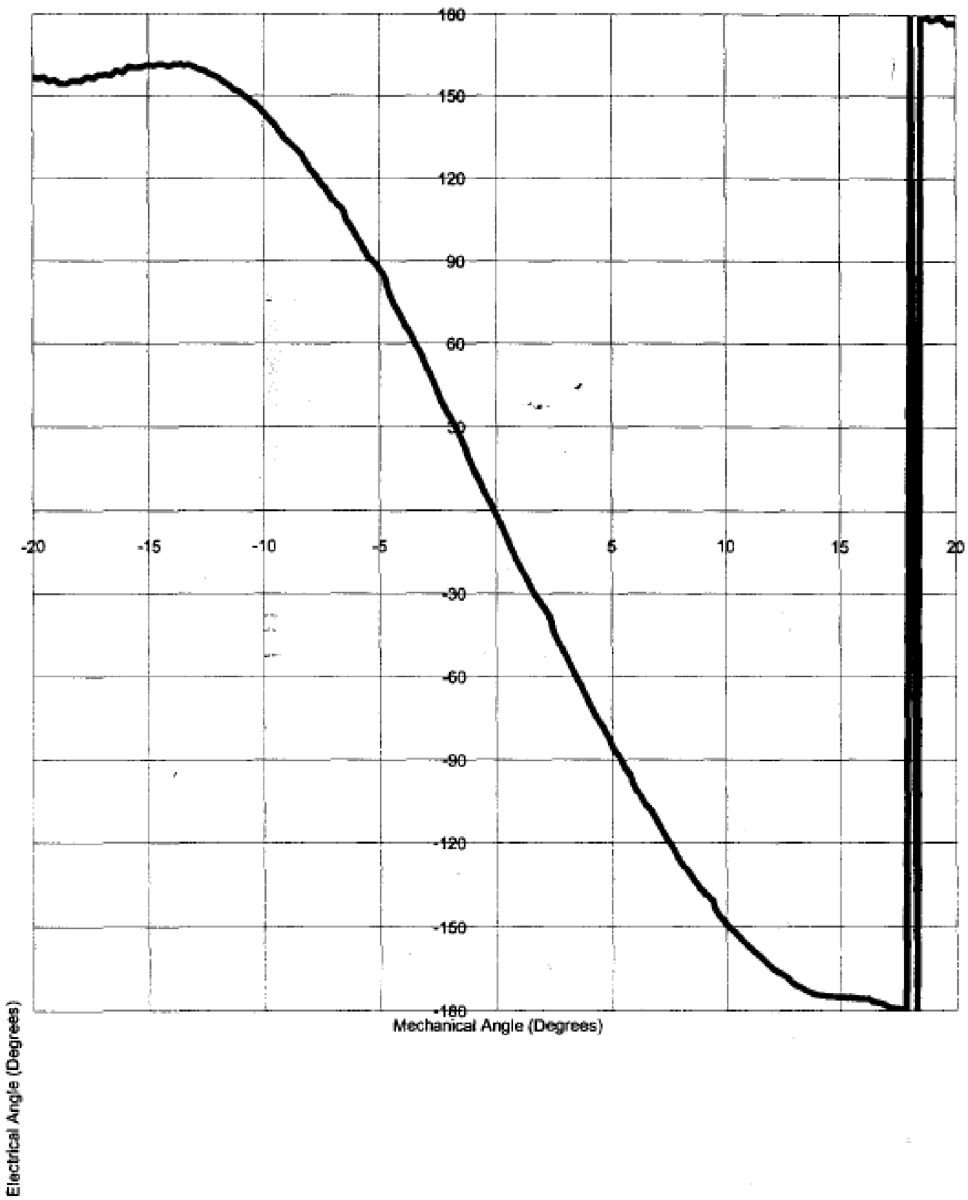

-continued-

Hydroacoustic Technology Inc. Copyright © 1996

Collected By: BK, GH
Date June 05, 2002
Time 7:14:45
Sounder S/N 1320758 241
Transducer S/N 926451 6x10
Cable S/N 1302026+030 400'

Depth 4.57 m
Sep. Dist. 6.1 m
Water Temp 55 F
Bandwidth N/A Hz

-3dB Beamwidth = 6.12 Deg
BoreSite = 13.72 dBv @ 186.63 RAM Deg
Largest Left Side Lobe = -20.46 dB @ -11.91 Deg
Largest Right Side Lobe = -19.72 dB @ 12.80 Deg

Processes: Clip=C Smooth=S Boresite=B Normalize=N
Performed: C,C,S,S,N,N,B,B,

Comments: PLOT-90 IS UP: 451A90N

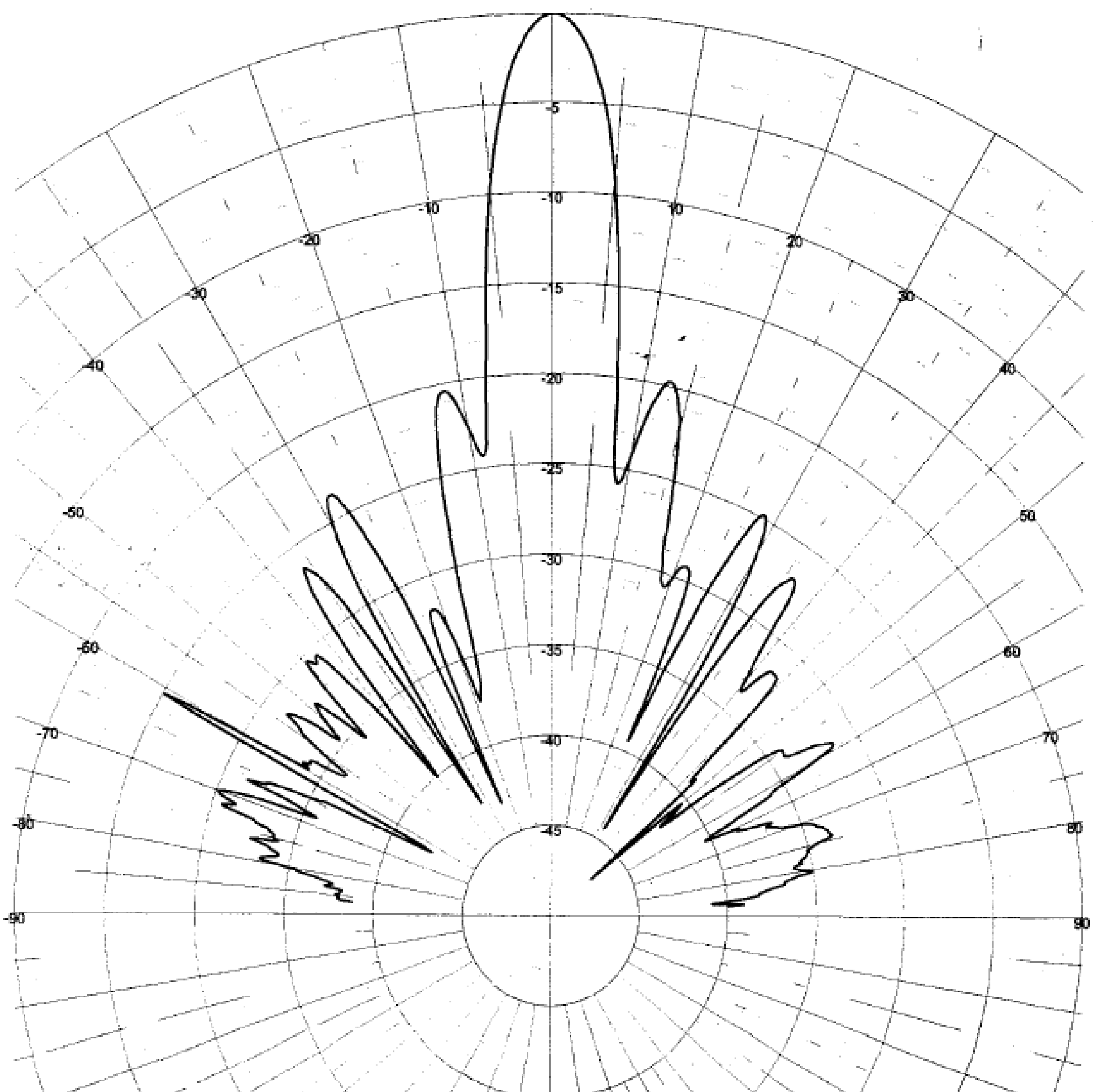

Printed: June 05, 2002 @ 7:15:17

-continued-

Left-Right Stiffness. HTI Copyright © 1996

Collected By: BK, GH
Date June 05, 2002
Time 7:14:45
Sounder S/N 1320758 241
Transducer S/N 926451 6x10
Cable S/N 1302026+030 400'
Comments: PLOT-90 IS UP: 451A90N

Depth 4.57 m
Sep. Dist. 6.1 m
Water Temp 55 F
Bandwidth N/A Hz

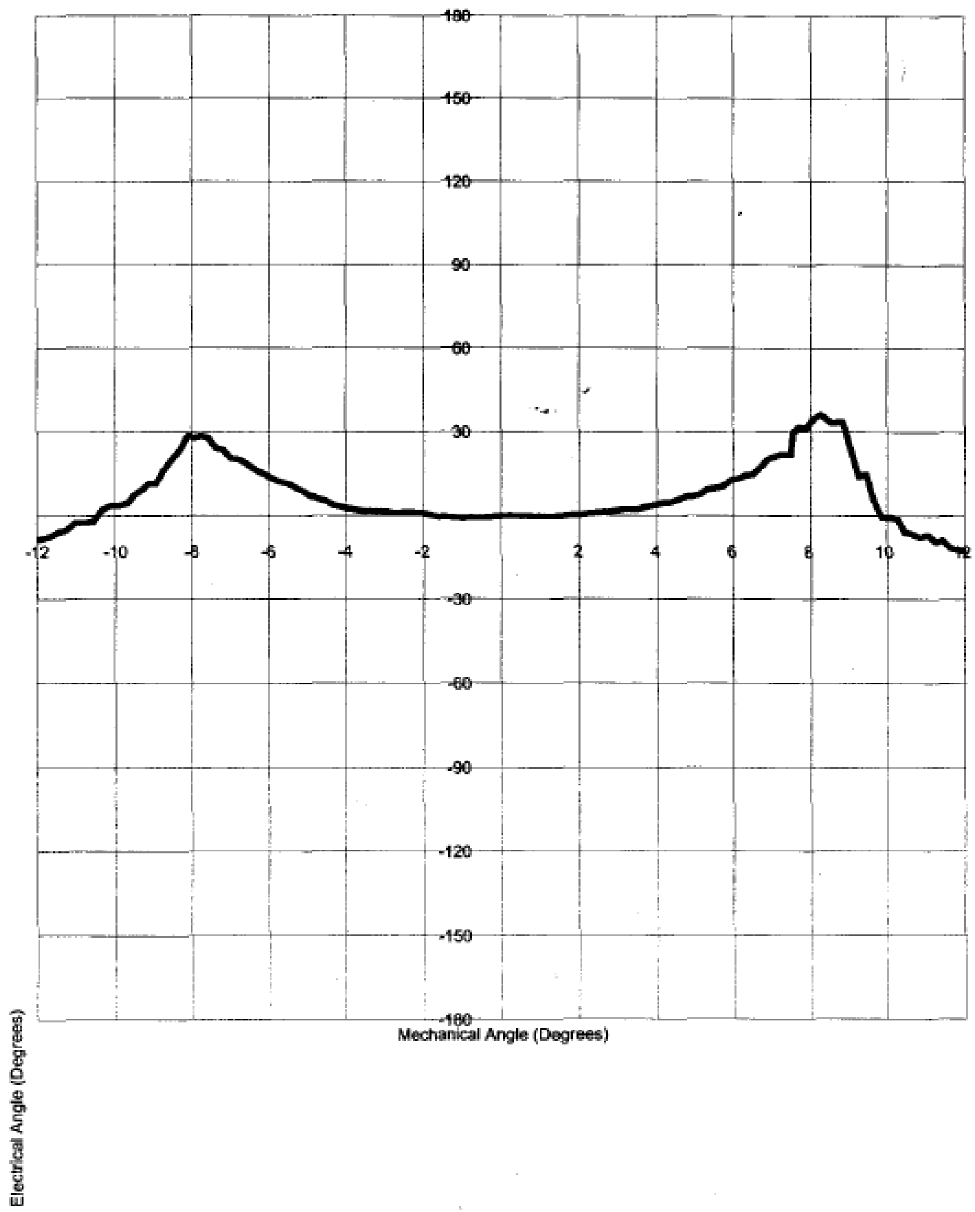

-continued-

Up-Down Stiffness

Collected By: BK, GH
Date June 05, 2002
Time 7:14:45
Sounder S/N 1320758 241
Transducer S/N 926451 6x10
Cable S/N 1302026+030 400'
Comments: PLOT-90 IS UP; 451A90N

Depth 4.57 m
Sep. Dist. 6.1 m
Water Temp 55 F
Bandwidth N/A Hz

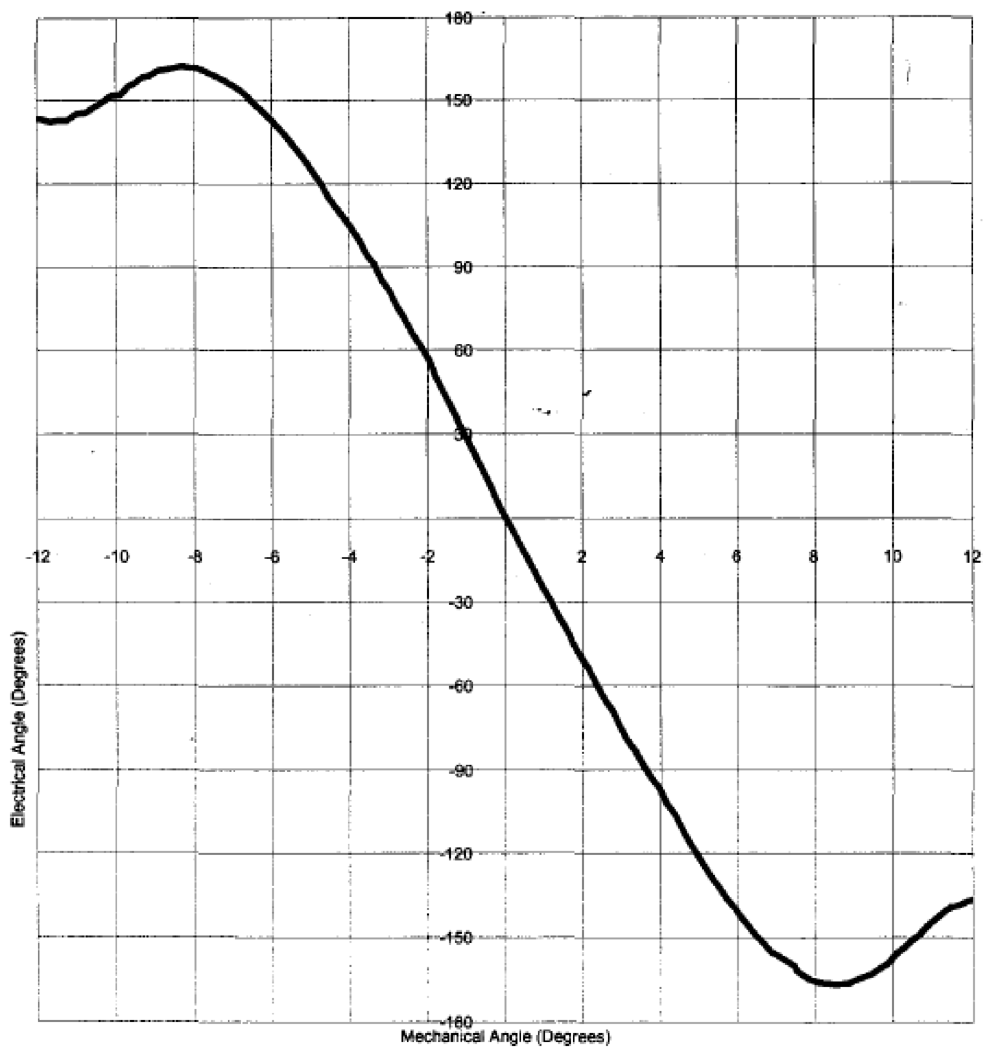

-continued-

Transducer S/N 926451 6x10 Up/Sum Stiffness processed Jun 05, 2002 07:16:01
Comments: PLOT-90 IS UP: 451A90N
Calibrated on HTI Impulse: Date June 05, 2002 Time 7:14:45

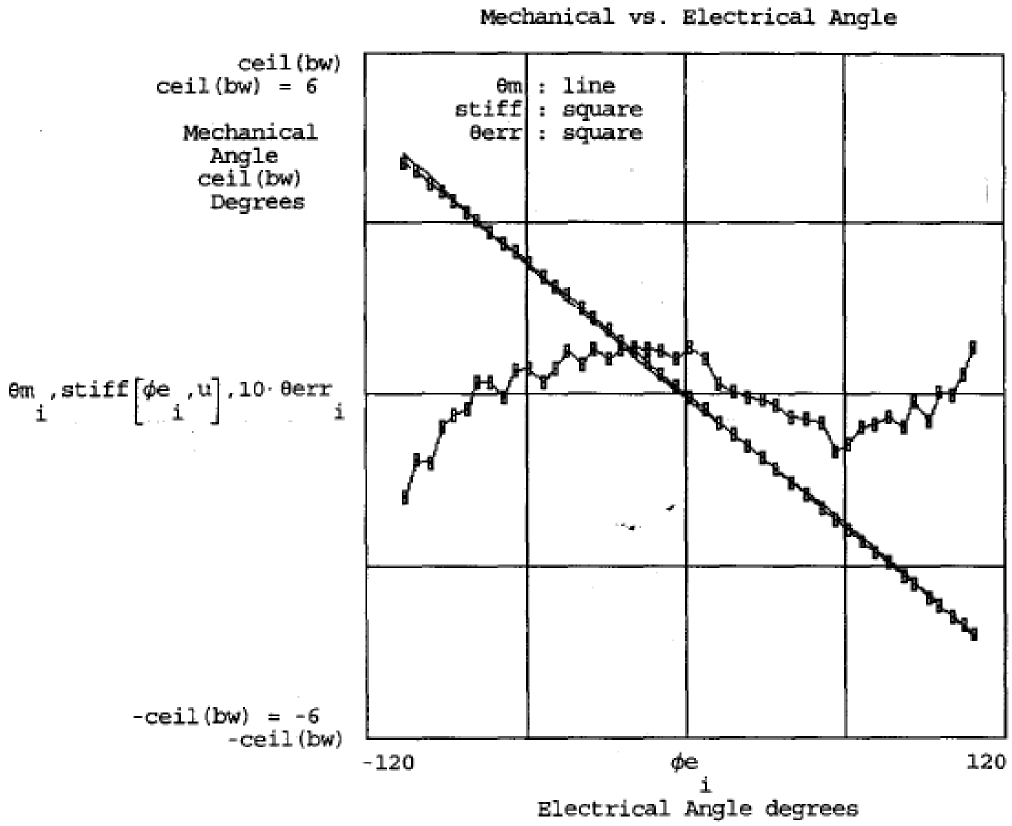

Stiffness constant: U = -25.930956

-continued-

```
Transducer S/N 926451 6x10 Up/Sum Stiffness processed Jun 05, 2002  07:16:01
Comments: PLOT-90 IS UP: 451A90N
Calibrated on HTI Impulse:                      Date June 05, 2002 Time 7:14:45
```

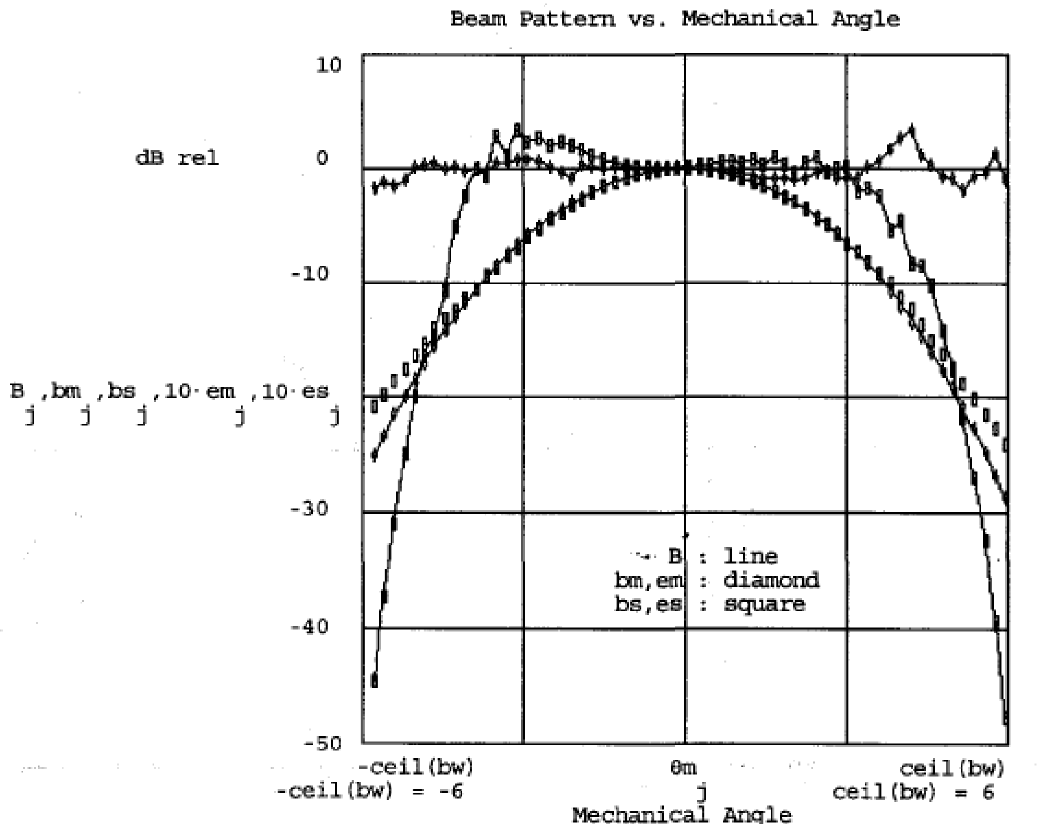

Symbols:
- B beam pattern factor
- θm mechanical angle
- ϕe electrical angle

Beam pattern fit plot:
- B: pattern plotted against mechanical angle, θm
- bm: fit of pattern, θm -> bm
- bs: pattern predicted from stiffness, ϕe -> θm' -> bm

Beam fit coefficients: Measured beamwidth: bw = 5.853
Beamwidth from fit: bw_fit = 5.859

$$c = \begin{array}{cc} \left[\begin{array}{r} 0 \\ 0.000117 \\ -0.678245 \\ -0.004425 \\ -0.002733 \end{array}\right] & \begin{array}{c} a \\ b \\ c \\ d \\ e \end{array} \end{array}$$

-continued-

Squared Beam Pattern Factor Calculation for Rectangular Transducer Element

For XD: | **s/n 926451** | **200 KhZ, 6 x 10**

Actual 3dB beamwidth from beamfit - using coefficients

Vertical Plane:	5.86 °	2.759129 Ly/Lambda
Horizontal Plane:	9.30 °	1.739216 Lx/Lambda

Find squared beam pattern factor (b^2(theta,phi)):

Where:

Lx = transducer element size (wavelengths) in one plane
lambda = wavelength
BW = 3 dB one-way beamwidfth
constant1 = 0.1410112 is empirically determined

First find Lx/lambda and Ly/lambda:
Lx / lambda = constant / sin(BW/2)
10Log(b^2(theta,phi)) = 10Log((1/(Lx/lambda)) * (1/(Ly/lambda))) - 11.572

b^2(theta,phi) = Squared Beam Pattern Factor
constant2 = -11.572 is empirically derived

10Log(b^2(theta,phi)) = -18.3833

b^2(theta,phi) = 0.014510

These equations were developed by J. Ehrenberg,
after those expressed in Urick, 1963

-continued-

APPENDIX B.

Appendix B1.–Field calibration and aiming protocol for the split-beam sonar.

To field calibrate and aim the split-beam transducer, the protocols listed below were followed.

To field calibrate the split-beam transducer:

1. Mount the transducer so it is no more than 3-4 inches off the ground (you should barely be able to stick the toe of your boot under it).
2. Wrap a 1 ½ in tungsten carbide sphere in a mesh bag using 25-30 lb monofilament line. Tie a loop on the end of the line, far enough up so the knot will be above water level when the target is near the river bottom.
3. Attach the target to an extension pole and extend in front of the transducer just beyond the near field (1 m for a $6x10^{o}$ 200 kHz split-beam) lowering it to approximately mid-way between the river's surface and bottom to avoid reverberation interference from either surface. Note: a loop can be tied on the end of the line to the extension pole then the target's loop can be drawn through the pole's loop making it easier to remove and add targets.
4. Position the transducer beam so the target is centered both vertically and horizontally.
5. Set the sonar parameters as you would for sampling, except the threshold should be set as low as possible. Collect 1000 pings or more from the target. Note: if fish targets are present, it may be necessary to raise and lower the target until the operator is assured the echoes are coming from the target.
6. Determine the average target strength of the target and compare to the laboratory calibration. Adjust the calibration parameters if necessary. Document the target filename, the sonar parameters, and the average target strength in the logbook.

To aim the split-beam transducer:

1. Measure
    a. Distance from the river bottom to the bottom of the transducer
    b. Distance from river bottom to water's surface at the transducer
    c. Distance from transducer to shore
    d. Distance from transducer to the end of the weir
2. Wrap a salmon-size target (4 in diameter sphere partially filled with bb's) using 50 lb or heavier monofilament line. Tie a loop on the end of the line, far enough up so the knot will be above water level when the target is near the river bottom.
3. Attach the salmon-size target to an extension pole and extend in front of the transducer beyond the near field (1 m for a $6x10^{o}$ 200 kHz split-beam) Note: a loop can be tied on the end of the line to the extension pole, then the target's loop can be drawn through the pole's loop making it easier to remove and add targets.

-continued-

4. Follow directions #2-6 above to document the target strength of the salmon-size target.
5. Position the target so a line drawn from the transducer mount to the target would perpendicularly bisect a line parallel to the river's current, then lower the target to approximately 4 inches off the river bottom.
6. Aim the split-beam transducer so the target appears in the center of the beam horizontally and in the central portion of the lower half of the vertical beam. If the river bottom consists of a hard substrate, the transducer beam may have to be raised so the target rests closer to the lower edge of the beam. If the river bottom is soft, the transducer may be lowered slightly moving the target closer to the central axis of the beam.
7. Use the "Alt Print Screen" command to copy a picture showing the position of the target in the 2d graphs of HTI's DEP program, then paste to either a drawing program or a Microsoft PowerPoint presentation to document the aim. Note: if fish targets are present, it may be necessary to raise and lower the target until the operator is assured the echoes are coming from the target.
8. Pull the target out and reposition once again to recheck the aim.